

ADVANCED CONJUGATED SYSTEMS TOWARDS REALIZATION OF  
STABLE n-TYPE MATERIALS AND HIGH-PERFORMANCE  
ELECTROCHROMIC POLYMERS

A THESIS SUBMITTED TO  
THE GRADUATE SCHOOL OF NATURAL AND APPLIED SCIENCES  
OF  
MIDDLE EAST TECHNICAL UNIVERSITY

BY

KIANOUSH GHASEMI. A. F.

IN PARTIAL FULFILLMENT OF THE REQUIREMENTS  
FOR  
THE DEGREE OF MASTER OF SCIENCE  
IN  
POLYMER SCIENCE AND TECHNOLOGY

SEPTEMBER 2018



Approval of the thesis:

**ADVANCED CONJUGATED SYSTEMS TOWARDS REALIZATION OF  
STABLE n-TYPE MATERIALS AND HIGH-PERFORMANCE  
ELECTROCHROMIC POLYMERS**

submitted by **KIANOUSH GHASEMI. A. F.** in partial fulfillment of the requirements for the degree of **Master of Science in Polymer Science and Technology Department, Middle East Technical University** by,

Prof. Dr. Halil Kalıpçılar  
Dean, Graduate School of **Natural and Applied Sciences**

\_\_\_\_\_

Prof. Dr. Necati Özkan  
Head of Department, **Polymer Science and Technology**

\_\_\_\_\_

Assoc. Prof. Dr. Görkem Günbaş  
Supervisor, **Polymer Science and Technology, METU**

\_\_\_\_\_

**Examining Committee Members:**

Prof. Dr. Levent Toppare  
Department of Chemistry, METU

\_\_\_\_\_

Assoc. Prof. Dr. Görkem Günbaş  
Polymer Science and Technology, METU

\_\_\_\_\_

Prof. Dr. Ali Çırpan  
Department of Chemistry, METU

\_\_\_\_\_

Assist. Prof. Dr. Salih Özçubukçu  
Department of Chemistry, METU

\_\_\_\_\_

Prof. Dr. Yasemin Udum  
Dept. of Ad. Tech., Gazi Uni.

\_\_\_\_\_

Date: 07.09.2018

**I hereby declare that all information in this document has been obtained and presented in accordance with academic rules and ethical conduct. I also declare that, as required by these rules and conduct, I have fully cited and referenced all material and results that are not original to this work.**

Name, Surname: Kianoush Ghasemi. A. F.

Signature:

## ABSTRACT

### **ADVANCED CONJUGATED SYSTEMS TOWARDS REALIZATION OF STABLE n-TYPE MATERIALS AND HIGH-PERFORMANCE ELECTROCHROMIC POLYMERS**

Ghasemi. A. F., Kianoush  
Master of Science, Polymer Science and Technology  
Supervisor: Assoc. Prof. Dr. Gökem Günbaş

September 2018, 99 pages

Electrochromic materials attracted tremendous amount of interest both in academia and industry in recent decades. These materials owe their popularity to their fascinating fundamental spectroelectrochemical properties and their potential commercial applications. On the spectrum of electrochromic materials, electrochromic polymers drawn the attention of the scientific community due to properties such as high flexibility, low-power consumption, ease of processing and low processing cost. Polymers which represent one of the three complementary colors (red, green, and blue) in their reduced state and high transmissivity in oxidized state are fundamental for electrochromic devices and displays. With this regard and following previous works of our group in designing green to transmissive polymers utilizing EDOT as the donor unit, we aimed to create better performance green materials using ProDOT instead of EDOT. ProDOT containing conjugated systems are expected to outperform their EDOT analogues considering the fact that ProDOT homopolymers outperforms EDOT containing donor-acceptor type polymers. Hence, we introduced ProDOT units to benzoxadiazole and quinoxaline for reaching the required donor-acceptor match towards realization of a green to transmissive polymer with superior properties. Besides, despite the fact that stable n-dopable conjugated

polymers are infrequent, they have a broad potential of application in organic electrochemical transistors and OFETs. The stable n-type materials can be used for realization of complex organic electronic devices with p-i-n type junctions. On this path, perylene diimide (PDI) and its derivatives represent one of the most promising classes of electron acceptors because of their outstanding chemical and physical properties, including high electron mobility, strong intermolecular  $\pi$ - $\pi$  interactions, and high absorption coefficients. In this study, we coupled PDI with electron-rich EDOT units to realize easily n-dopable conjugated polymer systems that can be prepared by electrochemical polymerization techniques

Keywords: Electrochromism, Green to transmissive polymers, ProDOT, Conjugated polymers, n-type materials

## ÖZ

### **YÜKSEK PERFORMANSLI ELEKTROKROMİK POLİMERLERİN VE KARARLI n-TİPİ MALZEMELERİN GELİŞTİRİLMESİ İÇİN İLERİ SEVİYE KONJUGE SİSTEMLER**

Ghasemi. A. F., Kianoush  
Yüksek Lisans, Polimer Bilim ve Teknolojisi  
Tez Danışmanı: Doç. Dr. Görkem Günbaş

Eylül 2018, 99 sayfa

Elektrokromik malzemeler son yıllarda akademide ve endüstride yoğun ilgi çekmektedir. Bu malzemeler popülerliklerini etkileyici temel spektroeletrokimyasal özelliklerine ve potansiyel ticari uygulamalarına borçludurlar. Çeşitli elektrokromik malzemeler arasında yüksek esneklik, düşük güç tüketimi, işleme kolaylığı ve düşük işleme maliyeti özelliklerine sahip olan polimerler bilim camiasının özellikle ilgisini çekmiştir. İndirgenmiş hallerinde üç tamamlayıcı rengi (kırmızı, yeşil ve mavi) temsil eden ve oksitlenmiş hallerinde ise yüksek şeffaflık gösteren polimerler elektrokromik görüntüleme cihazlarında kullanılmaktadırlar. Araştırma grubumuzun daha önceki çalışmalarında donör ünitesi olarak EDOT kullanarak yeşilden şeffafa dönen polimerin daha yüksek performanslı olanlarını başarmak adına EDOT ünitesi ProDOT ünitesi ile değiştirilmiştir. ProDOT homopolimerlerin PEDOT'dan daha üstün özellik göstermesi ve ProDOT içeren donör-akseptör tipi polimerlerin de EDOT'lu olanlara oranla daha yüksek performans göstermektedir. Bu sebeple ProDOT ünitesi benzooksadiazol ve kuinoksalin ile eşleştirilerek uygun donör-akseptör eşleşmesini yakalayıp daha üstün özelliklere sahip yeşilden şeffafa dönen polimerler eldesi amaçlanmıştır. Ayrıca, yüksek kararlılığa sahip n-tipi doplanabilen konjuge polimerler çeşitlerinin seyrek olmasına rağmen organik elektrokimyasal transistör ve

OFET cihazların geniş bir uygulama potansiyeline sahiptirler. Kararlı n-tipi materyaller p-i-n tipi ekleme sahip kompleks organik elektronik cihazların geliştirilmesinde kullanılabilirler. Bu yolda, perilen diimide (PDI) ve türevleri; yüksek elektron hareketliliği, güçlü moleküller arası  $\pi$ - $\pi$  etkileşimleri, ve yüksek absorpsiyon katsayıları dahil olmak üzere etkileyici kimyasal ve fiziksel özellikleri sayesinde elektron alıcıları grubunda en önemli sınıflardan birini temsil etmektedirler. Bu çalışmada, PDI ünitesi elektronca zengin EDOT ünitesi bu sistem davranışlarında temel bilgiler ve yeni sonuçlar elde etmek üzere birleştirilmiş ve elektrokimyasal yöntemlerle polimerleştirilmiştir

Anahtar Kelimeler: Elektrokromizm, Yeşil-şeffaf polimerler, ProDOT, Konjuge polimerler

To family

## ACKNOWLEDGMENTS

Although words are so asthenic to take the responsibility to transfer what heart means, but we invented them and we split our path from our biological ancestors, so I try to harness the words to tender my sincere gratitude to the following esteemed people who were always on my side or in my mind and helped me to make this study happen.

My parents who gifted me life as the first blessing. Parents are such those things that are always there, since the time of your birth, like the sun and the moon, so you sometimes forget that you owe them everything, you owe them your life. I thank them for their kindness, understanding and their patience towards their stubborn son who always put them in hard tough emotional situations.

My dear lovely sister, Katayoon, whose soul, is my soul in another body. We have been all along throughout these decades of our lives, actually and spiritually, mentally and emotionally. I thank her so much because of carrying this heavy burden of being the child present with our parents within all these years of my absence, taking care of herself and consequently taking care of our parents. I love you.

My dear adviser Assoc. Prof. Dr. Gökem Günbaş for supervising, guiding and accompanying me in all steps of my work and more importantly giving me the chance of being a member of his research group and working in his laboratory. During the period of my study, he was always more of a friend whose leads had enlightened the blurry pathway of the new science.

Dear Prof. Dr. Yasemin Udum. No doubt that all of us owe her the electrochemistry part of our thesis, but it's not just that, because when it comes to electrochemistry we are all in rush to finish final works and we put this tremendous pressure on her to prioritize our work. She is so dedicated, hardworking and so kind to explain to me what I needed to know about her work in a short time, just like electrochemistry in a nutshell.

Dear Assist. Prof. Dr. Selcuk Yerci, who acquainted me in the first place with Dr.Günbaş and put the very first stone of this building.

The esteemed committee members, Prof. Dr. Levent Toppare, Prof. Dr. Ali Çırpan, Prof. Dr. Yasemin Udum, and Assist. Prof. Dr. Salih Özçubukçu for their kind consideration and making me honored by attending my thesis jury session.

And all my friends;

Dear lovely Gizem Atakan, the supervisor of our lab, for her kindness, conscientious, companion and friendship. I cannot even count how many times I interrupted her work just to check my NMR results and she never said no, not even once and that's not the only one.

My brother, Mustafa Yaşa, for those all days and nights of working together in the lab, the courses that we took with each other, his always and ever presence around at school never let me feel alone, answering my questions and accompanying me in researches and practical works. I have been around and he is one of the best people who I have ever seen in my life. He is a brilliant guy with a brilliant future.

Seza Göker, the hardworking companionate and brainy friend of mine. She may have come later than all friends who I had the opportunity to know in METU, but our friendship was immediately elevated to another level, that much I can say that sometimes she was more worried about me and my job than me.

Aliekber Karabağ, my strong friend who really is a delineation of hardworking and combatant. He was always patient and friendly the same as supporting and careful in devoting the knowledge that he earned through hard work out of difficulties. He is the man of acts.

Dear Figen Varlıoğlu, my lovely dreamer friend with a glass heart and an iron will. She was always so kind and so compassionate. I thank her so much for listening to my long never-ending boring speeches about life and philosophy of being, always patient, always merciful.

My man, Osman Karaman, for his generosity, brotherhood and friendship. I thank him so much because of being so munificent to share his glasses with me, accompany me with checking my NMRs and working shoulder by shoulder with me at weekend in the lab. I also thank him for listening to Arctic Monkeys for hours with me in the lab and never say enough.

Cansu İğci, for her kind help and warm welcome to me along with others when I came to the lab for the first time. She was and still is one of the bests and I learnt a lot from her.

Gülce Öklem. Everyone knows how to set up chromatography columns, I learnt her method and I got several pure products out of those chromatography columns.

Other dear friends from GÜNBAŞ research group, Dilay Kepil, Cevahir Ceren Akgül, Gülsüm Güneş, Merve Canyurt, Esra Bağ, Selin Akpınar, Sultan Çetin, Nihan Yılmaz and Hayriye Kocademirci for helping to make the meaning of the word “Group” real.

Last and the most, to my dear Simge for reminding me the blue sky.

With indulgences with everybody else that their names aren't mentioned here because of lack of my memory, I want to thank them by heart and propound this lovely message by Albert Camus, the French philosopher and journalist, to them; “But, heart has its own memory.”

## TABLE OF CONTENTS

|   |      |
|---|------|
| ABSTRACT.....                                   | v    |
| ÖZ .....  | vii  |
| ACKNOWLEDGEMENTS .....                          | x    |
| TABLE OF CONTENTS.....                          | xiii |
| LIST OF FIGURES .....                           | xvii |
| LIST OF ABBREVIATIONS.....                      | xxii |
| CHAPTERS  |      |
| CHAPTER 1 .....                                 | 1    |
| INTRODUCTION .....                              | 1    |
| 1.1. Conjugated Polymers .....                  | 1    |
| 1.2. Conduction in Conjugated Polymers .....    | 2    |
| 1.2.1. Band Theory .....                        | 2    |
| 1.2.2. Conduction in Conjugated Polymers .....  | 4    |
| 1.2.3. Solitons, Polarons, and Bipolarons ..... | 4    |
| 1.2.4. Doping .....                             | 5    |
| 1.2.5. What Affects the Band Gap? .....         | 6    |
| 1.2.6. Resonance Energy.....                    | 6    |
| 1.2.7. Electron-Withdrawing Groups.....         | 6    |
| 1.2.8. Electron-donating Groups.....            | 7    |
| 1.2.9. Donor Acceptor Approach.....             | 8    |
| 1.3. Stable N-Type Conjugated Polymers .....    | 8    |
| 1.4. Conducting Polymer Characterization.....   | 9    |

|   |           |
|---|-----------|
| 1.4.1. Chromism.....  | 10        |
| 1.4.2. Electrochromism .....  | 10        |
| 1.4.2.1. Electrochromic Material Types .....                              | 11        |
| 1.4.2.1.1. Viologens (1,1'-disubstituted-4,4'-bipyridylium salts) .....   | 11        |
| 1.4.2.1.2. Prussian Blue System .....                                     | 11        |
| 1.4.2.1.3. Metal Oxides.....  | 12        |
| 1.5. Conjugated Conducting Polymers .....                                 | 12        |
| 1.6. Utilized Color Models for Simple Electrochromic Display Devices..... | 14        |
| 1.6.1. Standard Red-Green-Blue (sRGB) Color Space.....                    | 14        |
| 1.6.1.1. Blue to Transmissive Electrochromic Polymers .....               | 15        |
| 1.6.1.2. Green to Transmissive Electrochromic Polymers .....              | 15        |
| 1.6.1.3. Red to Transmissive Electrochromic Polymers .....                | 16        |
| 1.6.2. Multicolor Electrochromic Polymers: Color Control .....            | 17        |
| 1.7. Polymerization Methods .....   | 21        |
| 1.7.1. Electropolymerization.....   | 21        |
| 1.7.2. Oxidative Chemical Polymerization .....                            | 23        |
| 1.7.2.1. Suzuki-Miyaura Coupling .....                                    | 23        |
| 1.7.2.2. Stille Coupling.....   | 24        |
| 1.7.2.3. Yamamoto Coupling .....  | 24        |
| 1.7.2.4. Knoevenagel Condensation .....                                   | 25        |
| 1.7.2.5. Tamao-Kumada-Corriu Coupling .....                               | 25        |
| 1.7.2.6. Sonogashira Coupling .....                                       | 25        |
| 1.8. Aim of This Work.....  | 26        |
| <b>CHAPTER 2 .....</b>  | <b>29</b> |
| <b>EXPERIMENTAL .....</b>   | <b>29</b> |
| 2.1. Materials & Methods .....  | 29        |
| 2.1.1. Synthesis of 2-decyl-1-tetradecylbromide .....                     | 30        |
| 2.1.2. Synthesis of N-(2-decyltetradecyl)phthalimide .....                | 30        |
| 2.1.3. Synthesis of 2-decyl-1-tetradecylamine.....                        | 31        |
| 2.2. Synthesis of (PDI-EDOT).....   | 31        |

|  |    |
|--|----|
| 2.2.1. Synthesis of PDI-2Br .....  | 32 |
| 2.2.2. Synthesis of N,N'-bis(2-decyltetradecyl)-1,6-dibromo-3,4,9,10-perylene diimide .....  | 32 |
| 2.2.3. Synthesis of tributyl(2,3-dihydrothieno[3,4-b][1,4]dioxin-5-yl)stannane .....   | 33 |
| 2.2.4. Synthesis of 2,9-bis(2-decyltetradecyl)-5,12-bis(2,3-dihydrothieno[3,4-b][1,4]dioxin-5-yl)anthrax[2,1,9-def:6,5,10-d'e'f']diisoquinoline-1,3,8,10(2H,9H)tetraone (PDI-EDOT) ..... | 34 |
| 2.3. Synthesis of stannylated Pro-DOT .....  | 35 |
| 2.3.1. Synthesis of diethyl 2,2-dipentadecylmalonate .....   | 35 |
| 2.3.2. Synthesis of 2,2-sipentadecyl-1,3-propanediol.....  | 36 |
| 2.3.3. Synthesis of 2,3,4,5-tetrabromothiophene .....  | 36 |
| 2.3.4. Synthesis of 3,4-dibromothiophene .....   | 37 |
| 2.3.5. Synthesis of 3,4-dimethoxythiophene.....  | 37 |
| 2.3.6. Synthesis of 3,3'-didodecyl-3,4-dihydro-2H thieno[3,4b][1,4]dioxepine (ProDOT).....   | 38 |
| 2.3.7. Synthesis of tributyl(3,3-diundecyl-3,4-dihydro-2H-thieno[3,4-b][1,4]dioxepin-6-yl) stannane .....  | 39 |
| 2.3.7.1. Synthesis of (3,3-didecyl-3,4-dihydro-2H-thieno[3,4-b][1,4]dioxepin-6-yl)trimethylstannane .....  | 40 |
| 2.4. Synthesis of QUIN-ProDOT .....  | 40 |
| 2.4.1. Synthesis of 5,8-dibromo-2,3-bis(4-((2-octyldodecyl)oxy)phenyl)quinoxaline.....   | 40 |
| 2.4.2. Synthesis of 5,8-bis(3,3-diundecyl-3,4-dihydro-2H thieno[3,4-b][1,4]dioxepin-6-yl)-2,3-bis(4 (dodecyloxy)phenyl)quinoxaline (Quin-ProDOT).....                                    | 41 |
| 2.5. Synthesis of (BENZ-ProDOT) .....  | 42 |
| 2.5.1. Synthesis of 4,7-bis(3,3-didecyl-3,4-dihydro-2Hthieno[3,4-b][1,4]dioxepin-6 yl)benzo[c][1,2,5]oxadiazole (BENZ-ProDOT) .....  | 42 |
| RESULTS and DISCUSSION .....   | 45 |

|   |    |
|---|----|
| 3.1. Monomer Syntheses.....   | 45 |
| 3.1.1. Synthesis of the PDI-EDOT.....                                     | 45 |
| 3.1.2. Synthesis of the QUIN-ProDOT.....                                  | 46 |
| 3.2.1. Electropolymerization of Monomers.....                             | 48 |
| 3.2.2. Spectroelectrochemistry Studies of Polymers.....                   | 48 |
| 3.2.3. Kinetic Studies of Polymers.....                                   | 48 |
| 3.2.4. Electrochemical and Electrochromic Properties of (PDI-EDOT).....   | 49 |
| 3.2.4.1. Electropolymerization of (PDI-EDOT).....                         | 49 |
| 3.2.4.2. Spectroelectrochemistry Studies of PPDI-EDOT.....                | 51 |
| 3.2.4.3. Kinetic Studies of PPDI-EDOT.....                                | 52 |
| 3.2.5. Electrochemical Polymerization of QUIN-ProDOT.....                 | 53 |
| 3.2.6. Electrochemical and Electrochromic Properties of (BENZ-Pro-DOT) .. | 54 |
| 3.2.6.1. Electropolymerization of (BENZ-Pro-DOT).....                     | 54 |
| 3.2.6.2. Spectroelectrochemistry Studies of PBENZ-Pro-DOT.....            | 56 |
| 3.2.5.3. Kinetic Studies of PBENZ-Pro-DOT.....                            | 57 |
| 3.3. Future Work.....   | 59 |
| CONCLUSION.....   | 61 |
| REFERENCES.....   | 63 |
| APPENDICES.....   | 69 |

## LIST OF FIGURES

|  |    |
|--|----|
| <b>Figure 1.1:</b> Structures of commonly known conjugated polymer systems .....   | 2  |
| <b>Figure 1.2:</b> Band structures of materials .....  | 3  |
| <b>Figure 1.3:</b> Charge carriers .....   | 4  |
| <b>Figure 1.4:</b> Band Structure of the polymer with bipolaron states .....   | 5  |
| <b>Figure 1.5:</b> Modification of band gap.....   | 7  |
| <b>Figure 1.6:</b> Representative electron-transporting polymer semiconductors.....  | 9  |
| <b>Figure 1.7:</b> Viologen redox states .....   | 11 |
| <b>Figure 1.8:</b> Illustrative example of electroactive conjugated conducting polymers<br>.....   | 13 |
| <b>Figure 1.9:</b> sRGB and CMYK color models.....   | 14 |
| <b>Figure 1.10:</b> Literature examples of blue to transmissive switching polymers ....  | 15 |
| <b>Figure 1.11:</b> Literature examples of green electrochromic polymers .....   | 16 |
| <b>Figure 1.12:</b> Literature examples of red to transmissive electrochromic copolymers<br>.....  | 17 |
| <b>Figure 1.13:</b> Tuning color by substituents.....  | 18 |
| <b>Figure 1.14:</b> Illustrative example of electrochromic polymers. “Color swatches are<br>representations of thin films based on measured CIE 1931 Yxy color coordinates.<br>Key: 0 = neutral; I = intermediate; + = oxidized; - and -- = reduced” ..... | 19 |
| <b>Figure 1.15:</b> Electropolymerization mechanism .....  | 23 |
| <b>Figure 1.16:</b> Oxidative chemical polymerization.....   | 23 |
| <b>Figure 1.17:</b> Suzuki coupling .....  | 24 |
| <b>Figure 1.18:</b> Stille coupling.....   | 24 |
| <b>Figure 1.19:</b> Yamamoto coupling.....   | 24 |
| <b>Figure 1.20:</b> Knoevenagel condensation.....  | 25 |
| <b>Figure 1.21:</b> Regioregular HT-P3ATs prepared using Ni-catalyzed Kumada<br>conditions: dppp = 1,2-bis(diphenylphosphino)propane .....   | 25 |
| <b>Figure 1.22:</b> Sonogashira coupling .....   | 26 |
| <b>Figure 2.1:</b> Synthesis of 2-decyl-1-tetradecylbromide.....   | 29 |
| <b>Figure 2.2:</b> Synthesis of N-(2-decyltetradecyl) phthalimide.....   | 30 |

|   |    |
|---|----|
| <b>Figure 2.3:</b> Synthesis of 2-decyl-1-tetradecylamine. ....   | 31 |
| <b>Figure 2.4:</b> Synthesis of PDI-2Br .....   | 31 |
| <b>Figure 2.5:</b> Synthesis of N,N'-bis(2-decyltetradecyl)-1,6-bibromo-3,4,9,10-<br>perylene diimide. ....   | 32 |
| <b>Figure 2.6:</b> Synthesis of tributyl(2,3-dihydrothieno[3,4-b][1,4]dioxin-5-<br>yl)stannane.....   | 33 |
| <b>Figure 2.7:</b> Synthesis of 2,9-bis(2-decyltetradecyl)-5,12-bis(2,3-dihydrothieno[3,4-<br>b][1,4]dioxin-5-yl)anthrac [2,1,9-def:6,5,10-d'e'f]diisoquinoline-1,3,8,10(2H,9H)-<br>tetraone (PDI-EDOT) ..... | 34 |
| <b>Figure 2.8:</b> Synthesis of diethyl 2,2-dipentadecylmalonate. ....  | 35 |
| <b>Figure 2.9:</b> Synthesis of 2,2-sipentadecyl-1,3-propanediol.....   | 35 |
| <b>Figure 2.10:</b> Synthesis of 2,3,4,5-tetrabromothiophene. ....  | 36 |
| <b>Figure 2.11:</b> Synthesis of 3,4-dibromothiophene. ....   | 37 |
| <b>Figure 2.12:</b> Synthesis of 3,4-dimethoxythiophene. ....   | 37 |
| <b>Figure 2.13:</b> Synthesis of 3,3'-didodecyl-3,4-dihydro-2H-thieno[3,4-<br>b][1,4]dioxepine(ProDOT).....   | 38 |
| <b>Figure 2.14:</b> Synthesis of tributyl(3,3-diundecyl-3,4-dihydro-2H-thieno[3,4-<br>b][1,4]dioxepin-6-yl)stannane. ....   | 39 |
| <b>Figure 2.15:</b> Synthesis of (3,3-didecyl-3,4-dihydro-2H-thieno[3,4-b][1,4]dioxepin-<br>6-yl)trimethylstannane.....   | 39 |
| <b>Figure 2.16:</b> Synthesis of 5,8-dibromo-2,3-bis(4-((2-<br>octyldodecyl)oxy)phenyl)quinoxaline.....   | 40 |
| <b>Figure 2.17:</b> Synthesis of 5,8-bis(3,3-diundecyl-3,4-dihydro-2H-thieno[3,4-<br>b][1,4]dioxepin-6-yl)-2,3-bis(4-(dodecyloxy)phenyl)quinoxaline .....   | 41 |
| <b>Figure 2.18:</b> Synthesis of 4,7-bis(3,3-didecyl-3,4-dihydro-2H-thieno[3,4-<br>b][1,4]dioxepin-6 yl)benzo[c][1,2,5]oxadiazole (BENZ-Pro-DOT).....   | 42 |
| <b>Figure 3.1:</b> Synthetic pathway of PDI-EDOT ( <b>12</b> ). ....  | 45 |
| <b>Figure 3.2:</b> Synthetic pathway of the central unit. ....  | 47 |
| <b>Figure 3.3:</b> Synthetic pathway of the central unit. ....  | 47 |
| <b>Figure 3.4:</b> Repeated scan polymerization of PDI-EDOT (WE: ITO, CE: Pt wire,<br>RE: Ag wire, 0.1 M TBAPF <sub>6</sub> /DCM/ACN 100 mV s <sup>-1</sup> , 10 cycles).....                                 | 49 |
| <b>Figure 3.5:</b> Single scan cyclic voltammetry of PDI-EDOT (WE: ITO, CE: Pt wire,<br>RE: Ag wire, 0.1 M TBAPF <sub>6</sub> /DCM/ACN 100 mV s <sup>-1</sup> ).....  | 50 |

|  |    |
|--|----|
| <b>Figure 3.6:</b> Spectroelectrochemistry studies of PPDI-EDOT (-0.1 V to 1.4 V with 0.1 V increments).....   | 51 |
| <b>Figure 3.7:</b> Photographs of the PPDI-EDOT at its neutral and oxidized states.....  | 51 |
| <b>Figure 3.8:</b> Electrochromic switching and optical absorbance change of PPDI-EDOT monitored at 402 nm (30 cycles).....  | 52 |
| <b>Figure 3.9:</b> Electrochromic switching and optical absorbance change of PPDI-EDOT monitored at 492 nm (30 cycles).....  | 53 |
| <b>Figure 3.10:</b> Electrochromic switching and optical absorbance change of PPDI-EDOT monitored at 1470 nm (30 cycles).....  | 53 |
| <b>Figure 3.11:</b> Repeated scan polymerization of BENZ-Pro-DOT (WE: ITO, CE: Pt wire, RE: Ag wire, 0.1 M TBAPF <sub>6</sub> /DCM/ACN, 100 mV s <sup>-1</sup> , 10 cycles). ..... | 54 |
| <b>Figure 3.12:</b> n-Doped polymerization of BENZ-Pro-DOT (WE: ITO, CE: Pt wire, RE: Ag wire, 0.1 M TBAPF <sub>6</sub> /DCM/ACN, 100 mV s <sup>-1</sup> ) .....                   | 55 |
| <b>Figure 3.13:</b> p-Doped polymerization of BENZ-Pro-DOT (WE: ITO, CE: Pt wire, RE: Ag wire, 0.1 M TBAPF <sub>6</sub> /DCM/ACN, 100 mV s <sup>-1</sup> ) .....                   | 56 |
| <b>Figure 3.14:</b> Spectroelectrochemistry studies of PBENZ-Pro-DOT (-0.1 V to 1.4 V with 0.1 V increments).....  | 56 |
| <b>Figure 3.15:</b> Photographs of the PBENZ-Pro-DOT at its neutral and oxidized states.....   | 57 |
| <b>Figure 3.16:</b> Electrochromic switching and optical absorbance change of PBENZ-Pro-DOT monitored at 400 nm (30 cycles).....   | 58 |
| <b>Figure 3.17:</b> Electrochromic switching and optical absorbance change of PBENZ-Pro-DOT monitored at 720 nm (30 cycles).....   | 59 |
| <b>Figure 3.18:</b> Electrochromic switching and optical absorbance change of PBENZ-Pro-DOT monitored at 1350 nm (30 cycles).....  | 59 |
| <b>Figure A.1.1:</b> <sup>1</sup> H-NMR spectrum 2-decyl-1-tetradecylbromide .....   | 69 |
| <b>Figure A.1.2:</b> <sup>13</sup> C-NMR spectrum of 2-decyl-1-tetradecylbromide.....  | 70 |
| <b>Figure A.2.1:</b> <sup>1</sup> H-NMR spectrum N-(2-decyltetradecyl)phthalimide.....   | 71 |
| <b>Figure A.2.2:</b> <sup>13</sup> C-NMR spectrum of N-(2-decyltetradecyl)phthalimide .....  | 72 |
| <b>Figure A.3.1:</b> <sup>1</sup> H-NMR spectrum 2-decyl-1-tetradecylamine.....  | 73 |
| <b>Figure A.3.2:</b> <sup>13</sup> C-NMR spectrum of 2-decyl-1-tetradecylamine .....   | 74 |
| <b>Figure A.4.1:</b> <sup>1</sup> H-NMR spectrum N,N'-bis(2-decyltetradecyl)-1,6-dibromo-3,4,9,10-perylene diimide .....   | 75 |

|   |    |
|---|----|
| <b>Figure A.5.1:</b> <sup>1</sup> H-NMR spectrum of tributyl(2,3-dihydrothieno[3,4-b][1,4]dioxin-5-yl)stannane .....  | 76 |
| <b>Figure A.5.2:</b> <sup>13</sup> C-NMR spectrum of tributyl(2,3-dihydrothieno[3,4-b][1,4]dioxin-5-yl)stannane .....   | 77 |
| <b>Figure A.6.1:</b> <sup>1</sup> H-NMR spectrum of PDI-e-Dot .....   | 78 |
| <b>Figure A.6.2:</b> <sup>13</sup> C-NMR spectrum of PDI-e-Dot .....  | 79 |
| <b>Figure A.7.1:</b> <sup>1</sup> H-NMR spectrum diethyl 2,2-dipentadecylmalonate .....   | 80 |
| <b>Figure A.7.2:</b> <sup>13</sup> C-NMR spectrum diethyl of 2,2-dipentadecylmalonate .....   | 81 |
| <b>Figure A.8.1:</b> <sup>1</sup> H-NMR spectrum of 2,2-dipentadecyl-1,3-propanediol .....  | 82 |
| <b>Figure A.8.2:</b> <sup>13</sup> C-NMR spectrum of 2,2-dipentadecyl-1,3-propanediol .....   | 83 |
| <b>Figure A.9.2:</b> <sup>13</sup> C-NMR spectrum of 2,3,4,5-tetrabromothiophene .....  | 84 |
| <b>Figure A.10.1:</b> <sup>1</sup> H-NMR spectrum of 3,4-dibromothiophene .....   | 85 |
| <b>Figure A.10.2:</b> <sup>13</sup> C-NMR spectrum of 3,4-dibromothiophene .....  | 86 |
| <b>Figure A.11.1:</b> <sup>1</sup> H-NMR spectrum of 3,4-dimethoxythiophene .....   | 87 |
| <b>Figure A.11.2:</b> <sup>13</sup> C-NMR spectrum of 3,4-dimethoxythiophene .....  | 88 |
| <b>Figure A.12.1:</b> <sup>1</sup> H-NMR spectrum of 3,3'-didodecyl-3,4-dihydro-2H-thieno[3,4-b][1,4]dioxepine(ProDOT) .....  | 89 |
| <b>Figure A.12.2:</b> <sup>13</sup> C-NMR spectrum of 3,3'-didodecyl-3,4-dihydro-2H-thieno[3,4-b][1,4]dioxepine(ProDOT) .....   | 90 |
| <b>Figure A.13.1:</b> <sup>1</sup> H-NMR spectrum of tributyl(3,3-diundecyl-3,4-dihydro-2H-thieno[3,4-b][1,4]dioxepin-6-yl)stannane .....                                 | 91 |
| <b>Figure A.13.2:</b> <sup>13</sup> C-NMR spectrum of tributyl(3,3-diundecyl-3,4-dihydro-2H-thieno[3,4-b][1,4]dioxepin-6-yl)stannane .....                                | 92 |
| <b>Figure A.14.1:</b> <sup>1</sup> H-NMR (3,3-didecyl-3,4-dihydro-2H-thieno[3,4-b][1,4]dioxepin-6-yl)trimethylstannane .....  | 93 |
| <b>Figure A.14.2:</b> <sup>13</sup> C-NMR (3,3-didecyl-3,4-dihydro-2H-thieno[3,4-b][1,4]dioxepin-6-yl)trimethylstannane .....   | 94 |
| <b>Figure A.15.1:</b> <sup>1</sup> H-NMR spectrum of 5,8-dibromo-2,3-bis(4-((2-octyldodecyl)oxy)phenyl)quinoxaline .....  | 95 |
| <b>Figure A.15.2:</b> <sup>13</sup> C-NMR spectrum of 5,8-dibromo-2,3-bis(4-((2-octyldodecyl)oxy)phenyl)quinoxaline .....   | 96 |
| <b>Figure A.16.1:</b> <sup>1</sup> H-NMR spectrum of 5,8-bis(3,3-diundecyl-3,4-dihydro-2H-thieno[3,4-b][1,4]dioxepin-6-yl)-2,3-bis(4-(dodecyloxy)phenyl)quinoxaline ..... | 97 |

|  |    |
|--|----|
| <b>Figure A.16.2:</b> $^{13}\text{C}$ -NMR spectrum of 5,8-bis(3,3-diundecyl-3,4-dihydro-2H-thieno[3,4-b][1,4]dioxepin-6-yl)-2,3-bis(4-(dodecyloxy)phenyl)quinoxaline..... | 98 |
| <b>Figure A.17.1:</b> $^1\text{H}$ -NMR spectrum of 4,7-bis(3,3-didecyl-3,4-dihydro-2H-thieno[3,4-b][1,4]dioxepin-6-yl)benzo[c][1,2,5]oxadiazole FF.....                   | 99 |

## LIST OF ABBREVIATIONS

|                              |  |
|------------------------------|--|
| ACN                          | Acetonitrile                             |
| BDT                          | Benzo[1,2-b:4,5-b']dithiophene           |
| BHJ                          | Bulk Heterojunction Cell                 |
| BTA                          | Benzo[d][1,2,3]triazole                  |
| CHCl <sub>3</sub>            | Chloroform                               |
| CIE                          | Commission Internationale de l'Eclairage |
| CV                           | Cyclic Voltammetry                       |
| D-A                          | Donor-Acceptor                           |
| D-A-D                        | Donor-Acceptor-Donor                     |
| DCM                          | Dichloromethane                          |
| DMF                          | Dimethyl Formamide                       |
| DMSO                         | Dimethyl Sulfoxide                       |
| EDOT                         | 3,4-Ethylenedioxythiophene               |
| E <sub>g</sub>               | Band Gap                                 |
| E <sub>g</sub> <sup>ec</sup> | Electronic Band Gap                      |
| E <sub>g</sub> <sup>op</sup> | Optical Band Gap                         |
| EtOH                         | Ethanol                                  |
| GPC                          | Gel Permeation Chromatography            |
| HRMS                         | High Resolution Mass Spectrometer        |

|                    |   |
|--------------------|---|
| HOMO               | Highest Occupied Molecular Orbital              |
| ITO                | Indium Tin Oxide                                |
| I-V                | Current Density-Voltage                         |
| $J_{sc}$           | Short-Circuit Current Density                   |
| L, a, b            | Luminance, Hue, Saturation                      |
| $LiClO_4$          | Lithium Perchlorate                             |
| LUMO               | Lowest Unoccupied Molecular Orbital             |
| n-BuLi             | n-Butyl Lithium                                 |
| $NaClO_4$          | Sodium Perchlorate                              |
| NBS                | N-Bromosuccinimide                              |
| NHE                | Normal Hydrogen Electrode                       |
| NIR                | Near-Infrared                                   |
| NMR                | Nuclear Magnetic Resonance Spectrometer         |
| OSC                | Organic Solar Cell                              |
| $PC_{71}BM$        | [6,6]-Phenyl $C_{71}$ Butyric Acid Methyl Ester |
| PCE                | Power Conversion Efficiency                     |
| PSS                | Polystyrene Sulfonate                           |
| Pt                 | Platinum  |
| <i>p</i> -TSA      | <i>p</i> -Toluene Sulfonic Acid                 |
| TBAPF <sub>6</sub> | Tetrabutylammonium Hexafluorophosphate          |
| THF                | Tetrahydrofuran                                 |
| TLC                | Thin Layer Chromatography                       |
| TPD                | Thieno[3,4-c]pyrrole-4,6-dione                  |

VIS

Visible

$V_{oc}$

Open-Circuit Voltage

## CHAPTER 1

### INTRODUCTION

#### 1.1. Conjugated Polymers

A similar electrical and optical property has been demonstrated by the great number of polymers that are being used commercially in our daily lives such as polyethylene, polyvinyl chloride or poly(methyl methacrylate). They have no mobile charge carriers and their lowest electronic transitions are mostly observed in UV region of the spectrum. On the other hand, there exists a different class of polymers with uniquely different characteristics. These materials with conjugated double bonds along their main chain are semiconductors, or with strong doping even conductors. During recent decades conjugated polymers have attracted an enormous amount of interest among scientists owing to their processability with solution-based methods, ease in modification of their band gap with structural changes, their low cost, and their potential for realization of flexible devices. Polthiazyl was the first member of synthetic conjugated polymers (inorganic) and this black powder materials were found to be a superconductor at 2K [1]. It was Alan J. Heeger, Hideki Shirakawa and Alan G. MacDiarmid were the leading scientist who brought conjugated carbon-based polymers into the realm of electronics. They proved how a plastic can be a good conductor of electricity in its oxidized and reduced states. The accidental use of the great amount of Ziegler-Natta catalyst in the process of the synthesizing of polyacetylene from methane resulted in a metal-like silvery black film [1]. The outcome of this discovery was the extraordinarily high conductivity ( $10^3$  S/cm) upon doping with iodine vapor at room temperature Shirakawa *et. al.* later showed that the trans polyacetylene, the thermodynamically stable form, shows higher conductivity compared to cis form of the same material. [2].  $\pi$ -conjugation is the main necessity for a polymer to be conductive. The process of adding the electron deficient chemicals such as halogens is called doping. Through doping, the conductivity of the plastic can be increased up to  $10^9$  fold and can match the conductivity of metals.

What doping does is to provide free movement of electrons which results in conduction. The reward of discovery and development of conductive polymers for Heeger, Shirakawa and MacDiarmid was the Nobel Prize in chemistry in 2000. The shortcomings of polyacetylene which are low solubility and sensitivity to air and humidity led the scientists to the development of significantly more stable conducting polymers most based on heterocycles which capable of being used as active layers in variety of applications such as organic solar cells (OSCs), organic light emitting diodes (OLEDs), organic field effect transistors (OFETs), electrochromic devices (ECDs) and organic electrochemical transistors (OECTs). It was found that polymers of heterocyclic units such as thiophene, fluorene, pyrrole, aniline, and carbazole which are less sensitive to air and humidity compare to polyacetylene.

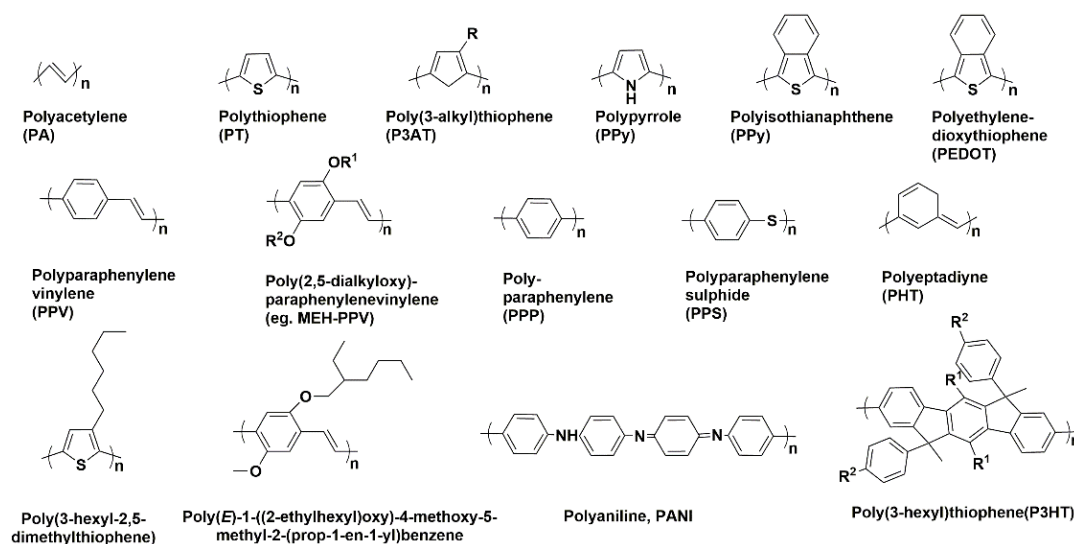


**Figure 1.1:** Structures of commonly known conjugated polymer systems

## 1.2. Conduction in Conjugated Polymers

### 1.2.1. Band Theory

The energy spacing between the valence band (VB) and conduction band (CB) is defined as the band gap. (HOMO) the highest occupied molecular orbital and (LUMO) the lowest unoccupied molecular orbital are also other definitions of the valence band and conduction band respectively. The characteristic of insulator,

semiconductors, and metals are explained by the band theory. Based on this theory, conducting polymers represent mostly semiconductor properties however conducting polymers with metallic conductivity are also known. Charge carriers are divided into holes (p-type) and electrons (n-type). In insulators since the band gap between two bands is large it causes no movement of charge carriers and also no conductivity as the result. The absence of band gap between empty conduction band and partially filled valence band in metals led the charge carriers to move easily between these two overlapped band and cause conductivity as result. With semiconductors, the small gap between filled valence band and empty conduction band gives the chance to electrons to move from valence to conduction band which results in conduction at ambient temperature. There are ways to calculate band gap, for instance, through the  $\pi$ - $\pi^*$  transition in the UV-Vis spectrum and when the polymer is both p and n dopable by measuring the oxidation and reduction onset values by using cyclic voltammetry.

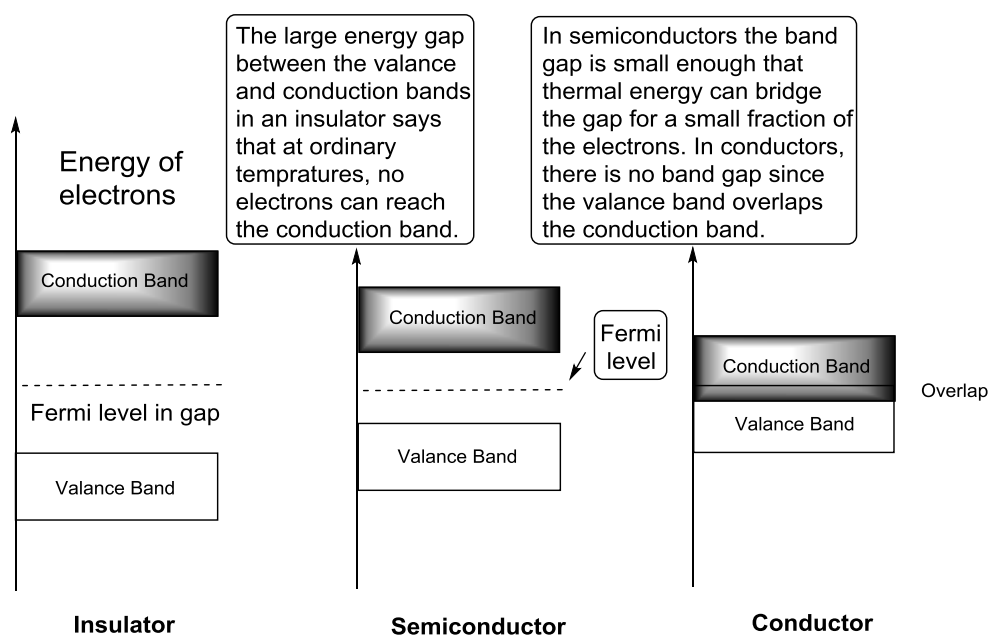


**Figure 1.2:** Band structures of materials

### 1.2.2. Conduction in Conjugated Polymers

Although there are several techniques available for preparation of conducting polymers such as photochemical, solid state and pyrolysis; the two broadly employed methods for synthesizing conductive polymers are the chemical (coupling chemistry and oxidative chemical polymerization) and electrochemical polymerizations [3]. The method of polymerization should be determined carefully towards synthesis of a polymer with desired set of properties such conductivity, processability and stability.

### 1.2.3. Solitons, Polarons, and Bipolarons

The term for a free radicalic structure in conjugated polymers with a degenerate ground state energy, like in polyacetylene, is a neutral soliton, but unlike polyacetylene, most conducting polymers do not possess degenerate ground states, therefore there is no indication for the formation of solitons. It is stated by Su *et. al.* that the structural defects in the backbone are the results of the formation of charged radicals in the polymerization process [4].

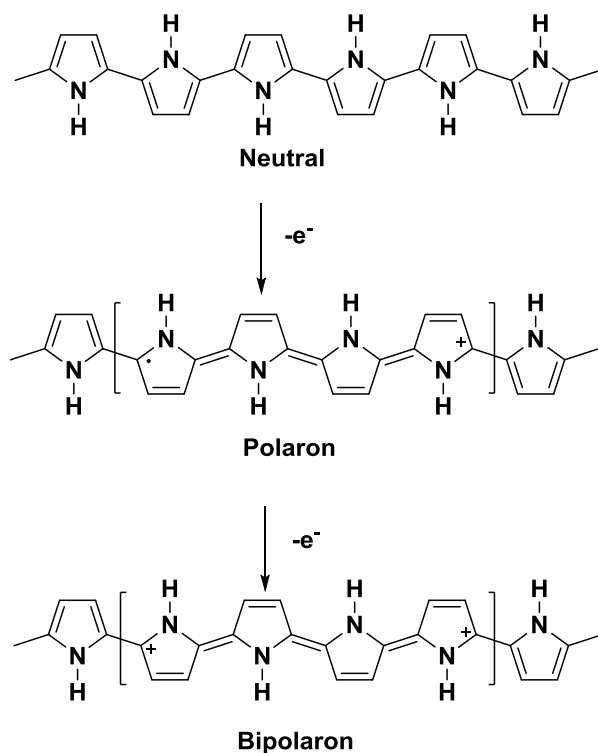


**Figure 1.3:** Charge carriers [118]

When the polymer oxidized the energy of the orbital will be raised by removing electrons. ‘Polaron’ is the radical resulted by the removal of one electron. Polarons have both spin and charge [5, 6]. Through further exothermic chain oxidation reactions, dications namely known as bipolarons will be formed [7]. In these reactions, it is also possible for two polarons to be formed; however, due to the electronic repulsion caused by two charges, bipolarons are thermodynamically more stable.

#### 1.2.4. Doping

Doping is the introduction of charge carriers to the polymer backbone through a redox process. p-Doping is the removal of an electron from the polymer chain whereas n-doping is the addition of an electron to the polymer chain. Since both neutral and heavily doped states are diamagnetic in nature, there is no net spin defined for them. Most heavily doped materials conduct electricity [6].

Forming interbands between conduction and valence bands is how doping lead conjugated polymers to become conductors. All the optical, magnetic, and mechanical properties of the polymers can be completely changed because of the formation of polaronic and bipolaronic bands [3]. The fact that anions are relatively more sensitive to oxygen and air than cations, defines p-type doped conjugated systems are more common than n-type ones.

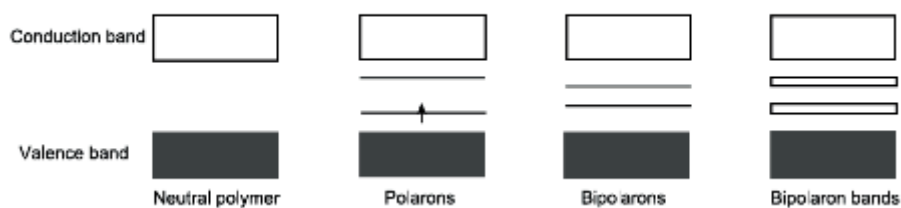


**Figure 1.4:** Band Structure of the polymer with bipolaron states

### **1.2.5. What Affects the Band Gap?**

The band gap of conjugated polymers can be controlled to achieve desired properties for a target application mainly by devising synthetic strategies for the design of the conducting polymers. So many properties of materials, such as absorption wavelength, conductivity, and electronic properties are determined by the band gap. There are variety of approaches for band gap control in conducting polymers such as inducing planarity, reducing bond length alternation, resonance effects, interchain effects and donor-acceptor approach.

### **1.2.6. Resonance Energy**

The most proper basic structures because of their stability and structural flexibility are aromatic systems to be used in synthesizing low band gap  $\pi$ -conjugated polymers. One of the most important facts that play an important role in reducing the band gap in aromatic conjugated systems is the double bond introduction to the backbone. As an example, in the case of paraphenylenevinylene (PPV), steric interactions between adjacent phenyl rings can be reduced by introduction of ethylene linkages and provide a planar structure for the conjugated system. Besides, since the rotational freedom around the single bonds reduces by the double bonds, (for instance in thiophene ring), the result will be a planar geometry Moreover, band gap increases with increasing the aromaticity, due to an increase in the rigidity of the system, as a consequence, double bonds in the  $\pi$ -conjugated system reduces the band gap by decreasing total aromaticity. The double bond interaction in paraphenylenevinylene causes reducing of the band gap from 3.20 eV to 2.60 eV [8].

### **1.2.7. Electron-Withdrawing Groups**

The HOMO and LUMO energy levels of a conjugated polymers can be altered by introduction of electron-releasing and electron-accepting functional groups. For example, when nitro or cyano as the electron withdrawing groups are introduced in the 3-position of thiophene, oxidation potential increases compared to that of thiophene. "A cyano group introduction to the vinylene linkage of dithienylethylene was shown to lead to band gap reduction for the corresponding polymers" as Roncali's group stated [9]. High lying LUMO levels cause an unstable neutral state

of the system, the effect of electron-withdrawing groups such as cyano is to decrease the LUMO level and leads to stabilization of neutral state system [10]. Theoretical studies offer that the increase in the quinoid character of the ground system can lower the band gap, however, the drawback of this approach is that generally a major increase is the oxidation potential which results in difficulties during electrochemical or oxidative chemical polymerization methods.

### 1.2.8. Electron-donating Groups

The HOMO level increases by introducing the electron-donor groups in a conjugated system which results in a reduced band gap. Studies show that the inductive effect of alkyl groups can cause a decrease in oxidation potential of the materials [11]. In case of linear alkyl chains, considering the length of the chain the increase in lipophilic interactions between polymer chains can reduce the band gap [12, 13]. The HOMO level increases effectively by introducing the strong electron donors such as alkoxy groups. The formation of a highly strong donor in case of thiophene is the result of oxygen attached to thiophene with an ethylene bridge as electron releasing groups. The mentioned group can easily be polymerized through chemical or electrochemical methods yielding a highly-conductive polymer such shows significantly lower band gap compared to polythiophene [14, 15].

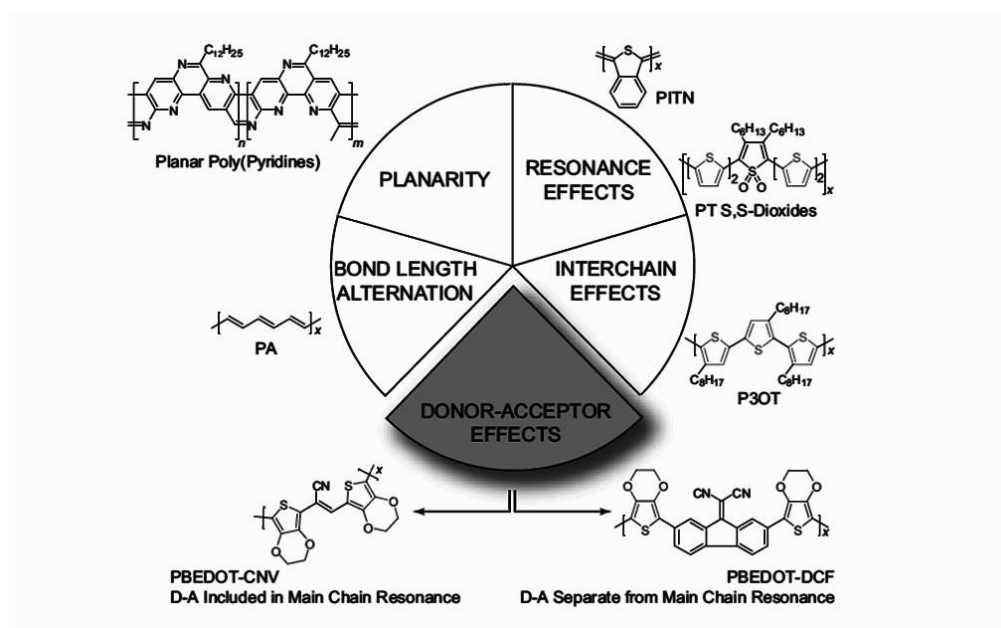


**Figure 1.5:** Modification of band gap

### 1.2.9. Donor Acceptor Approach

“Electron rich donor unit is combined with electron poor acceptor unit in close conjugation” is known as the D-A approach. Band gap reduction is the result of donor and acceptor groups with regular alternation causes valence and conduction band broadening [16]. With this consideration, “the highest occupied molecular orbital (HOMO) of the donor unit contributes to HOMO level of the polymer whereas the lowest unoccupied molecular orbital (LUMO) of the acceptor group contributes to the LUMO level of the polymer” [17].

### 1.3. Stable N-Type Conjugated Polymers

Conjugated polymers can be doped in a p-type and n-type manner. It has been shown that some heavily p-type doped polymers such polypyrrole and polyaniline can be very stable under ambient conditions. Conjugated polymers that shows high stability in their undoped or slightly p-doped states, such as variety of polythiophene are also demonstrated. However, air-stable and soluble n-type (electron-transporting) conjugated polymers are still quite rare. The difficulty to achieve such a polymer is related to the well-documented instability of carbon-based anions. Carbanions are readily oxidized in contact with air or water [18, 19].

The reason of rare nature of n-type semiconductors is due to external effect; the adversity of keeping out oxygen and moisture while fabricating and testing was the most reason for the lack of n-type organic semiconductors. High electron density along the  $\pi$ -conjugated backbones in unsubstituted form which results in LUMO energy levels in the range of  $-2.0$  eV to  $-3.5$  eV relative to the vacuum is the distinctive attribute of organic semiconductors. In such situation, a great energy barrier is encountered by the electron for injection from standard metal electrodes such as gold which shows a high work function around  $4.3$ – $5.5$  eV.

Reducing the electron density in the  $\pi$ -conjugated backbone in the neutral state is the simple rule for prospering n-type organic semiconductors; with this regard, introducing functional groups such as fluorides [20, 21, 22], nitriles [23, 24], amides and imides [25, 26, 27], has been broadly studied. The functionality of this approach is to obtain low-lying LUMO and HOMO energy levels to be able to effectively

inject electrons and, stabilize the molecules with low reorganization energy. The LUMO energy level lower than  $-3$  eV is the energy level needed for the efficient electron injection. Considering the fact that anionic form is less sensitive to air which results in higher stability, the preferred LUMO energy level for an n-type material is around  $-4$  eV. The exact same approach with regard to molecules and design has been applied to synthesize electron transporting polymers. Most high-performance-type polymer semiconductors have LUMO energy levels in the range between  $-3.8$  eV and  $-4.2$  eV [28, 29, 30, 31, 32].

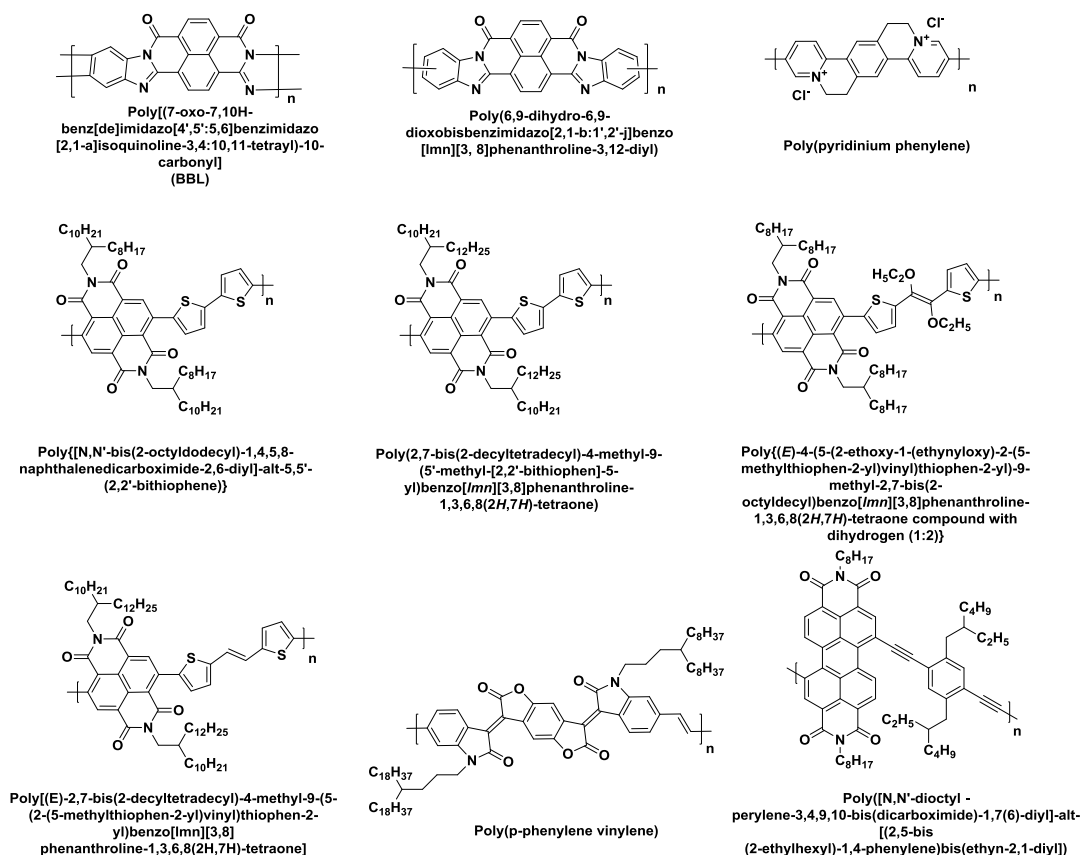


**Figure 1.6:** Representative electron-transporting polymer semiconductors [33]

#### 1.4. Conducting Polymer Characterization

Characterization of conducting polymers can be conducted through a variety of methods and the most commonly utilized ones are conductivity and mobility measurements, cyclic voltammetry, spectroelectrochemistry. Structural characterizations can be performed by NMR spectroscopy, IR spectroscopy and gel

permeation chromatography. The detection of the redox properties of polymers is mainly studied via cyclic voltammetry. In spectroelectrochemistry, optical properties of the materials are evaluated as a function of applied potential and a variety of valuable information such as the band gap ( $E_g$ ), absorption maxima ( $\lambda_{max}$ ), polaron and bipolaron characteristics can be deduced. In kinetic studies, stepping repeated potential between the neutral and oxidized states reveals the percent transmittance changes and the time required for the switching these states. The number average molecular weight, weight average molecular weight, and polydispersity index of the polymer are the properties determined by gel permeation chromatography. Polymer formation information can also be studied by  $^1H$  NMR spectra. Also, the idea of the copolymer ratio for random copolymers can be provided by  $^1H$  NMR spectroscopy.

#### **1.4.1. Chromism**

Chromism is the reversible color change of materials upon external stimulus. Different types of the chromism includes thermochromism, piezochromism, solvatochromism, halochromism, and electrochromism.

#### **1.4.2. Electrochromism**

Electrochromism can be broadly defined as the reversible optical changes occur in a polymer film upon applied external potential. The color change can occur between two colored states or one colored and one highly transmissive state. More than two colors can also be observed which is named as multichromism [34]. Electrochromism was initially observed in thin films of  $WO_3$  and  $MoO_3$  in late sixties [35]. The potential of the electrochromic materials to be used in optical devices, not only made them so popular but also a new gate to the development of new materials. Metal oxides, viologens, metal hexacyanometallates, metal coordination complexes, and conjugated conducting polymers are the different classes for electrochromic materials [36]. The reason that made the conducting polymers a good choice for the construction of electrochromic devices is the fact that their optical properties can be easily tuned, they are low cost, flexible devices can be generated and polymers generally have good UV stability and reasonable operation temperature range. The important required parameters for electrochromic devices made from the polymers

are high coloration efficiency, good stability, high optical contrast, optical memory and short response time. The most important fact to meet all these parameters at the same time is the molecular design of these materials. Among variety of possible application areas, car rear view mirrors, protective eyewear, and smart windows are the ones that utilization of electrochromic devices are commonly envisioned [37, 38].

### 1.4.2.1. Electrochromic Material Types

#### 1.4.2.1.1. Viologens (1,1'-disubstituted-4,4'-bipyridylium salts)

1,1'-Disubstituted-4,4'-bipyridylium salts are synthesized by alkylation of 4,4'-bipyridyls. Viologens are widely used in the form of methyl viologen. In viologens upon reduction radical cations form and these species are intensely colored due to intramolecular electronic transition observed in the delocalized positive charge. Three most common viologen redox states are shown in Figure 1.7. The most stable state belongs to dication which is colorless [34]. Aryl substitution on the nitrogens generally results in a green color for the radical cation whereas use of alkyl groups incite a violet-blue color.

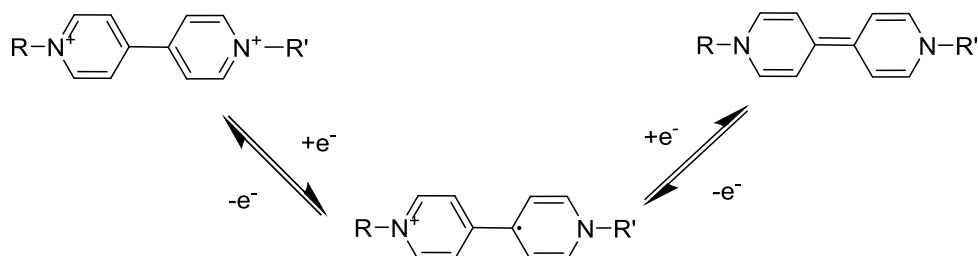


**Figure 1.7:** Viologen redox states

#### 1.4.2.1.2. Prussian Blue System

Prussian Blue was discovered as the first synthetic pigment in the very early decades of 18<sup>th</sup> century. Compare to ultramarine or other blue pigments at that time, ferric hexacyanoferrate(II) or Prussian Blue was more available, less expensive and easier to be produced as compound; besides, apart from alkaline medias where Prussian Blue was unstable this new pigment was known as quite stable pigment. How Prussian Blue was discovered is ambiguous and no reliable research has been done about it, but today, Prussian Blue not only is used as a pigment, but also it is

used in other fields of applications such as electrochromic and poison antidotes sensors. [39].

#### **1.4.2.1.3. Metal Oxides**

Cerium oxide, chromium oxide, cobalt oxide, iridium oxide, iron oxide, manganese oxide, molybdenum oxide, nickel oxide, palladium oxide, ruthenium oxide, tungsten oxide and vanadium oxide are the metal oxides which represent electrochromic properties. [40]. the oxides of tungsten, molybdenum, nickel and iridium has shown the most intense color change among all metal oxides used as metallic electrochromic. A severe electronic absorption band upon reduction is revealed by the transparent thin films of those metal oxides. Tungsten trioxide,  $WO_3$ , with a high band gap is known as the most popular electrochromic material. In a study done by Berzelius in 1815 it was shown that through the reduction of pure tungsten trioxide under hydrogen the color will change [41]. A similar experiment was also done by Wöhler. In 1824, he used sodium to show the color change of  $WO_3$  a through reduction [42]. Tungsten trioxide is colorless or presenting a very pale yellow in its oxidized form, it has the oxidized state of six (WVI) in contrast with the fact that a deep blue color is formed by WV sites upon electrochemical reduction. As more examples of electrochromic materials Molybdenum and vanadium oxides can be mentioned [43, 44].

#### **1.5. Conjugated Conducting Polymers**

Some common examples from electrochemically active conducting polymers we polythiophenes, polyanilines, polypyrroles and polycarbazoles. These materials can be prepared by both electrochemical and chemical methods [45]. The possibility of tuning spectral properties of materials has made conducting polymers favorable for electrochromic devices. Delocalized  $\pi$  electron systems and positive charge carriers balanced with anions are observed in p-doped states. n-Doped states are not as stable as p-doped ones and their applications are rare [36]. Reduction of the polymer electrochemically leads to electrically insulator materials by the virtue of the removal of conjugation [46]. The electrochromic properties of the molecule are determined

by the band gap in the neutral state. Almost all of the polymers are colored in their undoped form. If the band gap of materials is large (higher than 3 eV) no color in the undoped form will be revealed, but in their doped form, they absorb visible region of the light. Considering the fact that materials with moderate band gaps (1.7-1.9 eV) absorb in their neutral form, whereas absorption is really weak in the visible region and free charge carriers are shifted to near IR region in the doped form. Materials with smaller band gaps can show a variety of different colors. The certain aromatic molecules which have initially been introduced at the beginning of this paragraph are commonly benefited from an evenly distributed electron density, which makes them resonance-stabilized from this electron delocalization. Five membered rings with one heteroatom substitutions are one class of these molecules. For example, thiophene (with a sulfur substitution), pyrrole (nitrogen substitution) and furan (oxygen substitution). The other class based on six-membered rings fused with five-membered ones (such as carbazole, azulene, and indole), with various substitutions. Aniline is also another member of this class. Chemical or electrochemical oxidation of these substances produces electroactive conjugated conducting polymers.

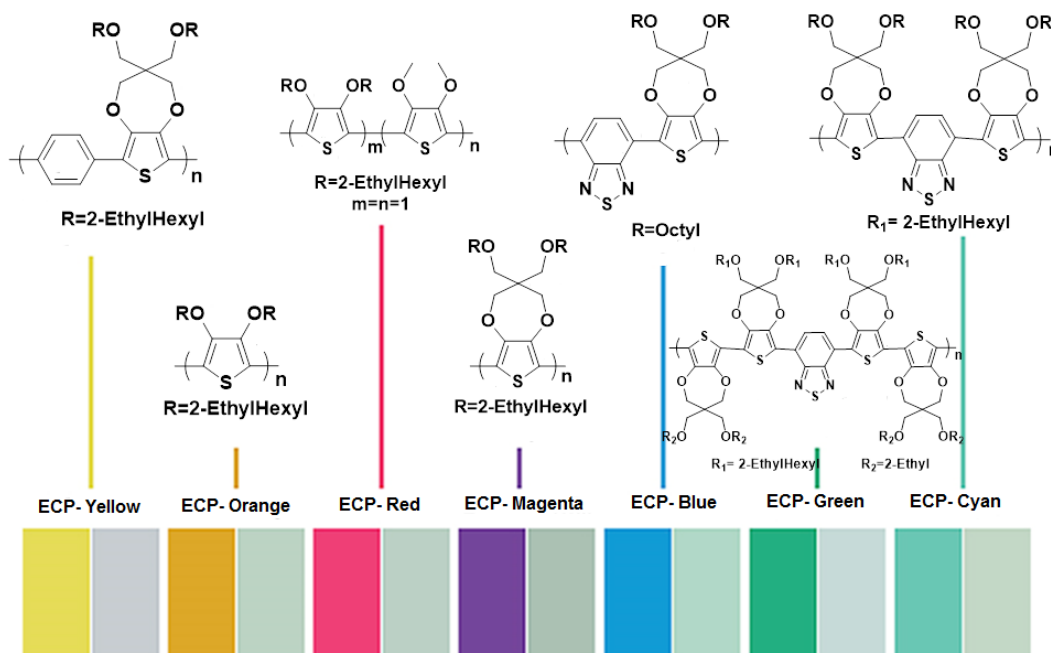


**Figure 1.8:** Illustrative example of electroactive conjugated conducting polymers [47]

## 1.6. Utilized Color Models for Simple Electrochromic Display Devices

One of the forefront topics in material researches these days is non-emissive display technologies utilizing electrochromic materials. Inexpensive printing techniques, fabrication of the large area devices and having the ability to be viewed in a wide variety of lighting conditions are the attractive benefits of electrochromic devices. Materials that can exhibit three primary colors are utilized in electrochromic displays. These materials can be employed to create full-colour displays through the control of the contribution of each primary color. Towards realization of a simple electrochromics based display device such as an e-paper, polymer that shows intense RGB and/or CMYK colors in their reduced state that switches to a highly transmissive oxidized state are required [48].

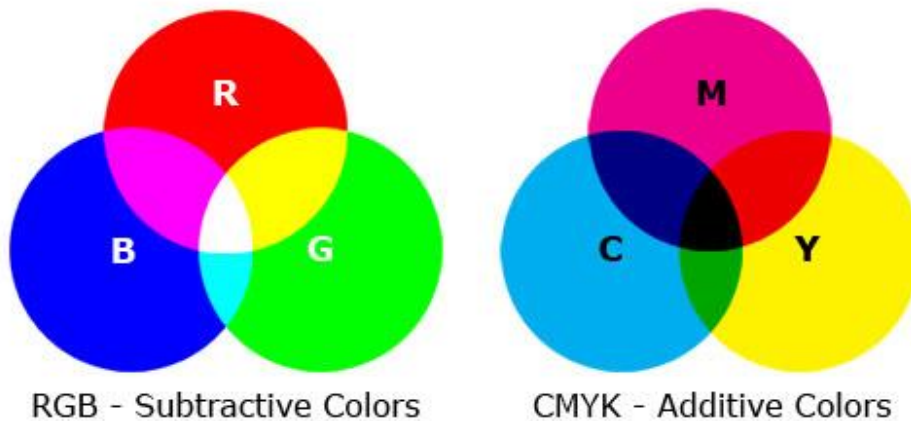


**Figure 1.9:** sRGB and CMYK color models [48]

### 1.6.1. Standard Red-Green-Blue (sRGB) Color Space

The trichromatic model of RGB is based on the additive primary colors of red (R), green (G) and blue (B) [49,50]. RGB model is mainly used in display of images in electronic systems, because the RGB model correlate with most closely to the sensors of colored light. To come up with a color formation in the RGB model; the three components of the light must be superimposed and emit from a black screen or being reflected from a white screen. Throughout mixing a combination of different components with different intensities the complete color scheme can be achieved. The color black, as the darkest color, would be the result of the zero intensity and in

full intensity, the color white will be achieved. The reason that the RGB color model is also known as the additive color model is that final colored is formed by the three components adding together which means their light spectra add wavelength to wavelength [51, 52].

### 1.6.1.1. Blue to Transmissive Electrochromic Polymers

PEDOT has a good electrochromic properties and chemical stability, which made it one of the best candidates to be used in structure of blue to transmissive switching polymers. This polymer shown to have intense blue color in the neutral state that switches to a highly transmissive light blue oxidized state [53]. A great number of blue to transmissive electrochromic polymers with enhanced electrochromic properties were realized using EDOT or EDOT like molecules (molecules number 1-4), were studied during recent years [54, 55, 56, 57, 58].

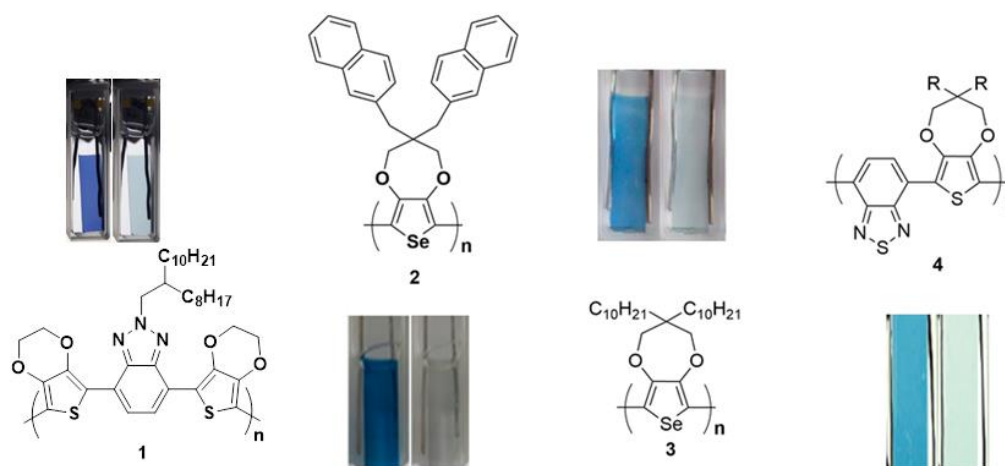


**Figure 1.10:** Literature examples of blue to transmissive switching polymers [54-57]

### 1.6.1.2. Green to Transmissive Electrochromic Polymers

Studies performed in conducting polymers research, convince the fact that a great number of electrochromic polymers reflecting red and blue color in their neutral states, whereas polymers reflecting green color have not been broadly studied. The reason behind this fact is comprehensible, to reflect red or blue color in reduced state, the materials have to absorb at only one dominant wavelength, with contrast, to show

green color, at least two simultaneous absorption bands in the red and blue regions should exist of the visible spectrum and these bands should be controlled with the same applied potential. when in 2007, Toppare group could synthesize the first green to transmissive electrochromic polymer, only two studies have been reported related to polymers reflecting green color [59, 60]. This work was a conception for other studies on green to transmissive electrochromic polymers [61, 62, 63]. Some of the green to transmissive electrochromic polymers (Number 5-9) are shown in Figure 1.11.

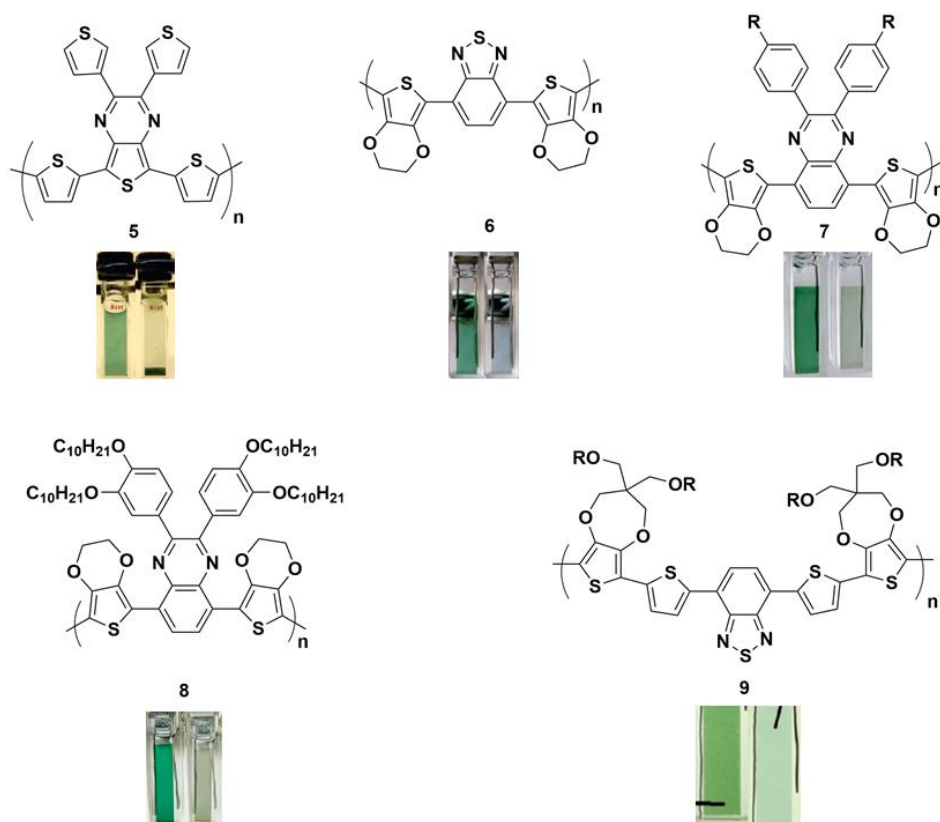


**Figure 1.11:** Literature examples of green electrochromic polymers [59-63]

### 1.6.1.3. Red to Transmissive Electrochromic Polymers

The literature shows few numbers of random copolymers with high optical contrast and good stability with regards to red to transmissive electrochromic polymers in recent years [64, 65, 66]. The downside with these polymers is that two or three monomer units are employed from these polymers by oxidative polymerization,

which might cause reproducibility issue, besides, another disadvantage was switching time. These polymers had switching times of couples of seconds, which later on was studied and improved to tens of a second in a study by Günbas group in early 2016 [67]. Figure 1.12 shows some of these polymers listed from number 10-12.

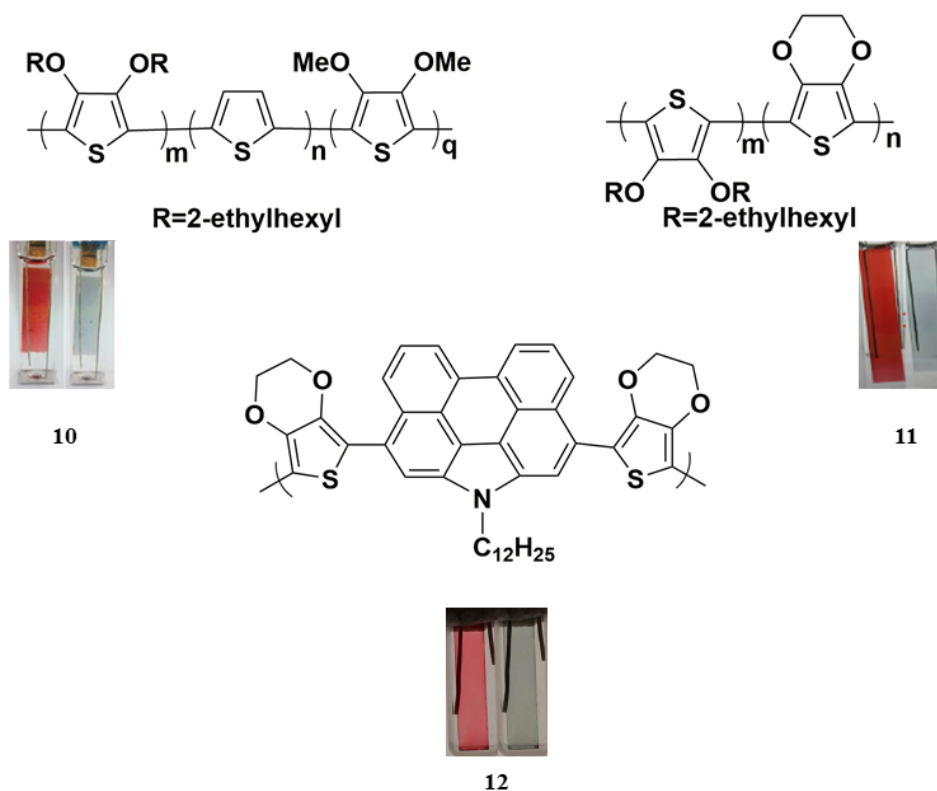


**Figure 1.12:** Literature examples of red to transmissive electrochromic copolymers [64-67]

### 1.6.2. Multicolor Electrochromic Polymers: Color Control

With regard to the electrochromic materials, what makes conjugated polymers advantageous is the fact that their electrochromic properties can be tailored through modification of the polymer structure. The accessible color states in both the doped and neutral forms of the polymer can be varied just via band gap control. The band gap of conjugated polymers is possible to be tuned by countless synthetic strategies [68]. Practically, the tuning of the band gap is achievable basically via the modification of the main chain and pendant group. The simplest method is

substitution. In substitution the band gap is affected by induced steric or electronic effects [69, 70].

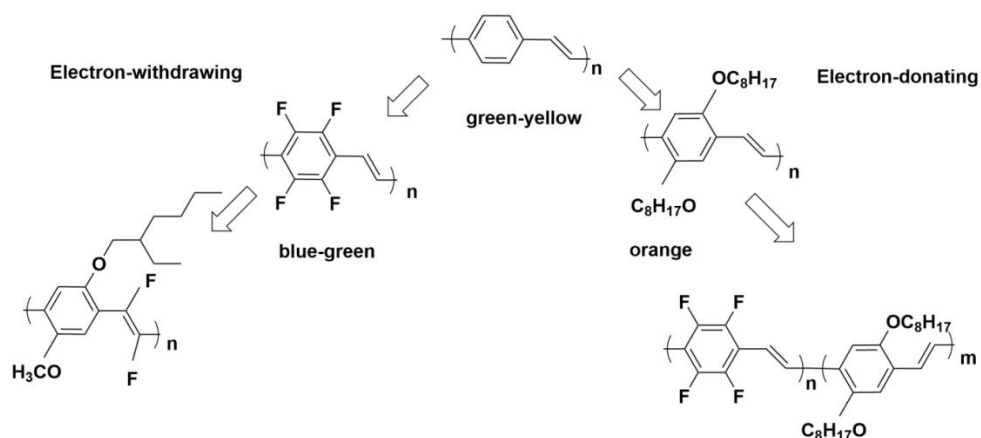


**Figure 1.13:** Tuning color by substituents

Interesting combination of the properties can be contributed by modification of main chain; this would be possible through copolymerization of distinguished monomers or homopolymerization of comonomers.

Conjugated polymers employed in blends, laminates, or composites to have an effect on the ultimate color exhibited by the material.

EDOT and EDOT containing conjugated polymers have been used as the platforms to make a broad range of variable-gap electrochromic polymers. Structural modification performed on the monomer and copolymerization approaches have been demonstrated to be efficient. Few more examples are mentioned from the literature in the following part to explain further about color control in conjugated polymers.

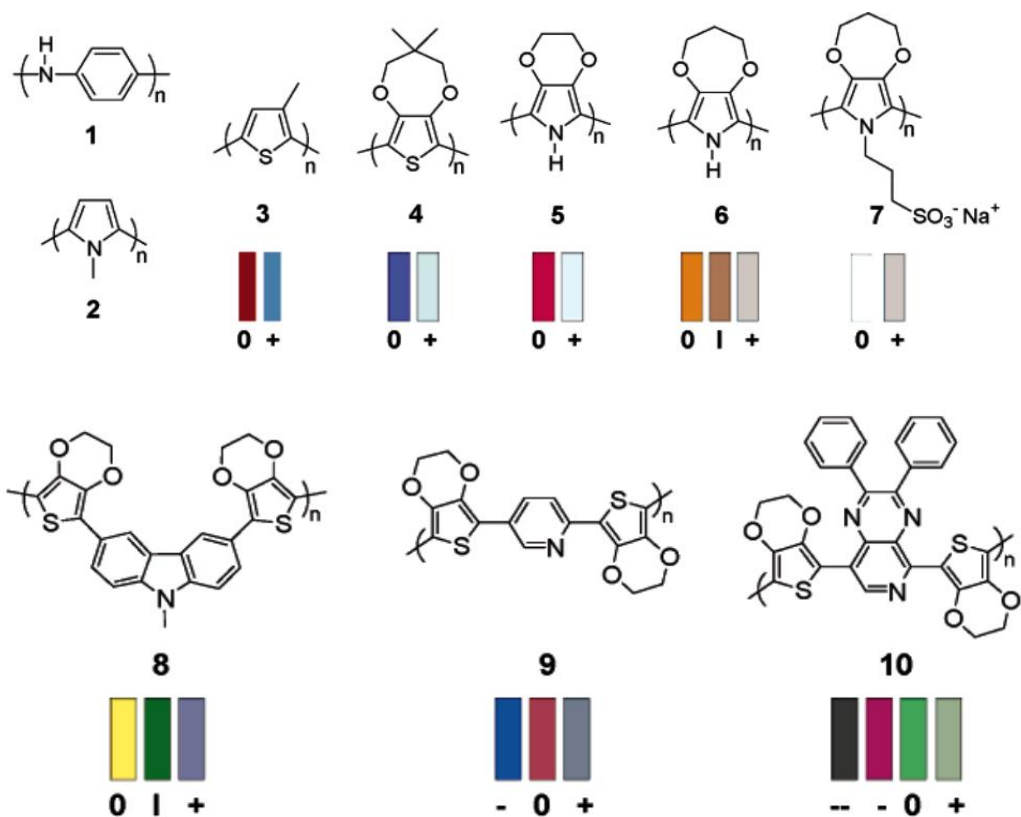


**Figure 1.14:** Illustrative example of electrochromic polymers. “Color swatches are representations of thin films based on measured CIE 1931 Yxy color coordinates. Key: 0 = neutral; I = intermediate; + = oxidized; - and -- = reduced”. [81]

Electropolymerization has been the centerpiece of electrochromic polymer research due to ease of preparation. Thanks to electropolymerization, a great number of various structurally diverse electrochromic polymers have been produced. In figure 1.14 and illustrative example of 10 polymers is shown that how multicolor electrochromic polymers are produced through tuning the band gap by structural modification of the monomer repeat unit.

Depending on the oxidation state of the polymer film, PANI (1) presents multiple colored forms include leucoemeraldine (bright yellow), emeraldine (green), and pernigraniline (dark blue). [71,72,73] After poly(N-methylpyrrole) (PN-MePy) and poly(3-methylthiophene) (P<sub>3</sub>MeTh) (2, 3) were found to be stable and electrochromic, researchers became attentive to develop derivatized pyrrole- and thiophene-based polymers with improved electrochromic properties.

The driving force behind developing polymers 4-10 was to signify that through making quite minimal change in the structures, various colors can be achieved in doped and neutral forms. PProDOT-Me<sub>2</sub> (4) is a good example from the PXDOT family with minimal difference in color compared to PEDOT. These two are cathodically colouring materials and they are strongly colored in their neutral states, and they show a high level of transmissivity upon their oxidation [74].

PEDOP (5) (poly(3,4-ethylenedioxyppyrole)) is a member of the of PXDOP family [75, 76]. In this example, the electron-rich pyrrole results in increase in material bandgap to 2.0 eV and as a result, red color was observed in the neutral state and upon oxidation a transmissive blue state was achieved.

PProDOP (6) (poly(3,4-propylenedioxyppyrole)) shows how a drastic change in the accessible color states can be the result of a quite minimal modification in the structure of the monomer, relative to the PEDOP. Here, an orange neutral state was observed in PProDOP with a band gap of 2.2 eV, an intermediate brown state, and a grey/blue oxidized state.

N-substitution modification in the repeat unit results in N-PrS-PProDOP (7) (poly(N-sulfonatopropoxy-ProDOP)). A drastic increase in the band gap ( $\geq 3.0$  eV) is the result of unfavorable steric interactions between polymer repeat units based on the bulky sulfonatopropoxy. As an anodically coloring polymer it was observed that this polymer shows changes in color from a completely transmissive colorless state in its neutral form to a light grey color in its oxidized state [77].

PBEDOT-NMeCz (8) (poly(bis-EDOT-N-methylcarbazole)) [78] is a three-color electrochromic polymer. PBEDOT-NMeCz is formed from a multiring monomer (comonomer). The polymer is a higher gap material ( $E_g = 2.5$  eV) in the neutral form and the reason is that the conjugation is limited by the 3,6-linked incorporation of the carbazole into the main chain. Two additional color states have been observed upon oxidative doping, as a result of two distinct redox processes. At intermediate potentials the material reveals the color of green and in fully oxidized state the color of blue was observed.

Other examples of multichromic polymers are PBEDOT-Pyr (9) and PBEDOT-PyrPyr (10) [79, 80]. In their case, the donor-acceptor conjugated backbone resulted in materials with low band gaps and both materials were shown to be both p- and n-type dopable. The band gap for PBEDOT-Pyr was observed at 1.9 eV since the electron withdrawing capacity of pyridine as an acceptor is weak. The polymer shows three colors as a result of three distinct redox states. For PBEDOT-PyrPyr, two n-doped states, a neutral state and a p-doped state are the result of the significantly lower bandgap polymer (1.2 eV) due to pyridopyrazine unit serving as a stronger acceptor compared to pyridine [81].

## **1.7. Polymerization Methods**

The main polymerization techniques are listed in the following:

- ❖ electrochemical polymerization;
- ❖ photochemical polymerization;
- ❖ metathesis polymerization;
- ❖ solid-state polymerization;
- ❖ chemical polymerization;
- ❖ inclusion polymerization;
- ❖ plasma polymerization [82]

Among all the mentioned techniques, electrochemical and chemical polymerization are the most favorable methods both in academia and industry [83].

### **1.7.1. Electropolymerization**

To synthesize a conjugated polymer electrochemically a supporting electrolyte in an inert organic solvent is needed. Irreversible oxidation and irreversible reduction are respectively proceeded by anodic and cathodic polymerization. Having a tendency for oxidation, anodic polymerization is used to synthesize homopolymers of electron rich units such as pyrrole [7]. One of the advantages of the electropolymerization is that there is no requirement for further purification. In electropolymerization the properties of the polymer are severely affected by the concentration of monomer,

solvent and electrolyte types, and electrodes. Other advantageous of electropolymerization can also be mentioned as morphology, conductivity upon applied potential, ease of production of an electrochemically active conductive polymer film and control of film thickness, scan rate and time [84]. The anodes can be used in electropolymerization can be listed as platinum, gold, glassy carbon, and indium–tin oxide (ITO) coated glass. Electropolymerization is carried out potentiostatically or galvanostatically. Potentiostatic (constant potential) or galvanostatic (constant current) methods are the two ways for the electropolymerization to be achieved. Since these techniques are easier to describe quantitatively, they have been broadly utilized to investigate the nucleation mechanism and the macroscopic growth. Potentiodynamic techniques such as cyclic voltammetry correlate with a repetitive triangular potential waveform applied at the surface of the electrode. The last method has been chiefly used to acquire qualitative data about the redox processes engaged in the early stages of the polymerization reaction, and to examine the electrochemical behavior of the polymer film after electrodeposition. [85]. An appropriate solvent will be chosen and the monomer is dissolved in it. Care must have taken to choose the solvent and electrolyte; solvent and electrolyte should be stable at the oxidation potential of the monomer. The solvents of choice for electropolymerization are acetonitrile and propylene carbonate due to their high relative dielectric permittivity and large potential range. After the monomer initially oxidized the radical cation will be formed. Then, through the reaction of radical cation with other monomers present in solution a neutral dimer will be formed; this happens by losing of another electron and two protons. With regard to form oligomers, the oxidized radical cations react with monomers until the polymer is formed [86, 87]. At the same time, the polymer is also doped while it is synthesized electrochemically. Because of extended conjugation in the system the oxidation potential of the polymer is lower than that of the monomers.

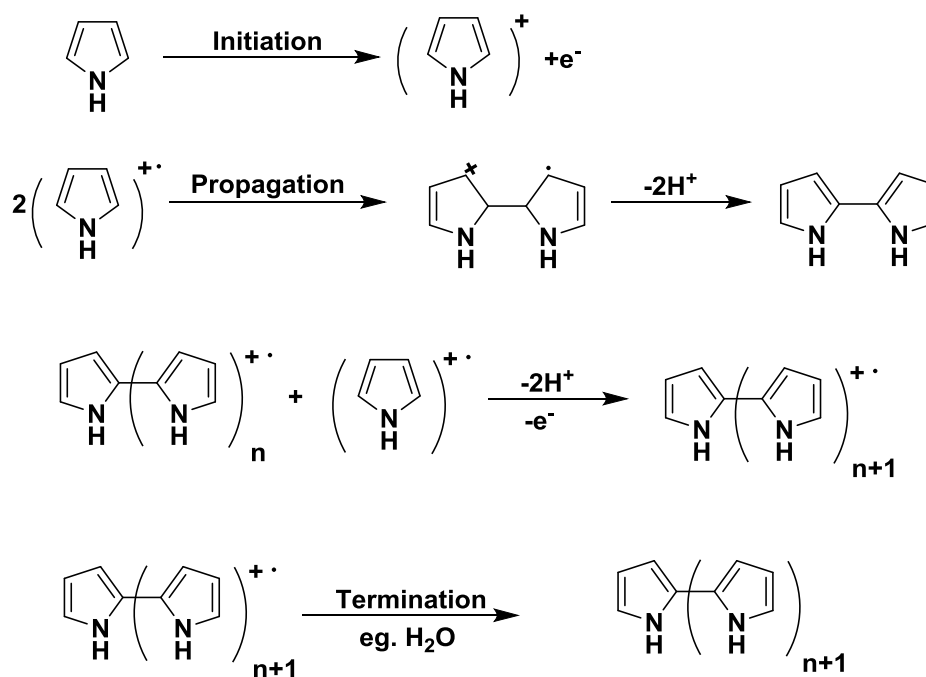


**Figure 1.15:** Electropolymerization mechanism

### 1.7.2. Oxidative Chemical Polymerization

In chemical oxidation polymerization, Lewis acid catalysts like  $\text{MoCl}_5$ ,  $\text{FeCl}_3$ ,  $\text{RuCl}_3$  react with heterocyclic compounds to provide high molecular weight polymers with relatively high conductivity. The solvents are generally anhydrous chloroform or dioxane. The polymers synthesized through chemical polymerization are alike with electrochemically synthesized polymers in their properties. By oxidative cationic polymerization, polymers of furan, thiophene, pyrrole or alkyl substituted thiophene can be prepared [88].

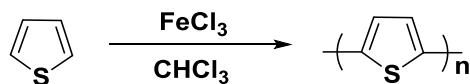


**Figure 1.16:** Oxidative chemical polymerization.

#### 1.7.2.1. Suzuki-Miyaura Coupling

Reactions of organic halides with organometallics through the formation of C-C bonds in the presence of transition metal catalysts are known as Suzuki-Miyaura Coupling [3, 89].

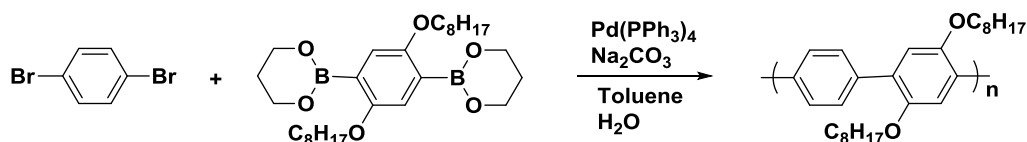


**Figure 1.17:** Suzuki coupling [90]

### 1.7.2.2. Stille Coupling

Stille coupling is known as one of the most efficient C-C bond forming reactions. In Stille coupling, two distinct monomers, stannanes and halides are utilized to synthesize alternating and random copolymers [91].

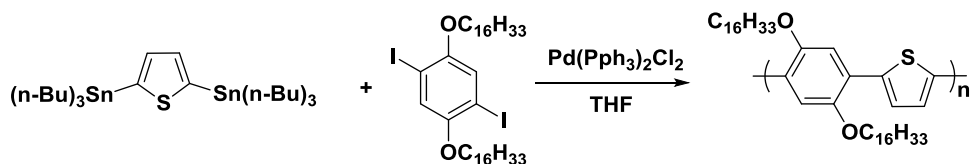


**Figure 1.18:** Stille coupling [92]

### 1.7.2.3. Yamamoto Coupling

In this type polycondensation reaction, the coupling of the organometallic C-C is promoted by NiCl<sub>2</sub>/bpy/Mg/DMF system. NiCl<sub>2</sub>, 2,2'-bipyridine (bpy), and Mg are mixed in DMF. Mg in this reaction has the duty of reducing agent for [Ni<sup>II</sup>Lm] to form [Ni<sup>0</sup>Lm]; another metal which can be used as reducing metal is Zinc to generate [Ni<sup>0</sup>Lm] from [Ni<sup>II</sup>Lm] for basic C-C coupling and dehalogenative polycondensation. The reaction generally carried out in N,N-dimethylacetamide (DMAc) and DMF as solvents. For this type of polycondensation, other offers can be NiBr<sub>2</sub>, PPh<sub>3</sub>, and bipyridine [93].

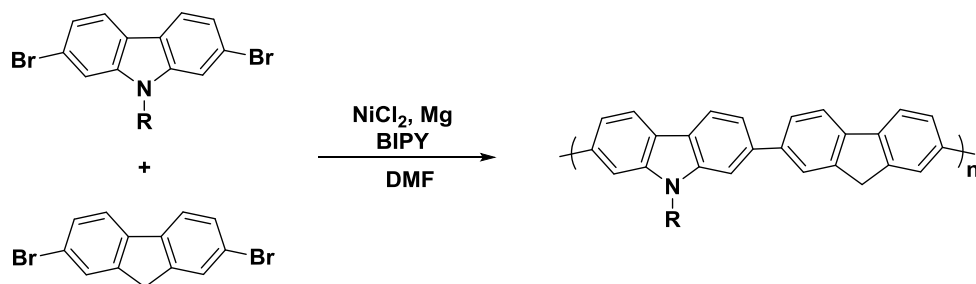


**Figure 1.19:** Yamamoto coupling [93]

#### 1.7.2.4. Knoevenagel Condensation

The C-C bond formation between carbonyl compounds and active methylene species is known as Knoevenagel condensation. In this condensation reaction the products can be formed by using heterogeneous catalysis producing a high yield. The catalysts of Knoevenagel condensation are alkali metal hydroxides or organic bases like primary, secondary and tertiary amines [94, 95].

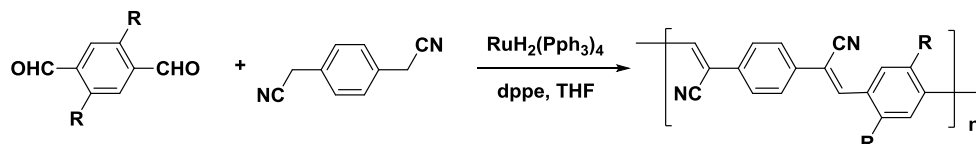


Figure 1.20: Knoevenagel condensation [96]

#### 1.7.2.5. Tamao-Kumada-Corriu Coupling

Tamao-Kumada-Corriu coupling represents another class of polycondensation reaction. In this type of reactions coupling of either alkyl or aryl Grignard reagent is achieved with halogenated aryl or vinyl species. The catalysts of this reaction can be nickel or palladium catalysis [97, 98, 99, 100].

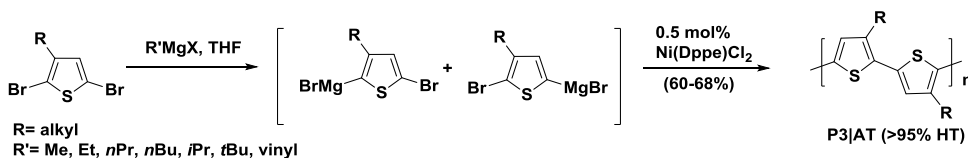
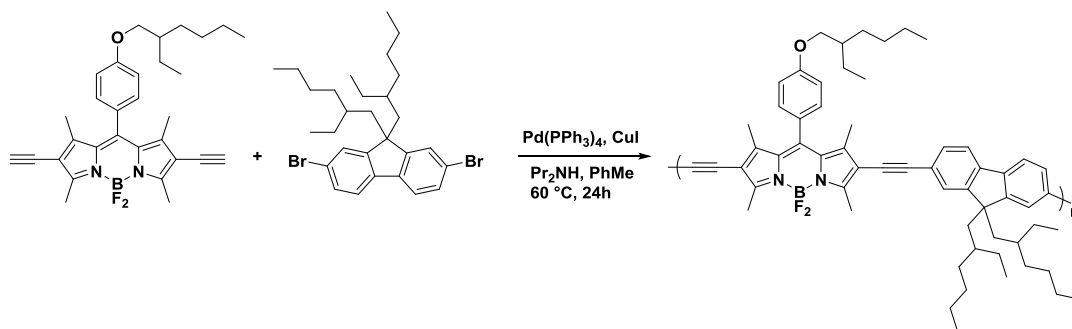


Figure 1.21: Regioregular HT-P3ATs prepared using Ni-catalyzed Kumada conditions: dppp = 1,2-bis(diphenylphosphino)propane. [101]

#### 1.7.2.6. Sonogashira Coupling

This type of coupling was firstly reported by Kenkichi Sonogashira and Nobue Hagihara in 1975. In Sonogashira coupling in the presence of a palladium catalyst the acetylenic hydrogen will be substituted by iodoarenes, bromoalkenes or bromopyridines [102].



**Figure 1.22:** Sonogashira coupling [103]

### 1.8. Aim of This Work

The aim of this work is two-fold: 1) Realization of a stable n-dopable conjugated polymer via electropolymerization and 2) Realization of a superior high-performance soluble green to the transmissive electrochromic polymer.

1) Stable n-dopable conjugated polymers are rare however there are a variety of application eras such OFETs and organic electrochemical transistors. Additionally, these stable n-type materials can be used for the realization of complex organic electronic devices with p-i-n type junctions. The rare examples of stable n-type materials generally produced with chemical polymerization methods since the structures are highly electron deficient making the oxidation potentials are quite high for electrochemical polymerizations. We wanted to solve this paradox by using one of the strongest electron acceptors known as PDI, and couple it with electron-rich EDOT units to make electrochemical polymerization possible. This approach was not examined before and the results will be important in fundamental understanding of how these systems behave.

2) Previous work from our group established the design strategy for green to transmissive polymers and quite a good number of examples have been realized. Most of these materials utilized EDOT as the donor unit. It has been shown that ProDOT homopolymer outperforms PEDOT and additionally, ProDOT containing donor-acceptor type polymers also tends to outperform their EDOT analogues. However, it has been shown that while benzothiadiazole-EDOT couple gives a true green color whereas benzothiadiazole-ProDOT couple is cyan. The absorption maxima are generally blue shifted when EDOT is exchanged with ProDOT. Here we

envisioned that switching benzothiadiazole with benzoxadiazole or quinoxaline might result in a better donor-acceptor match towards the realization of a green to transmissive polymer with superior properties. We incorporated ProDOT units with long alkyl-chains towards the realization of soluble polymers.



## CHAPTER 2

### EXPERIMENTAL

#### 2.1. Materials & Methods

The commercially available reagents and reactants used in this study were acquired from Sigma, Across, TCI or Merck. All purification procedures took place under argon unless otherwise noted. Anhydrous were provided from a solvent purification system. A Voltalab 50 potentiostat in a three-electrode system was used to investigate the electrochemical properties of each monomer. This system contained an ITO coated glass slide as the working electrode, platinum wire as the counter electrode, and Ag wire as the pseudo reference electrode which was calibrated against ferrocene. GAMRY Reference 600 potentiostat was used for cyclic voltammetry (CV) measurements of polymers, these measurements were done under inert atmosphere at standard temperature and pressure. The monomers and polymers were analyzed with regard to their spectroelectrochemical properties by using Jasco V-770 UV-Vis spectrophotometer. HOMO and LUMO energy values were determined by taking NHE value as -4.75 eV in the formula of  $HOMO = -(4.75 + E_{onset}^{ox})$  and  $LUMO = -(4.75 + E_{onset}^{red})$ .  $^1H$  and  $^{13}C$  NMR spectra were acquired using Bruker Spectrospin Avance DPX-400 Spectrometer with using either  $CDCl_3$  or DMSO as the solvent. Chemical shifts were reported relative to TMS as the internal standard. HRMS, Waters Synapt MS System was used to measure the accurate mass for each novel product. Purification of the product of each step too place in Silica Gel Column Chromatography with silica gel (35–70  $\mu m$ ).

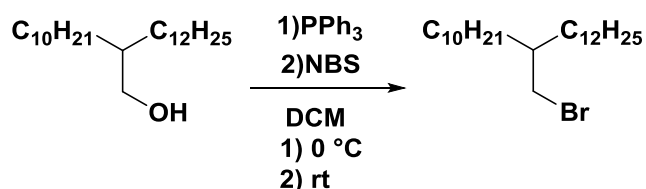


**Figure 2.1:** Synthesis of 2-decyl-1-tetradecylbromide

### 2.1.1. Synthesis of 2-decyl-1-tetradecylbromide

2-Decyl-1-tetradecylbromide was prepared according to the literature [104]. 2-Decyl-1-tetradecanol (7.63 g, 21.5 mmol) was dissolved in DCM (20 mL) and the mixture was cooled to 0 °C by an ice/H<sub>2</sub>O bath. PPh<sub>3</sub> (8.11 g, 30.9 mmol) was added and the mixture was stirred for 30 minutes at 0 °C. After that, NBS (5.24 g, 29.4 mmol) was added portion-wise over 30 minutes at 0 °C and the reaction was stirred at room temperature for 16 hours. The solvent was removed under reduced pressure and the residue was washed with hexane several times. The hexane washings were combined, the solvent evaporated and the residue was purified by column chromatography (SiO<sub>2</sub>, Hexane) to yield the product as a colorless oil (8.49 g, 95% yield). <sup>1</sup>H NMR (400MHz, CDCl<sub>3</sub>) δ: 3.43 (d, 2H), 1.57 (m, 1H), 1.24 (m, 40H), 0.86 (m, 6H). <sup>13</sup>C NMR (100MHz, CDCl<sub>3</sub>) δ: 38.65, 38.52, 31.59, 30.95, 28.82, 28.71, 28.67, 28.62, 28.39, 25.59, 21.72, 13.13

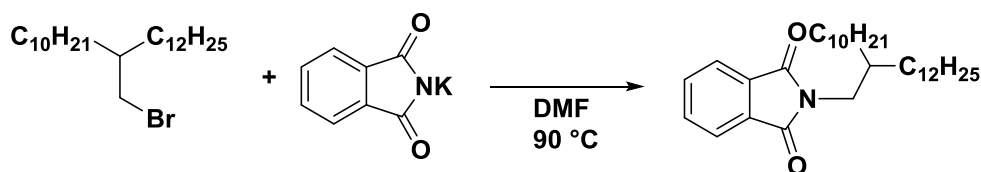


**Figure 2.2:** Synthesis of N-(2-decyltetradecyl) phthalimide.

### 2.1.2. Synthesis of N-(2-decyltetradecyl)phthalimide

N-(2-decyltetradecyl)phthalimide was prepared according to the literature [104]. Potassium phthalimide (4.037 g, 21.80 mmol) was added to a solution of 2-decyl-1-tetradecylbromide (8.49 g, 20.33 mmol) in 25 ml dry DMF. The reaction was stirred for 16 hours at 90 °C. After cooling to room temperature, the reaction mixture was poured into water (150 mL) and extracted with DCM (3×50 mL). The combined organic layers were washed with 100 mL of 0.2 N KOH, water, saturated ammonium chloride, dried over anhydrous MgSO<sub>4</sub>, and concentrated under reduced pressure. The resulting crude yellow oil was purified via column chromatography (silica gel: dichloromethane) giving N-(2-decyltetradecyl)phthalimide as a pale yellow oil (9.67 g, 92% yield) <sup>1</sup>H NMR (400MHz, CDCl<sub>3</sub>) δ: 7.75 (m, 2H), 7.62 (m, 2H), 3.49 (d, 2H), 1.80 (m, 1H), 1.25 (m, 40H), 0.81 (m, 6H). <sup>13</sup>C NMR (100MHz, CDCl<sub>3</sub>) δ: δ 168.63, 133.75, 132.14, 123.10, 42.27, 37.01, 31.92, 31.48, 29.95, 29.68, 29.63,

29.59, 29.36, 29.34, 26.28, 22.69, 14.11. (Note: some peaks in  $^{13}\text{C}$  NMR spectrum overlap).

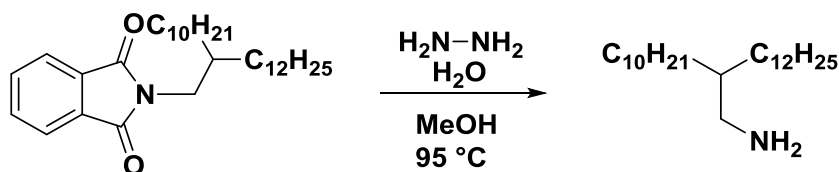


**Figure 2.3:** Synthesis of 2-decyl-1-tetradecylamine.

### 2.1.3. Synthesis of 2-decyl-1-tetradecylamine

2-Decyl-1-tetradecylamine was prepared according to the literature [104]. N-(2-decyl-1-tetradecyl)phthalimide (9.0 g, 0.020 mol), hydrazine hydrate (hydrazine, 51%) (4.0 mL, 65 mmol) and MeOH (100 mL) were stirred at 95 °C and monitored by TLC. After disappearance of the starting imide, the methanol was evaporated under reduced pressure, the residue diluted with DCM (100 mL) and washed with 10% KOH (2×50 mL). Aqueous layers were combined and extracted with dichloromethane (3×20 mL). The combined organic layers were washed with brine (2×50 mL) and dried over  $\text{MgSO}_4$ . The removal of the dichloromethane afforded yellow oil as product which was used in synthesis without further purification (6.66 g, 94% yield).  $^1\text{H}$  NMR (400MHz,  $\text{CDCl}_3$ )  $\delta$ : 2.53 (d, 2H), 1.42 (m, 1H), 1.18 (br, 40H), 0.81 (m, 6H)  $^{13}\text{C}$  NMR (100 MHz,  $\text{CDCl}_3$ )  $\delta$  45.40, 41.09, 32.06, 31.70, 30.25, 29.82, 29.79, 29.49, 26.94, 22.82, 14.23.

### 2.2. Synthesis of (PDI-EDOT)

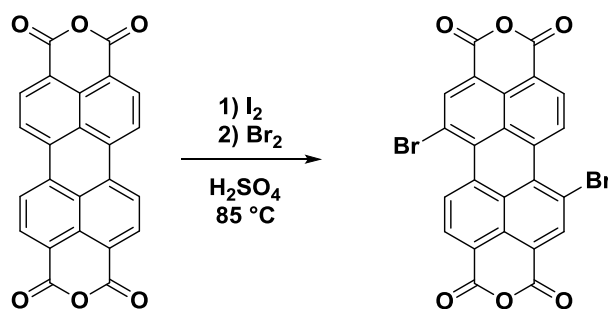


**Figure 2.4:** Synthesis of PDI-2Br

### 2.2.1. Synthesis of PDI-2Br

PDI-2Br was prepared based on a literature process [105]. A mixture of perylene-3,4:9,10-tetracarboxylic acid bisanhydride (2.0 g, 5.1 mmol) and 98 wt% H<sub>2</sub>SO<sub>4</sub> (8 mL) was stirred at room temperature for 12 h. I<sub>2</sub> (52 mg, 0.26 mmol) was then added, the mixture was heated to 85 °C with vigorous stirring for 30 min. Then bromine (4.88 g, 30.6 mmol) was added drop wise over a time period of 3 h and the reaction mixture was stirred for 16 h at 85 °C. After being cooled to room temperature, the mixture was poured into 100 g of ice. The precipitate was filtered, washed with 100 mL 50% sulfuric acid and then a large amount of H<sub>2</sub>O until neutral. The residue was dried to give 2.46 g of red powder. The crude product was used for the next step directly.

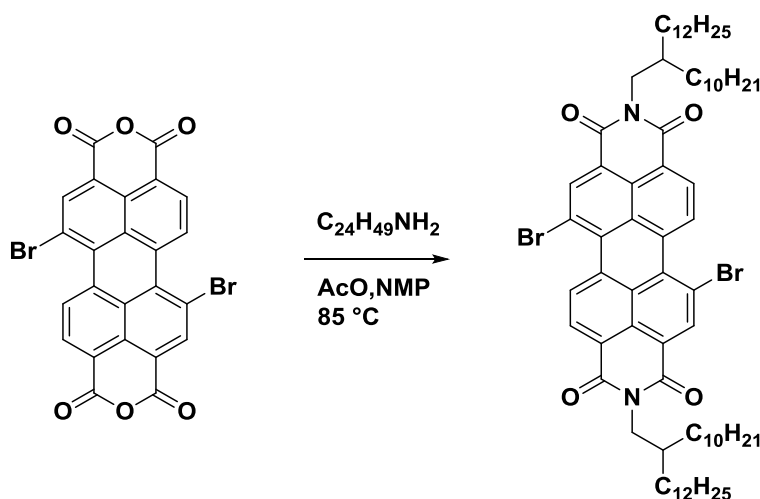


**Figure 2.5:** Synthesis of N,N'-bis(2-decyltetradecyl)-1,6-bibromo-3,4,9,10-perylene diimide.

### 2.2.2. Synthesis of N,N'-bis(2-decyltetradecyl)-1,6-dibromo-3,4,9,10-perylene diimide

N,N'-Bis(2-decyltetradecyl)-1,6-dibromo-3,4,9,10-perylene diimide was prepared based on the literature [106, 107]. A suspension of brominated perylene bisanhydrides (0.250 g) obtained in the above reaction, 2-decyl-1-tetradecylamine (0.520 g, 14.8 mmol), and acetic acid (0.2 mL) in N-methyl-2 pyrrolidinone (6.25 mL) was stirred at 85 °C under N<sub>2</sub> for 12 h. After the mixture was cooled to room temperature, the precipitate was separated by filtration, washed with MeOH (50 mL),

and dried in a vacuum. The crude product was purified by silica gel column chromatography (Silica gel, eluent, Hexane and DCM, 10:3) giving 0.110 g (20% yield) of the pure product of N,N'-bis(2-decyltetradecyl)-1,6-dibromo-3,4,9,10-perylene diimide.  $^1\text{H}$  NMR (400 MHz,  $\text{CDCl}_3$ )  $\delta$  9.38 (d,  $J = 8.2$  Hz, 2H), 8.82 (s, 2H), 8.59 (d,  $J = 8.2$  Hz, 2H), 4.06 (d,  $J = 7.2$  Hz, 4H), 1.92 (s, 2H), 1.26 – 1.07 (m, 80H), 0.80 – 0.76 (m, 12H).

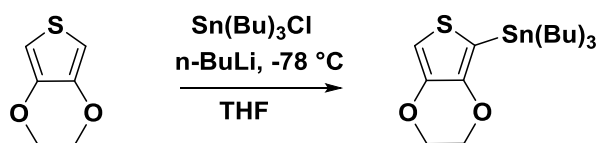


**Figure 2.6:** Synthesis of tributyl(2,3-dihydrothieno[3,4-b][1,4]dioxin-5-yl)stannane.

### 2.2.3. Synthesis of tributyl(2,3-dihydrothieno[3,4-b][1,4]dioxin-5-yl)stannane

Tributyl(2,3-dihydrothieno[3,4-b][1,4]dioxin-5-yl)stannane was prepared according to published procedure [108]. 3,4-ethylenedioxythiophene (3.0 g, 21 mmol) was dissolved in anhydrous THF (60 mL) in a two-neck round bottom flask. The reaction mixture was cooled down to  $-78$  °C and *n*-butyllithium (2 M, 9.3 mL, 23 mmol) was added dropwise at  $-78$  °C and the solution was stirred for 1.5 hours at this temperature. Tributyltinchloride (8.2 g, 25 mmol) was then added to the solution at the same temperature. The reaction was allowed to slowly warm to room temperature and stirred overnight. The solvent was evaporated under vacuum to afford a crude yellow-brown oil (9.0 g, 99%) which was used in the next step without any further purification.

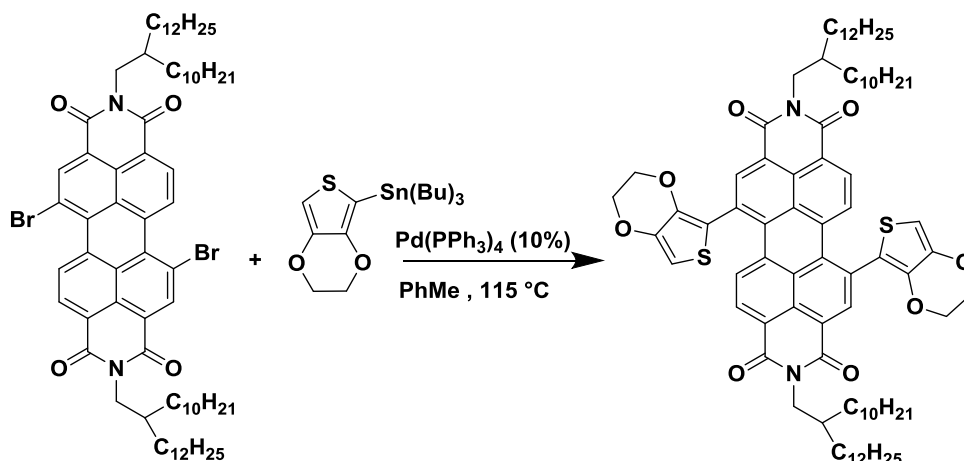


**Figure 2.7:** Synthesis of 2,9-bis(2-decyltetradecyl)-5,12-bis(2,3-dihydrothieno[3,4-b][1,4]dioxin-5-yl)anthrax [2,1,9-def:6,5,10-d'e'f']diisoquinoline-1,3,8,10(2H,9H)-tetraone (PDI-EDOT)

#### 2.2.4. Synthesis of 2,9-bis(2-decyltetradecyl)-5,12-bis(2,3-dihydrothieno[3,4-b][1,4]dioxin-5-yl)anthrax[2,1,9-def:6,5,10-d'e'f']diisoquinoline-1,3,8,10(2H,9H)tetraone (PDI-EDOT)

Under an argon atmosphere N,N'-Bis(2-decyltetradecyl)-1,6-dibromo-3,4,9,10-perylene diimide (110 mg, 90.1  $\mu\text{mol}$ ), 2-(tributylstannyl)-3,4-ethylenedioxythiophene (117 mg, 270  $\mu\text{mol}$ ) and Pd(PPh<sub>3</sub>)<sub>2</sub>Cl<sub>2</sub> (7.00 mg, 9.97 mmol) were added to the reaction flask and dissolved in anhydrous toluene (7 mL). At 115 °C for 24 h the mixture was stirred and then cooled to the room temperature. To the resulting greenish dark black oil H<sub>2</sub>O was added and the extraction of the aqueous layers was done by DCM several times. The combined organic layers were washed with brine and dried over anhydrous Na<sub>2</sub>SO<sub>4</sub>. The resulted product of the step was filtered and the solvent was reduced under pressure. The resulting greenish dark black sticky oil was then purified by column chromatography (SiO<sub>2</sub>, Hexane 1:3 DCM). The target product was obtained as a black sticky oil (42 mg, 38%) <sup>1</sup>H NMR (400 MHz, CDCl<sub>3</sub>)  $\delta$  8.59 (s, 2H), 8.22 (dd,  $J$  = 17.9, 8.2 Hz, 4H), 6.49 (s, 2H), 4.07 (d,  $J$  = 4.3 Hz, 4H), 4.04 (d,  $J$  = 7.3 Hz, 4H), 3.95 (d,  $J$  = 3.6 Hz, 4H), 2.05 – 1.81 (m,  $J$  = 22.1 Hz, 2H), 1.39 – 1.03 (m, 80H), 0.78 (td,  $J$  = 6.9, 3.4 Hz, 12H). <sup>13</sup>C NMR (100 MHz, CDCl<sub>3</sub>)  $\delta$  162.00, 161.93, 140.72, 136.29, 134.13, 133.71, 131.71, 128.31, 128.09, 127.06, 126.00, 125.76, 120.57, 120.30, 115.61, 99.71, 62.99, 34.97, 30.20, 30.03, 28.38, 27.94, 27.64, 24.82, 20.96, 12.39, -0.70.

### 2.3. Synthesis of stannylated Pro-DOT

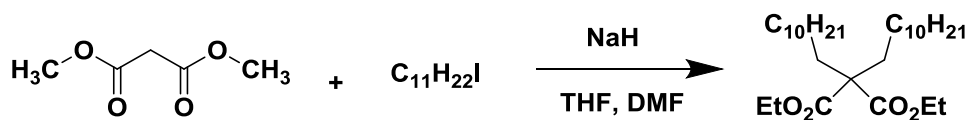


**Figure 2.8:** Synthesis of diethyl 2,2-dipentadecylmalonate.

#### 2.3.1. Synthesis of diethyl 2,2-dipentadecylmalonate

Diethyl 2,2-dipentadecylmalonate was prepared based on the literature [109]. A solution of NaH (1.2 g, 52.2 mmol) in THF (100 mL) and DMF (30 mL) was prepared at 0 °C under argon. Diethyl malonate (1.66 g, 12.6 mmol) was added slowly to this solution. After attiring the mixture at room temperature for 15 min, 1-iodoundecane (10.60 g, 37.69 mmol) was added, and the mixture was heated under reflux for 6 h. The reaction mixture was concentrated in vacuo, and the resultant oil was suspended in water (100 mL). The extraction was done first with hexane (2 × 50 mL) and then with a 1:1 mixture of pentane/diethyl ether (1 × 50 mL). The organic layers were washed with H<sub>2</sub>O (3 × 30 mL), dried over MgSO<sub>4</sub>, and were dried through evaporation. The crude product was purified by column chromatography on silica gel (hexane/diethyl ether, 1/0 to 10/1), affording diethyl 2,2-dipentadecylmalonate (2.4 g) in 42% yield. <sup>1</sup>H NMR (400 MHz, CDCl<sub>3</sub>) δ 4.18 – 4.01 (m, 4H), 1.86 – 1.68 (m, 4H), 1.30 – 0.93 (m, 36H), 0.87 – 0.67 (m, 6H). <sup>13</sup>C NMR (100 MHz, CDCl<sub>3</sub>) δ 172.06, 60.88, 31.90, 29.84, 29.62, 29.53, 29.34, 23.88, 22.68, 14.10.

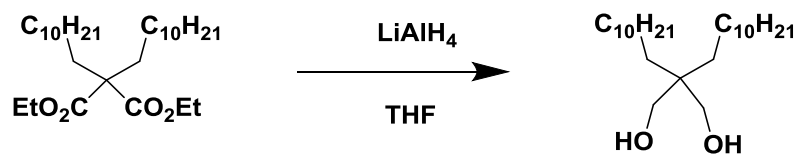


**Figure 2.9:** Synthesis of 2,2-sipentadecyl-1,3-propanediol.

### 2.3.2. Synthesis of 2,2-sipentadecyl-1,3-propanediol

2,2-Dipentadecyl-1,3-propanediol was prepared based on the literature [109]. Lithium aluminium hydride (1.2 g, 31.7 mmol) was added to a solution of diethyl 2,2-dipentadecylmalonate (4.60 g, 7.93 mmol) in THF at room temperature. The reaction mixture was heated under reflux for 2 h. The reaction was quenched by conducting Fieser method. Removal of the solvents under vacuum afforded crude 2,2-dipentadecyl-1,3-propanediol in 94% yield.  $^1\text{H}$  NMR (400 MHz,  $\text{CDCl}_3$ )  $\delta$  3.56 (s, 4H), 1.32 – 1.22 (m, 40H), 0.88 (t,  $J = 6.8$  Hz, 6H).  $^{13}\text{C}$  NMR (100 MHz,  $\text{CDCl}_3$ )  $\delta$  69.45, 31.93, 30.78, 30.60, 29.69, 29.66, 29.62, 29.58, 29.37, 22.86, 14.13

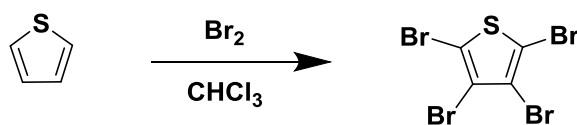


**Figure 2.10:** Synthesis of 2,3,4,5-tetrabromothiophene.

### 2.3.3. Synthesis of 2,3,4,5-tetrabromothiophene

2,3,4,5-Tetrabromothiophene was prepared according to the literature [110]. To the reaction flask. Thiophene (1.0 g, 10 mmol) was added and dissolved in  $\text{CHCl}_3$  (1 mL). The toxic gas of HBr was turned into the harmless NaBr salt by using a trap filled with saturated NaOH solution. The reaction mixture was cooled down to  $0\text{ }^\circ\text{C}$ , a mixture of  $\text{CHCl}_3$  (4 mL) and  $\text{Br}_2$  (3.7 mL, 71 mmol) were added dropwise to the reaction flask. The mixture was stirred at  $0\text{ }^\circ\text{C}$  for 3 h. then, the ice bath was removed and the reaction mixture was warmed to room temperature.  $\text{Br}_2$  (0.6 mL) was added additionally. The mixture was refluxed for 3 h and was left to be cooled to the room temperature. To eliminate the excess amount of  $\text{Br}_2/\text{NaOH}$  solution (80 mL) was added dropwise to the reaction mixture. The reaction mixture was stirred at  $95\text{ }^\circ\text{C}$  for 1 h and then gradually warmed to  $25\text{ }^\circ\text{C}$ . The resulted crystals were filtered and dissolved in DCM. Water was added and extraction was performed. The water layer extracted with DCM several times. The combined organic layers were then dried ( $\text{Na}_2\text{SO}_4$ ) and the solvent was evaporated. The recrystallization from methanol was done and the crystals were washed repeatedly with cold MeOH. The desired product was obtained as white crystals (3.1 g, 80%).

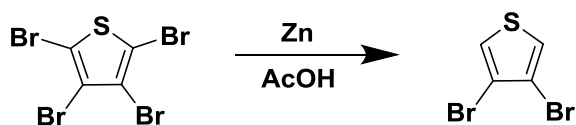


**Figure 2.11:** Synthesis of 3,4-dibromothiophene.

### 2.3.4. Synthesis of 3,4-dibromothiophene

3,4-Dibromothiophene was prepared according to the literature [110]. The reaction flask equipped with a magnetic stir bar was charged with an acetic acid/water mixture (1:2 v/v, 180 mL) followed by the addition of powdered zinc (13 g, 0.20 mol) and 2,3,4,5-tetrabromothiophene (25 g, 0.063 mmol) in small portions. The resulting mixture was subsequently stirred at room temperature for 1 h, and then under reflux for 3 h under argon atmosphere. The mixture was passed through a plug of celite (~4 cm thick), and then the filtrate was extracted with diethyl ether. After drying with anhydrous  $\text{Na}_2\text{SO}_4$ , the solvent was removed via rotary evaporation, and the crude product was distilled under vacuum to yield a colorless liquid (13 g, 87%):  $^1\text{H-NMR}$  (400 MHz,  $\text{CDCl}_3$ ):  $\delta$  (ppm) 7.19 (s, 2H).

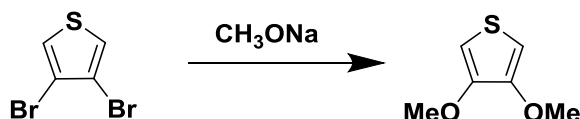


**Figure 2.12:** Synthesis of 3,4-dimethoxythiophene.

### 2.3.5. Synthesis of 3,4-dimethoxythiophene

3,4-Dimethoxythiophene was prepared according to the literature [111]. A flame dried 250 mL round-bottom flask equipped with a magnetic stir bar was charged with 60 mL anhydrous methanol, and sodium metal (~5 g, 0.22 mol) was added slowly over 30 min. 3,4-Dibromothiophene (12 g, 0.50 mol) was added to the alkaline solution at room temperature. The cupric oxide (2.8 g, 35 mmol) and KI (0.85 g, 5.0 mmol) were quickly added to the above mixture, and then the reaction mixture was stirred and heated to reflux for 3 days under argon atmosphere. After cooling to room temperature and the most of the solvent was removed and water (80

mL) was added and stirred 10 min. Then it was extracted three times with diethyl ether (3×50 mL), and the combined organic layer was washed with water (50 mL) and brine (100 mL), respectively. The organic layer was dried over MgSO<sub>4</sub>, and concentrated via rotary evaporation. The resulting product was purified via distillation under reduced pressure and the compound was obtained as a clear oil (5.5 g, 77 %). <sup>1</sup>H NMR (400 MHz, CDCl<sub>3</sub>) δ 6.11 (s, 1H), 3.77 (s, 3H). <sup>13</sup>C NMR (100 MHz, CDCl<sub>3</sub>) δ 147.82, 96.28, 57.54.

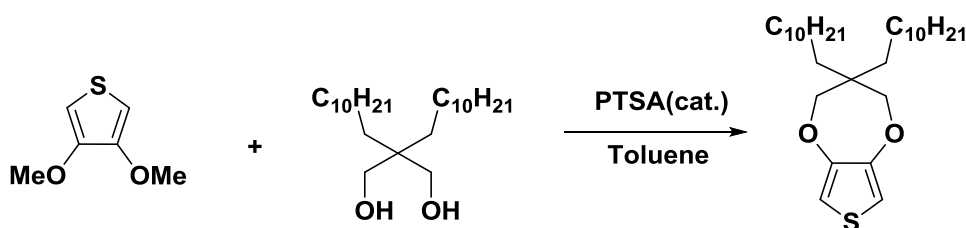


**Figure 2.13:** Synthesis of 3,3'-didodecyl-3,4-dihydro-2H-thieno[3,4-b][1,4]dioxepine(ProDOT)

### 2.3.6. Synthesis of 3,3'-didodecyl-3,4-dihydro-2H thieno[3,4b][1,4]dioxepine (ProDOT)

3,3'-Didodecyl-3,4-dihydro-2H-thieno[3,4-b][1,4]dioxepine(ProDOT) was prepared according to the literature [111]. A 250 mL roundbottom flask equipped with a magnetic stir bar was charged with toluene (120 mL). 3,4-Dimethoxythiophene (0.197 g, 1.36 mmol), 2,2'-didodecyl-1,3 propanediol (0.745 g, 2.72 mmol) and *p*-toluenesulfonic acid monohydrate (0.026 g, 0.136 mmol) were added. The resulting mixture was stirred at reflux for 2 days under N<sub>2</sub> atmosphere. After cooling down to room temperature, the reaction mixture was washed with water (100 mL). The toluene was removed under reduced pressure, and the crude product was purified by column chromatography on silica gel with methylene chloride/hexane (1:9, v/v ) as an eluent to yield colorless oil (370 mg, 78%) . <sup>1</sup>H NMR (400 MHz, CDCl<sub>3</sub>) δ 6.33 (s, 2H), 3.76 (s, 4H), 1.30 – 1.07 (m, 40H), 0.81 (t, *J* = 6.8 Hz, 6H). <sup>13</sup>C NMR (100 MHz, CDCl<sub>3</sub>) δ 149.75, 104.61, 77.54, 43.75, 31.95, 31.88, 30.51, 29.66, 29.56, 29.38, 22.83, 22.72, 14.13.

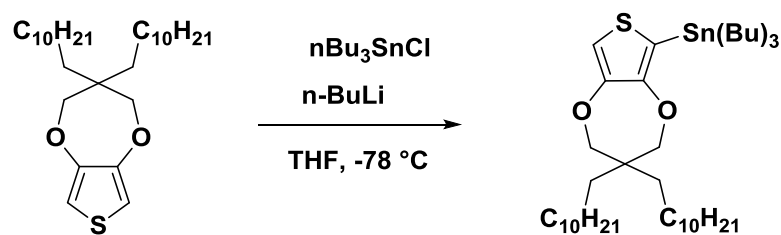


**Figure 2.14:** Synthesis of tributyl(3,3-diundecyl-3,4-dihydro-2H-thieno[3,4-b][1,4]dioxepin-6-yl)stannane.

### 2.3.7. Synthesis of tributyl(3,3-diundecyl-3,4-dihydro-2H-thieno[3,4-b][1,4]dioxepin-6-yl) stannane

Tributyl (3,3-diundecyl-3,4-dihydro-2H-thieno[3,4-b][1,4]dioxepin-6-yl) stannane was synthesized similar to published procedures with small modifications [112]. 3,3'-Didodecyl-3,4 dihydro-2H-thieno[3,4-b][1,4]dioxepine(ProDOT) (300 mg), 0.645 mmol) was dissolved in dry THF (6 mL) and the mixture was cooled to -78 °C. n-Butyllithium (2.5 M, 0.51 mL, 1.28 mmol, in hexanes) was added dropwise at -78 °C and the mixture was maintained at this temperature for 90 minutes. Tributyltinchloride (216 mg, 0.645 mmol) was then added at the same temperature and the resulting mixture was gradually warmed to room temperature and stirred for 16 hours. The solvent was evaporated to afford a brown oil (400 mg, 82%) which was used in the next reaction without any further purification.

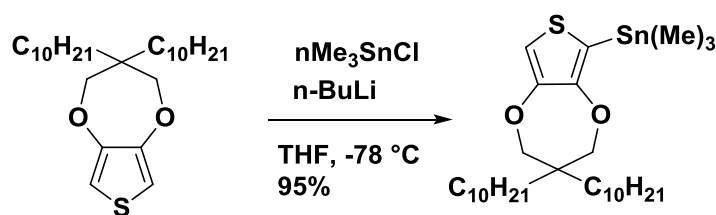


**Figure 2.15:** Synthesis of (3,3-didecyl-3,4-dihydro-2H-thieno[3,4-b][1,4]dioxepin-6-yl)trimethylstannane.

### 2.3.7.1. Synthesis of (3,3-didecyl-3,4-dihydro-2H-thieno[3,4-b][1,4]dioxepin-6-yl)trimethylstannane

(3,3-Didecyl-3,4-dihydro-2H-thieno[3,4-b][1,4]dioxepin-6-yl)trimethylstannane was synthesized similar to published procedures with small modifications [113]. 3,3-didecyl-3,4-dihydro-2H-thieno[3,4-b][1,4]dioxepine (ProDOT) (622 mg, 1.43 mmol) was dissolved in dry THF (6 mL) and the mixture was cooled to  $-78\text{ }^{\circ}\text{C}$ . *n*-Butyllithium (2.5 M, 0.7 mL, 1.77 mmol, in hexanes) was added dropwise at  $-78\text{ }^{\circ}\text{C}$  and the mixture was maintained at this temperature for 90 minutes. Tributyltinchloride (298 mg, 1.50 mmol) was then added at the same temperature and the resulting mixture was gradually warmed to room temperature and stirred for 16 hours. The solvent was evaporated to afford a brown oil (811 mg, 8295%) which was used in the next reaction without any further purification.

### 2.4. Synthesis of QUIN-ProDOT

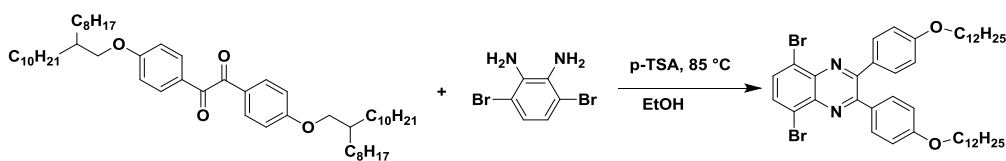


**Figure 2.16:** Synthesis of 5,8-dibromo-2,3-bis(4-((2-octyldodecyl)oxy)phenyl)quinoxaline

#### 2.4.1. Synthesis of 5,8-dibromo-2,3-bis(4-((2-octyldodecyl)oxy)phenyl)quinoxaline

5,8-Dibromo-2,3-bis(4-((2-octyldodecyl)oxy)phenyl)quinoxaline was prepared according to the literature [114]. To the heated vacuum dried reaction flask 1,2-Bis(4-((2-octyldodecyl)oxy)phenyl)ethane-1,2-dione (4.1 g, 5.1 mmol), 3,6-dibromobenzene-1,2-diamine (1.5 g, 5.6 mmol) and catalytic p-TSA (88 mg, 0.51 mmol) were added, and the mixture was dissolved with EtOH (50 mL). The mixture was undergone reflux overnight. To the resulted yellow mixture water was added. The extraction of the organic part was done by DCM several times. The combined

organic layers were washed with brine and dried over anhydrous  $\text{Na}_2\text{SO}_4$ . The resulted product of the step was filtered and the solvent was reduced under pressure. The purification of the resulted yellow product was done through column chromatography ( $\text{SiO}_2$ , Hexane 2:1 DCM). The target product was obtained as a yellow solid (4.3 g, 82%):  $^1\text{H}$  NMR (400 MHz,  $\text{CDCl}_3$ )  $\delta$  7.65 (d,  $J$  = 8.8 Hz, 2H), 6.87 (d,  $J$  = 8.9 Hz, 2H), 3.98 (d,  $J$  = 6.5 Hz, 2H).  $^{13}\text{C}$  NMR (101 MHz,  $\text{CDCl}_3$ )  $\delta$  160.49, 158.05, 139.03, 132.47, 131.68, 130.32, 123.45, 114.37, 68.12, 43.28, 31.94, 29.66, 29.60, 29.42, 29.37, 29.22, 26.05, 22.71, 18.44, 14.14.

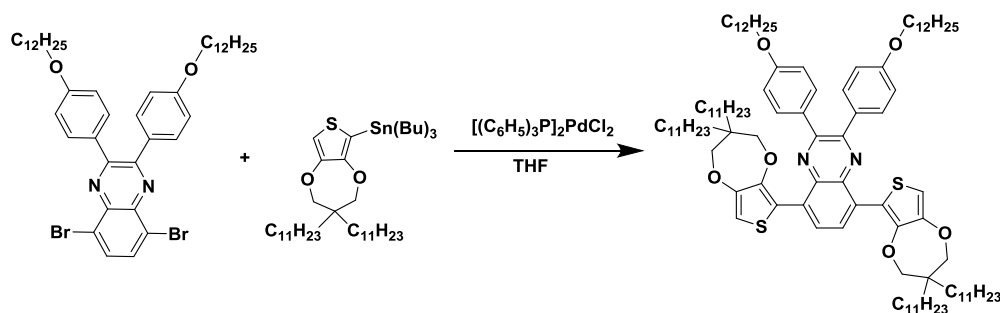


**Figure 2.17:** Synthesis of 5,8-bis(3,3-diundecyl-3,4-dihydro-2H-thieno[3,4-b][1,4]dioxepin-6-yl)-2,3-bis(4-(dodecyloxy)phenyl)quinoxaline

#### 2.4.2. Synthesis of 5,8-bis(3,3-diundecyl-3,4-dihydro-2H thieno[3,4-b][1,4]dioxepin-6-yl)-2,3-bis(4 (dodecyloxy)phenyl)quinoxaline (Quin-Pro-DOT)

5,8-Bis(3,3-diundecyl-3,4-dihydro-2H-thieno[3,4-b][1,4]dioxepin-6-yl)-2,3-bis(4-(dodecyloxy)phenyl)quinoxaline was synthesized based on the procedure [115] with some modifications. Under an argon atmosphere 5,8-Dibromo-2,3-bis(4-(2-octyldodecyl)oxy)phenyl)quinoxaline (150 mg, 185  $\mu\text{mol}$ ), tributyl(3,3-diundecyl-3,4-dihydro-2H-thieno[3,4-b][1,4]dioxepin-6-yl)stannane (349 mg, 463  $\mu\text{mol}$ ) and Bis(triphenylphosphine)palladium(II) dichloride (13 mg, 19  $\mu\text{mol}$ ) were dissolved in THF (6 mL) in the reaction flask. For 24 h and at 74  $^\circ\text{C}$  the mixture was stirred and then cooled to the room temperature. To the resulted yellow-brown sticky oil  $\text{H}_2\text{O}$  was added and the extraction of aqueous layer was done by DCM. The combined organic layers were washed with brine and dried over anhydrous  $\text{Na}_2\text{SO}_4$ . The resulted product of the step was filtered and the solvent was reduced under pressure.

The purification of the resulting yellow-brown sticky oil was done by column chromatography (SiO<sub>2</sub>, Petroleum Ether 1:1 DCM). The target product was obtained as yellowish-orange sticky oil (110 mg, 38%) <sup>1</sup>H NMR (400 MHz, CDCl<sub>3</sub>) δ 8.34 (s, 2H), 7.60 (d, *J* = 8.7 Hz, 4H), 6.79 (d, *J* = 8.7 Hz, 4H), 6.56 (s, 2H), 3.95 – 3.79 (m, 12H), 1.76 – 1.67 (m, 4H), 1.42 – 1.08 (m, 120H), 0.87 – 0.73 (m, 18H). <sup>13</sup>C NMR (100 MHz, CDCl<sub>3</sub>) δ 158.61, 149.29, 148.46, 146.66, 136.16, 130.68, 130.04, 128.15, 127.45, 116.44, 112.91, 105.75, 76.59, 76.41, 66.84, 42.54, 30.74, 29.34, 28.49, 28.47, 28.44, 28.41, 28.38, 28.26, 28.17, 28.11, 24.90, 21.67, 21.51, 12.92, -0.17.

## 2.5. Synthesis of (BENZ-ProDOT)

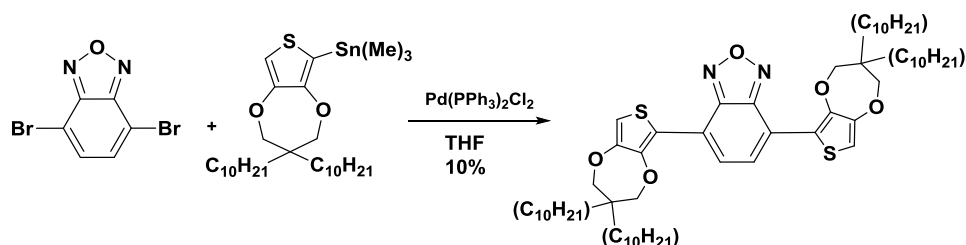


**Figure 2.18:** Synthesis of 4,7-bis(3,3-didecyl-3,4-dihydro-2H-thieno[3,4-b][1,4]dioxepin-6-yl)benzo[c][1,2,5]oxadiazole (BENZ-Pro-DOT)

### 2.5.1. Synthesis of 4,7-bis(3,3-didecyl-3,4-dihydro-2Hthieno[3,4-b][1,4]dioxepin-6-yl)benzo[c][1,2,5]oxadiazole (BENZ-ProDOT)

4,7-Bis(3,3-didecyl-3,4-dihydro-2H-thieno[3,4-b][1,4]dioxepin-6-yl)benzo[c][1,2,5]oxadiazole was synthesized based on the procedure [115] with some modifications. 4,7-dibromobenzo[c][1,2,5]oxadiazole (150 mg, 540 μmol), (3,3-didecyl-3,4-dihydro-2H-thieno[3,4-b][1,4]dioxepin-6-yl)trimethylstannane (809 mg, 1.35 mmol) and Bis(triphenylphosphine)palladium(II) dichloride in catalytic amount (53 mg) were dissolved in THF (5 mL) in the reaction flask. For 24 h and at 74 °C the mixture was stirred and then cooled to the room temperature. To the resulted yellow-brown sticky oil H<sub>2</sub>O was added and the extraction of aqueous layer was done by DCM. The combined organic layers were

washed with brine and dried over anhydrous  $\text{Na}_2\text{SO}_4$ . The resulted product of the step was filtered and the solvent was reduced under pressure. The resulting dark-red sticky oil was then purified by column chromatography resulted in 53 mg of pure product (yield 10%). ( $\text{SiO}_2$ , petroleum ether 1:1 DCM).  $^1\text{H}$  NMR (400 MHz,  $\text{CDCl}_3$ )  $\delta$  7.99 (s, 2H), 6.57 (s, 2H), 3.99 (s, 4H), 3.88 (s, 4H), 1.59 – 0.93 (m, 64H), 0.81 (t,  $J = 6.8$  Hz, 12H).



## CHAPTER 3

### RESULTS and DISCUSSION

#### 3.1. Monomer Syntheses

##### 3.1.1. Synthesis of the PDI-EDOT

Figure 3.1 shows the synthetic pathway for the central PDI monomer unit.

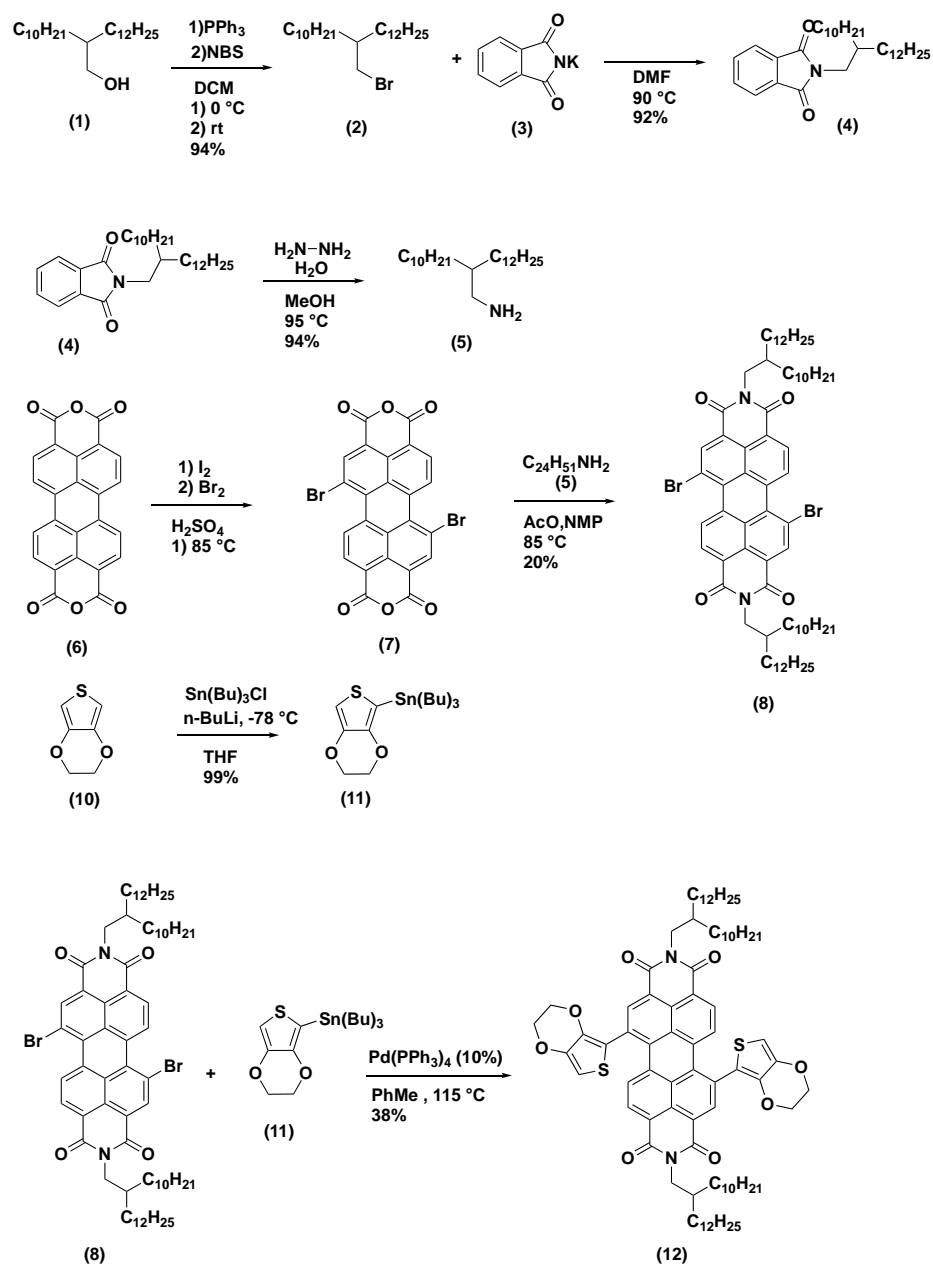
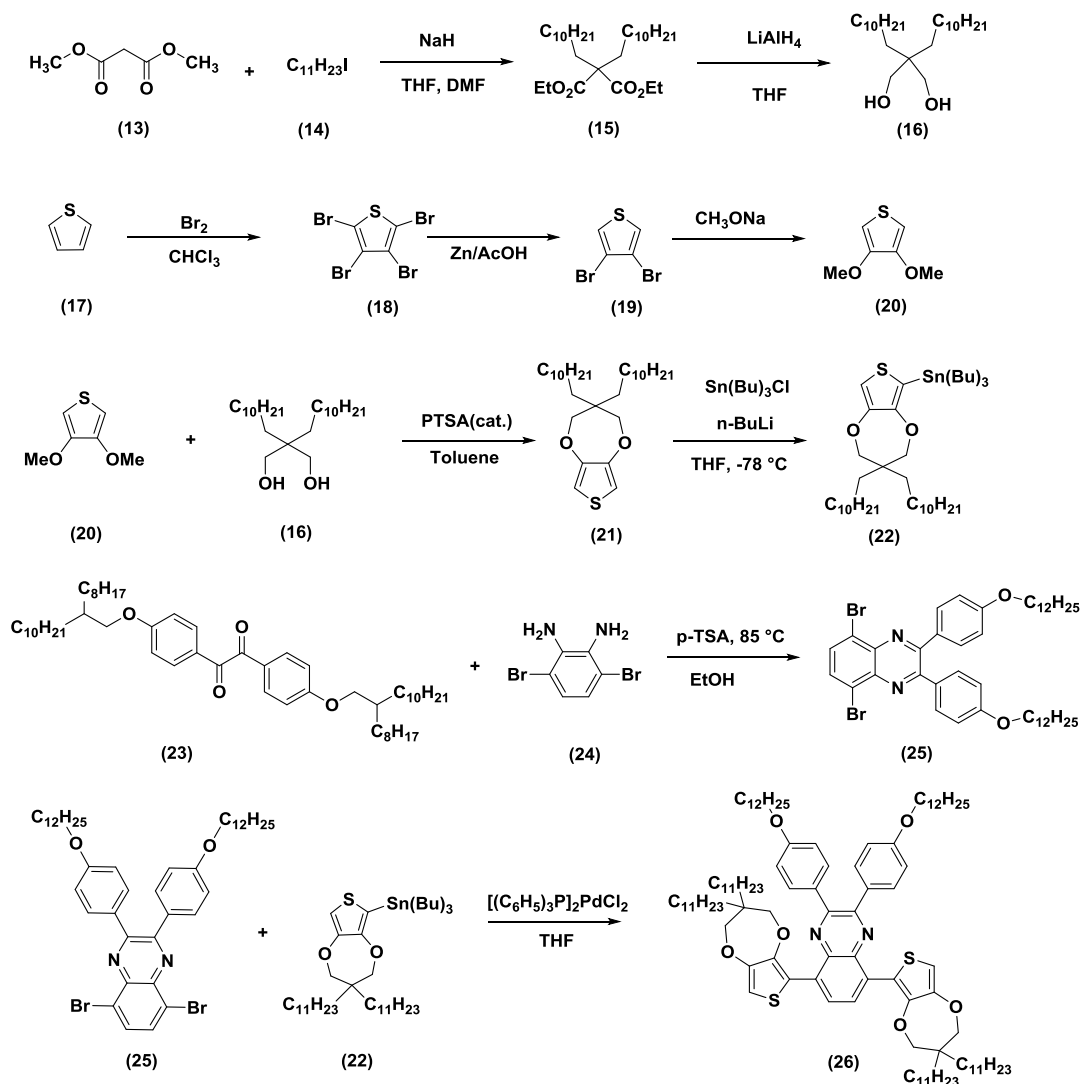


Figure 3.1: Synthetic pathway of PDI-EDOT (12).

The synthetic approach to PDI-ProDOT is shown in Figure 3.1. The synthesis started with the commercially available alcohol **1**. Bromination with NBS/PPh<sub>3</sub> system gave the bromo **2** in high yields. Towards the synthesis of the target amine **5** Gabriel synthesis was applied. Thus, potassium phthalimide (**3**) was reacted with the bromo **2** and compound **4** was synthesized. Removal of the protecting group with hydrazine/water gave the desired amine **5**. Then perylene tetracarboxylic dianhydride **6** was dibrominated in the presence of bromine/iodine and sulfuric acid to give the dibromo compound **7**. Condensation of anhydride **7** and amine **5** gave the desired dibromo PDI **8**. EDOT (**10**) was stannylated successfully and the resulting compound **11** was coupled with PDI **8** under Stille coupling conditions to give target compound **12**.

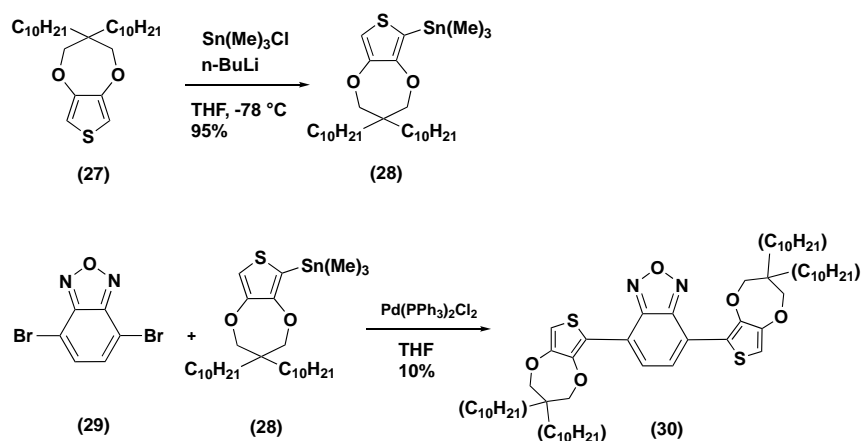
### 3.1.2. Synthesis of the QUIN-ProDOT

Figure 3.2 shows the synthetic pathway for the QUIN-ProDOT monomer unit. Commercially available diester **13** and alkyl iodide **14** was reacted in the presence of NaH to yield the doubly alkylated product **15**. Diester **15** was reduced completely to diol **16** in the presence of LiAlH<sub>4</sub>. Separately thiophene (**17**) was tetrabrominated in the presence of bromine then the bromines at 2 and 5 positions were selectively reduced to give 3,4-dibromothiophene (**19**). Etherification with NaOMe gave compound **20**. Transesterification between **20** and diol **16** gave the dialkyl ProDOT derivative **21**. Stannylation was performed in the presence of n-BuLi and Sn(Bu)<sub>3</sub>Cl to yield compound **22**. Alkylated diketone **23** and diamine **24** which were in our group inventory was condensed together to yield target dibromo quinoxaline **25**. Stille coupling between **25** and **22** gave the target donor-acceptor type monomer **26**.



**Figure 3.2:** Synthetic pathway of the central unit.

Figure 3.3 shows the synthetic pathway for the central BENZ-Pro-DOT monomer unit.



**Figure 3.3:** Synthetic pathway of the central unit.

A ProDOT derivative with different alkyl chain size that was in our group inventory was successfully stannylated to yield compound **28**. Coupling with commercially available 4,7-dibromo-2,1,3-benzoxadiazole (**29**) gave the target donor-acceptor type monomer **30**.

## **3.2. Electrochemical and Electrochromic Properties of Polymers**

### **3.2.1. Electropolymerization of Monomers**

Electropolymerizations in this study were taken place under the following system; the multiple scan voltammetry system was comprised of three electrodes where the counter electrode was a platinum wire, an Ag wire was utilized as the reference electrode and the ITO coated glass was introduced as the working electrode.

### **3.2.2. Spectroelectrochemistry Studies of Polymers**

Optical changed of the conjugated polymers upon doping processes were investigated via spectroelectrochemistry studies. These studies directly show the evolution of charge carriers when polymer is progressively deoped. Polymer films that are going to be used in this study were coated potentiodynamically on ITO . The UV-vis-NIR spectra were recorded at different applied potentials in a monomer free acetonitrile solution of 0.1 M TBAPF<sub>6</sub>.

### **3.2.3. Kinetic Studies of Polymers**

In order to probe changes in transmittance with time, the kinetic studies for the polymers were performed. To conduct such studies the polymer was repeatedly stepped between the neutral and oxidized states. The response times and switching abilities were investigated by performing the studies at the maximum absorption of the polymers in their neutral state. The polymer film was deposited on ITO glass slide by repeated scanning (15 cycles) in 0.1M TBAPF<sub>6</sub>/ACN (monomer free).

### 3.2.4. Electrochemical and Electrochromic Properties of (PDI-EDOT)

#### 3.2.4.1. Electropolymerization of (PDI-EDOT)

The potentiodynamic polymerization of PDI-EDOT on ITO coated glass slide was performed from a 10 mM solution of PDI-EDOT in DCM and ACN (5/95, v/v) and TBAPF<sub>6</sub> electrolyte solvent (Figure 3.4).

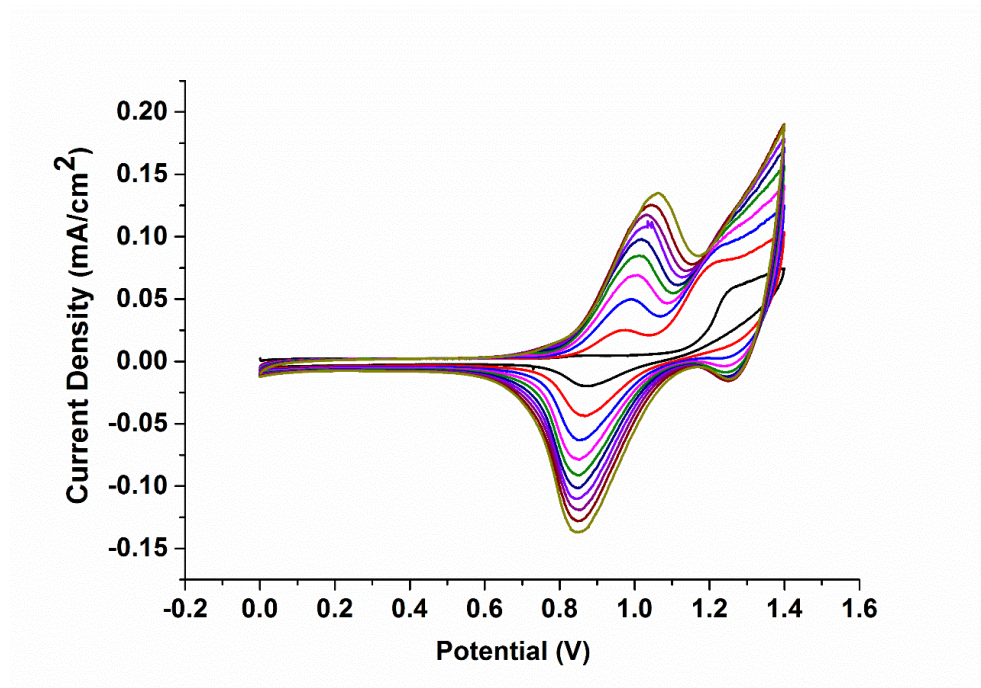


**Figure 3.4:** Repeated scan polymerization of PDI-EDOT (WE: ITO, CE: Pt wire, RE: Ag wire, 0.1 M TBAPF<sub>6</sub>/DCM/ACN 100 mV s<sup>-1</sup>, 10 cycles).

The monomer oxidation centered on EDOT unit was observed at 1.40 V and formation of an electroactive polymer was observed in the following cycles. The polymer oxidation and reduction potentials (10<sup>th</sup> cycle) were observed as 1.10 V and 0.87 V respectively. Even though currents were increasing in each cycle, a very thin coating of polymer was observed after 10 cycles. The coated polymer film was washed with ACN and CV was recorded in a monomer free solution. The polymer oxidation and reduction peaks for the p-type doping were observed at 1.2 V and 1.02 V respectively.

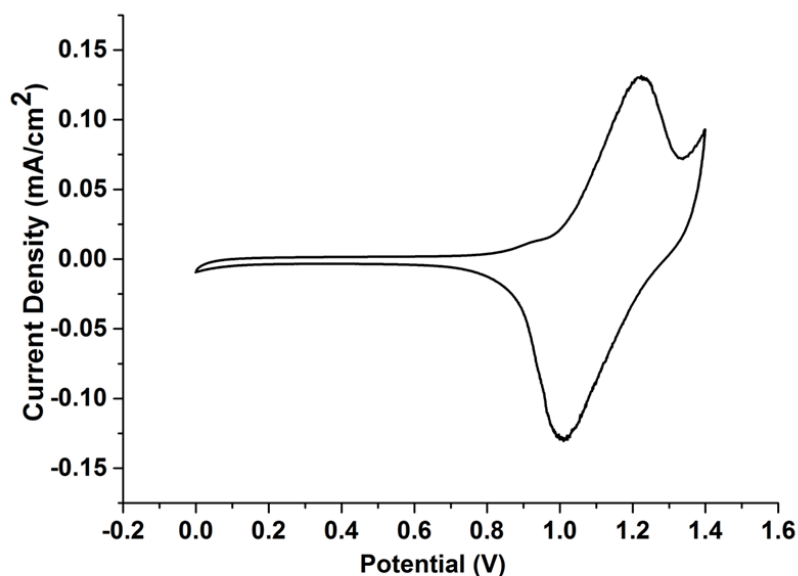


**Figure 3.5:** Single scan cyclic voltammetry of PDI-EDOT (WE: ITO, CE: Pt wire, RE: Ag wire, 0.1 M TBAPF<sub>6</sub>/DCM/ACN 100 mV s<sup>-1</sup>).

Quite interestingly the polymer can easily be n-doped. n-Doping redox peaks were observed at -0.75 V and -0.45 V which are quite unusual values for conjugated polymeric systems. The strong acceptor capacity of the central PDI unit was responsible for this phenomenon. As mentioned before a conjugated system with stable n-doped states are quite valuable towards the realization of complex organic electronic devices. However, it is important to note that a redox couple at negative potentials by themselves cannot be direct evidence for n-type doping. Observation of a spectral change needs accompanies the reduction waves observed in CV studies. Even though detailed spectroelectrochemical studies are not performed yet, we were quite happy to see that upon n-doping a significant color change was observed for the polymer. Hence we can confidentially claim that a true n-type doping process can be easily attained with very low potentials (absolute value). Actually, the results are among the lowest potentials reported for n-type conjugated polymers.

### 3.2.4.2. Spectroelectrochemistry Studies of PPDI-EDOT

For the UV-vis-NIR spectra of PPDI-EDOT, applied potential was between -0.1 V and 1.4 V with 0.1 V increments. The results are shown below (Figure 3.6). In its neutral state, the PPDI-EDOT shows a narrow absorption band centered at 402 nm. Additionally, a broad and low-intensity absorption peak at 756 nm and a small shoulder at 506 nm were observed. Upon applied potential, the absorption peak at 402 nm gradually depletes and a new strong absorption peak forms at 492 nm. The absorption at 756 nm also depletes to a certain extent and a new band forms centered at 836 nm. The bands at 492 and 836 nm are the polarons and strong absorption centered at 1400 nm represents the formation of bipolaronic species.

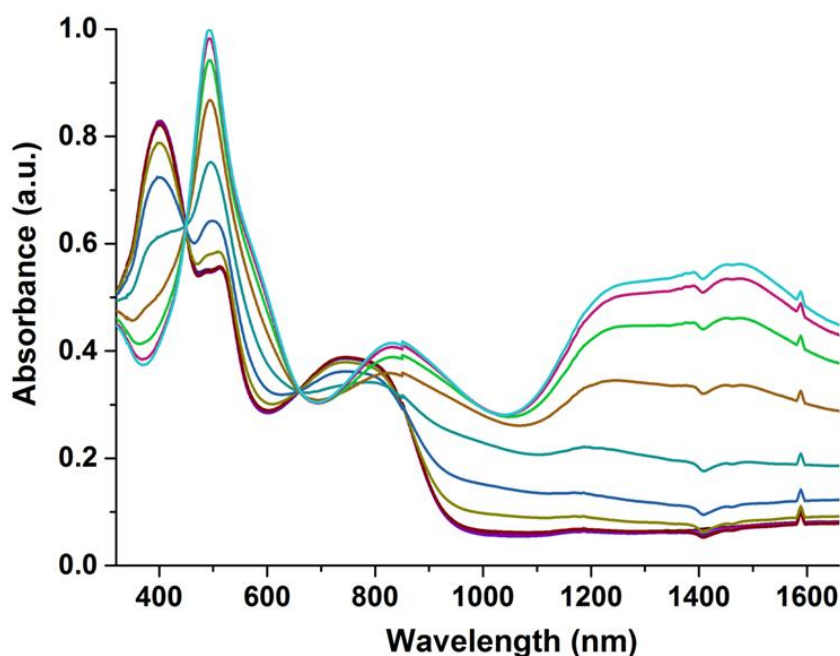


**Figure 3.6:** Spectroelectrochemistry studies of PPDI-EDOT (-0.1 V to 1.4 V with 0.1 V increments).

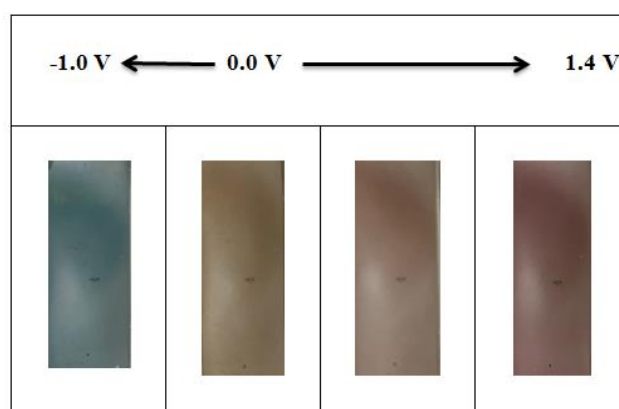


**Figure 3.7:** Photographs of the PPDI-EDOT at its neutral and oxidized states.

### 3.2.4.3. Kinetic Studies of PPDI-EDOT

The optical contrast of the PPDI-EDOT was found to be 10% at 402 nm 12% at 495 nm ( $\lambda_{\text{max}}$ ) (Figure 3.8) and 23% at 1470 nm ( $\lambda_{\text{max}}$ ) (Figure 3.9). These values are quite low for conjugated polymeric systems where optical contrasts up to 80% have been achieved. However, this material was synthesized for the purpose of generating a stable n-doped state. Optical changes that occur during n-type doping needs to be evaluated in detail. This will be discussed further in the future directions part. The switching times were also calculated at 402 nm, 492 nm and 1470 nm for oxidation and reduction respectively as 1.82 s and 1.83 s, 1.90 s and 1.91 s, 1.54 s, and 1.91 s.

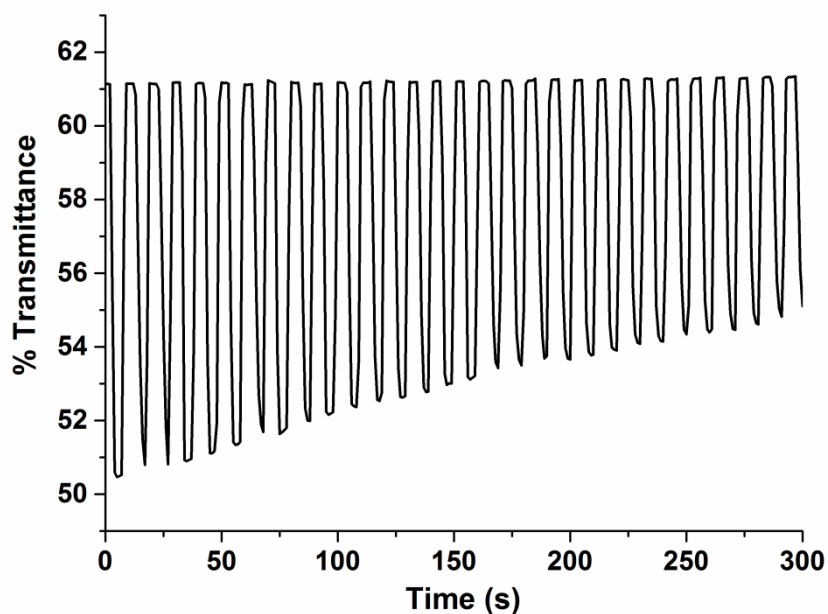


**Figure 3.8:** Electrochromic switching and optical absorbance change of PPDI-EDOT monitored at 402 nm (30 cycles).

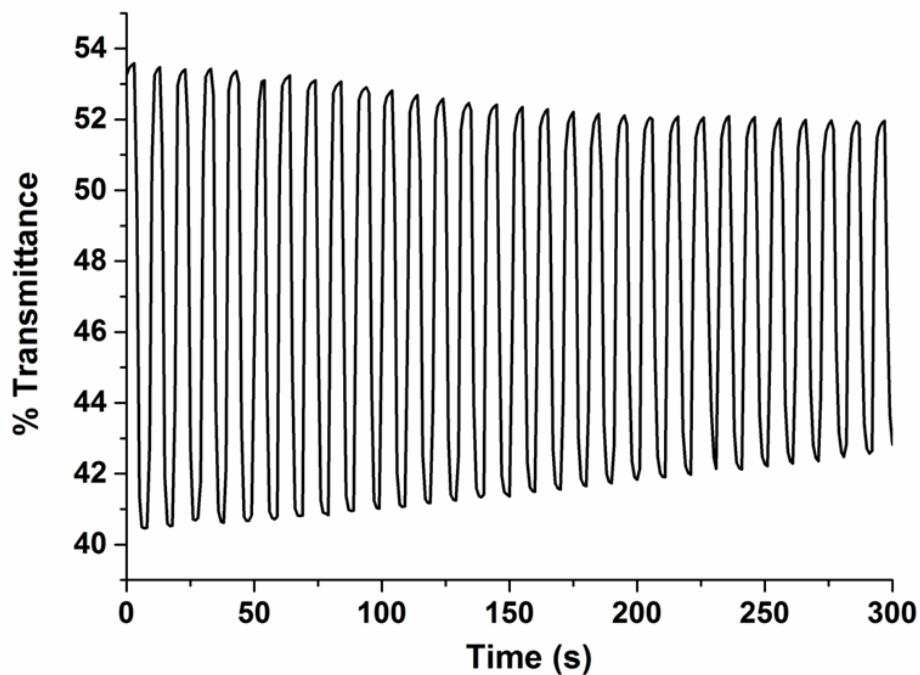


**Figure 3.9:** Electrochromic switching and optical absorbance change of PPDI-EDOT monitored at 492 nm (30 cycles).

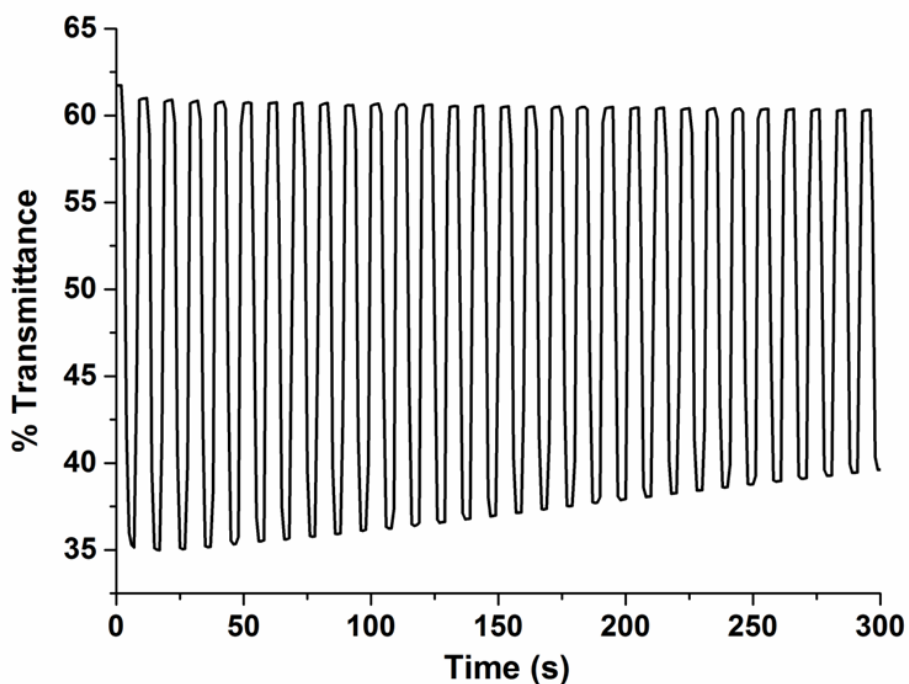


**Figure 3.10:** Electrochromic switching and optical absorbance change of PPDI-EDOT monitored at 1470 nm (30 cycles).

### 3.2.5. Electrochemical Polymerization of QUIN-ProDOT

The potentiodynamic polymerization of QUIN-EDOT on ITO coated glass slide was performed from a 10 mM solution of PDI-EDOT in variety of different

solvent/electrolyte couples. Unfortunately, the growth of CV cycles due to formation of an electroactive material on ITO surface was not observed. Even though a polymer formation is evident from the CV and a very thin coating on the electrode, the material is not electroactive and color change is not visible. This quite interesting considering that monomers that contain quinoxaline as acceptor and EDOT as donor electropolymerize easily to give highly electroactive conjugated [116].

### 3.2.6. Electrochemical and Electrochromic Properties of (BENZ-Pro-DOT)

#### 3.2.6.1. Electropolymerization of (BENZ-Pro-DOT)

A solution of BENZ-Pro-DOT (10 mM) was prepared in a mixture of DCM and acetonitrile (1/5, v/v) and TBAPF<sub>6</sub> was utilized as the supporting electrolyte. The potentiodynamic polymerization of (BENZ-Pro-DOT) on ITO coated glass slide was shown in Figure 3.11. The monomer oxidation centered on ProDOT unit was observed at 1.21 V. Upon formation of a well-defined redox couple, the formation of an electroactive polymer film was observed in the following cycles. The polymer oxidation and reduction potentials (10<sup>th</sup> cycle) were observed as 1.02 V and 0.62 V respectively.

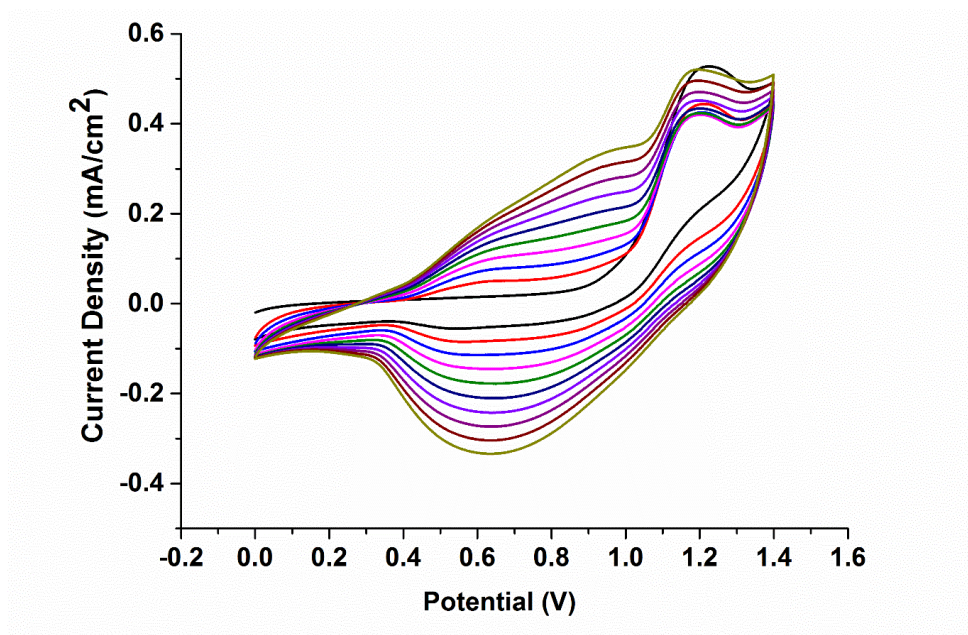


**Figure 3.11:** Repeated scan polymerization of BENZ-Pro-DOT (WE: ITO, CE: Pt wire, RE: Ag wire, 0.1 M TBAPF<sub>6</sub>/DCM/ACN, 100 mV s<sup>-1</sup>, 10 cycles).

P(BENZ-Pro-DOT) was also shown to be both p and n-dopable. On the p-doping site the redox couple is quite broad and CV resemble almost a square shape. This is one of important requirements for development of high performance supercapacitors with conjugated polymers. The supercapacitor properties of this material will be investigated in future. On the n-doping site a clear redox couple is observed with corresponding potentials of -1.43 V and -1.13 V. Although these values are not as low as that of the PPDI-EDOT discussed above, P(BENZ-Pro-DOT) is still a material that can be easily n-doped compared similar structures reported in the literature. As mentioned above to be able to demonstrate a clean n-doping process a redox couple at negative potentials are not enough. Spectral changes should also accompany the CV behaviour. This was also the case with P(BENZ-Pro-DOT) and blueish-green color in the neutral state switch to a brownish-grey color upon n-doping.

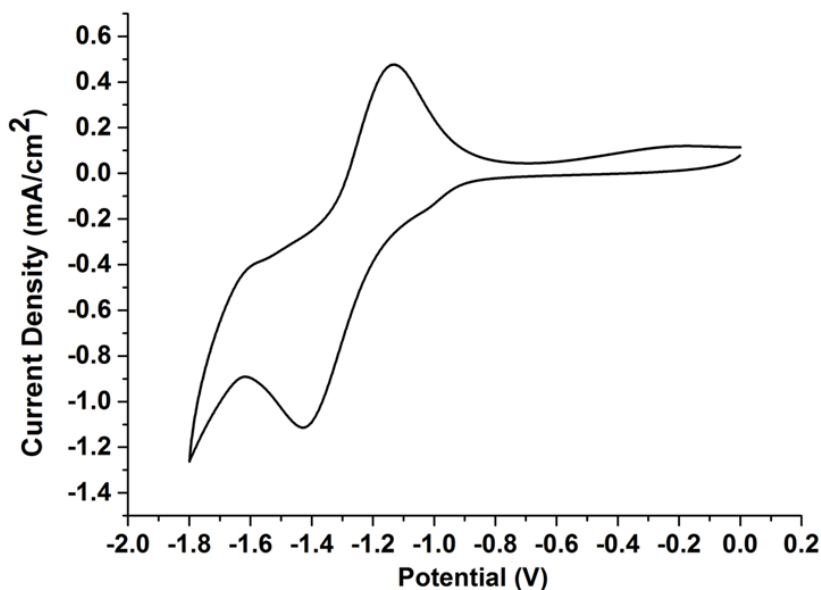


**Figure 3.12:** n-Doped polymerization of BENZ-Pro-DOT (WE: ITO, CE: Pt wire, RE: Ag wire, 0.1 M TBAPF<sub>6</sub>/DCM/ACN, 100 mV s<sup>-1</sup>)

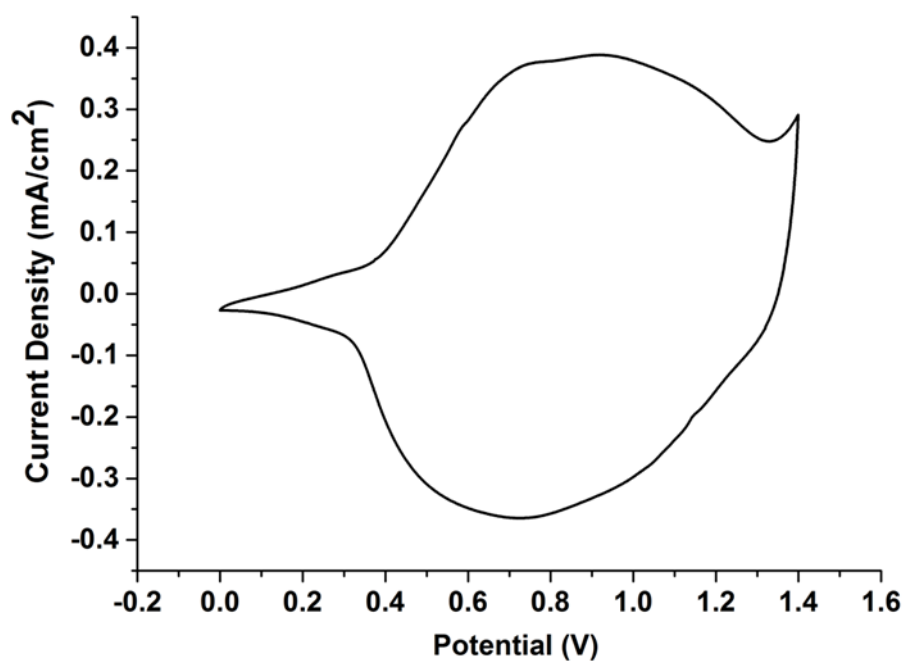


**Figure 3.13:** p-Doped polymerization of BENZ-Pro-DOT (WE: ITO, CE: Pt wire, RE: Ag wire, 0.1 M TBAPF<sub>6</sub>/DCM/ACN, 100 mV s<sup>-1</sup>)

### 3.2.6.2. Spectroelectrochemistry Studies of PBENZ-Pro-DOT

For the electrochemically synthesized PBENZ-Pro-DOT, UV-vis-NIR spectra were recorded between -0.1 V and 1.5 V with 0.1V increments is shown in Figure 3.14.

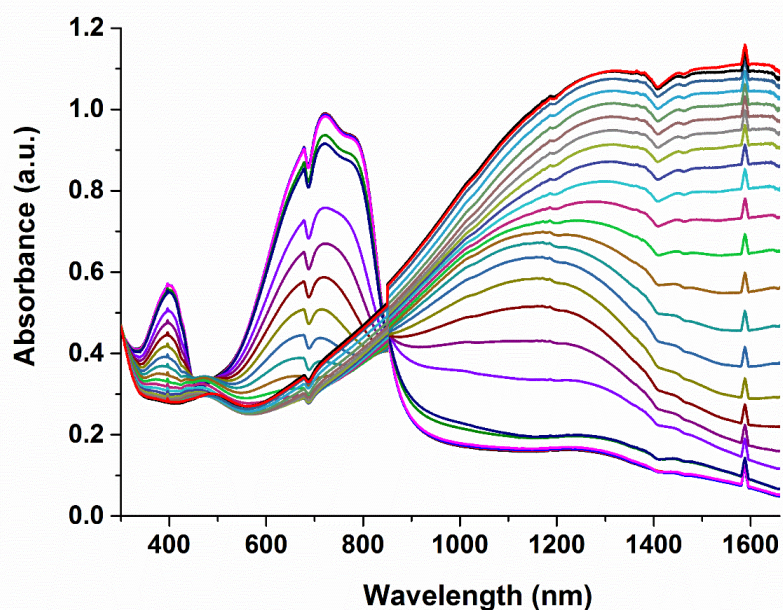


**Figure 3.14:** Spectroelectrochemistry studies of PBENZ-Pro-DOT (-0.1 V to 1.4 V with 0.1 V increments).

As mentioned in the aim of the work, we targeted to design and synthesize a high-performance soluble green to transmissive polymer. Two absorption bands centered at 400 nm and 720 nm were observed. Even though absorption centered at 720 nm is quite good for having a green color the absorption band centered at 400 nm is not appropriate. For observing a green color the lower wavelength band should be centered between 430-450 nm ranges [42]. Additionally, there is quite a big mismatch between the absorption intensities of the two peaks. This resulted in observation of a blueish-green color in the neutral state. Upon oxidation, both bands depleted strongly and a transmissive grey color was observed.

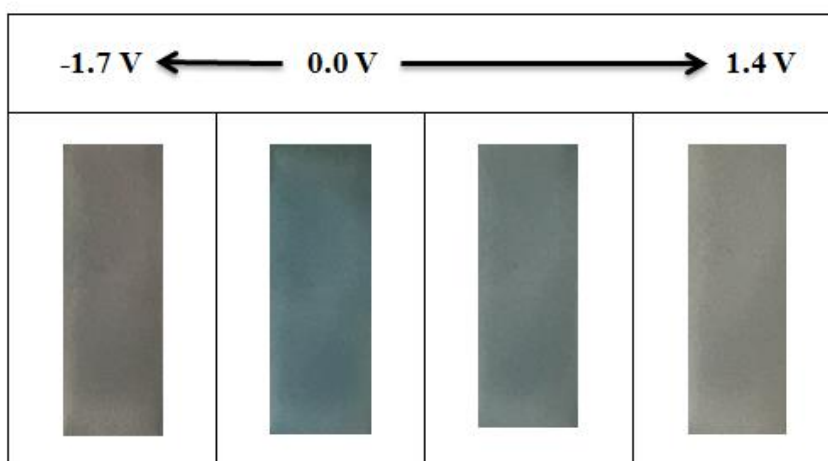


**Figure 3.15:** Photographs of the PBENZ-Pro-DOT at its neutral and oxidized states

### 3.2.5.3. Kinetic Studies of PBENZ-Pro-DOT

The optical contrast and the switching time of the electrochemically synthesized PBENZ-Pro-DOT were investigated. The results shown here are preliminary and detailed optimizations are still ongoing. The optical contrast values were found to be 17% at 400 nm ( $\lambda_{max}$ ) (Figure 3.15), 30% at 720 nm (Figure 3.16) and 50% at 1350 nm (Figure 3.17). Even though the optical contrast is slightly low at 400 nm, 30% optical contrast value at 720 nm is promising and comparable to similar materials in

the literature. The switching times were also calculated at 400 nm, 720 nm and 1350 nm for oxidation and reduction respectively as 1.81 s and 2.91 s, 1.91 s and 1.81 s, 1.86 s and 1.97 s.

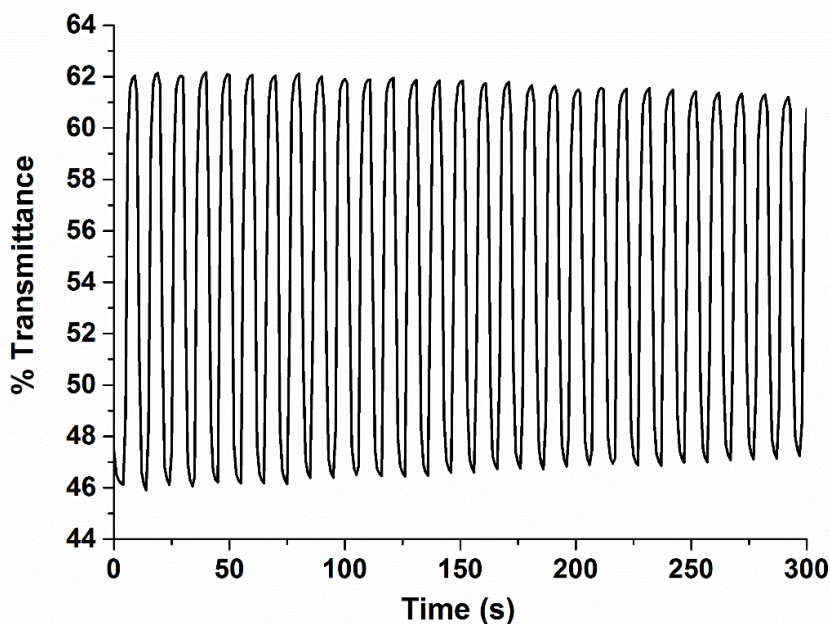


**Figure 3.16:** Electrochromic switching and optical absorbance change of PBENZ-Pro-DOT monitored at 400 nm (30 cycles)

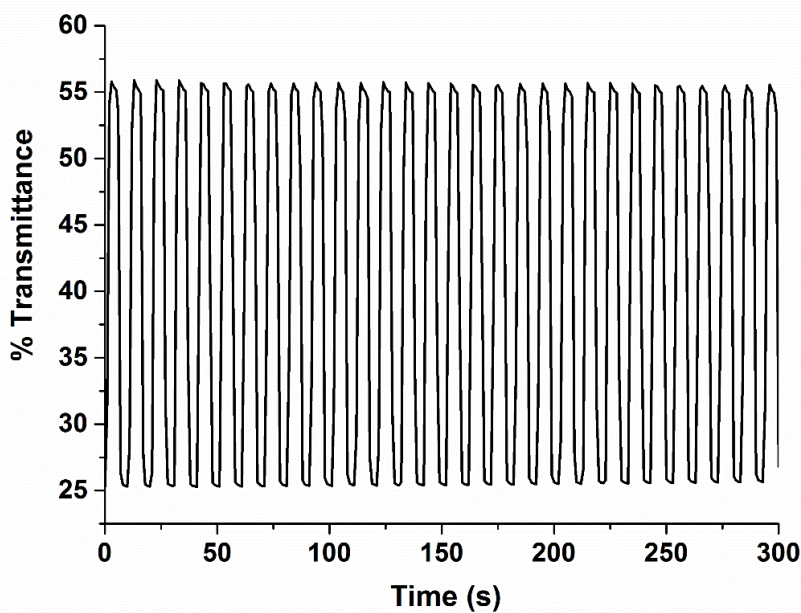


**Figure 3.17:** Electrochromic switching and optical absorbance change of PBENZ-Pro-DOT monitored at 720 nm (30 cycles)

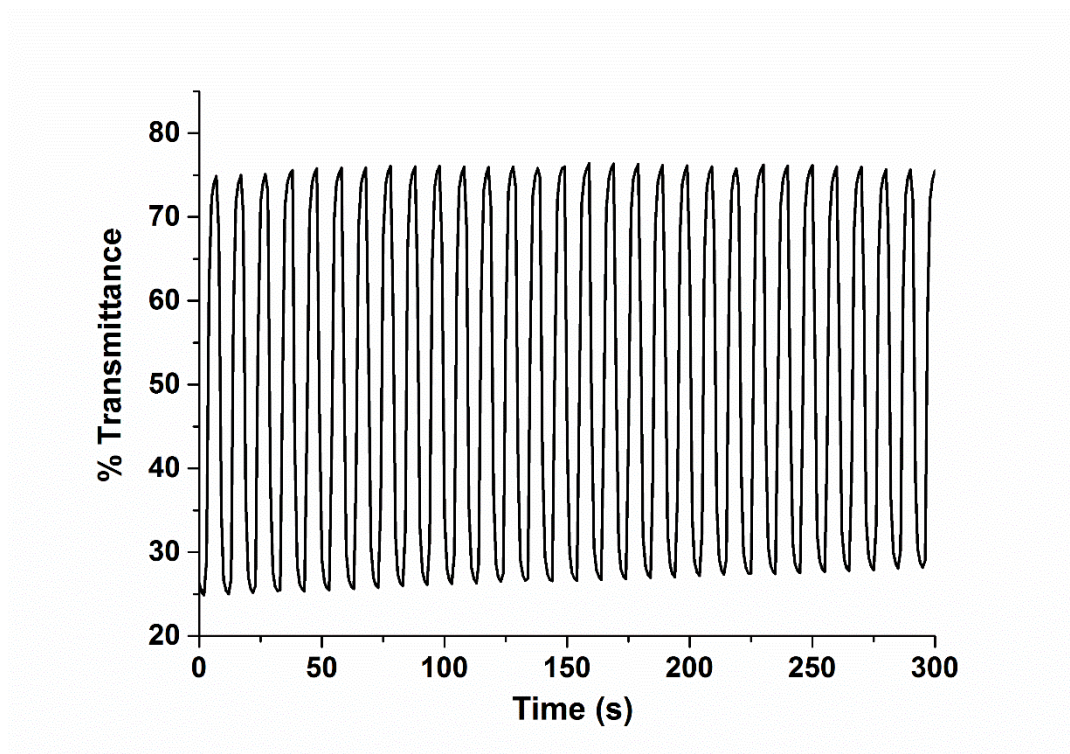


**Figure 3.18:** Electrochromic switching and optical absorbance change of PBENZ-Pro-DOT monitored at 1350 nm (30 cycles)

### 3.3. Future Work

Even though the main characteristics of both materials produced in this study were determined, additional characterizations are needed. For PPDI-EDOT spectroelectrochemistry studies at the negative region should be studied carefully to further determine the ease of n-doping process and related stability. Additionally, due to long alkyl chains on the PDI unit the polymer has the potential to be solution processable. Hence oxidative chemical polymerization methods will be applied to produce the polymer, and then solubility of the material will be tested. If the polymer is soluble it will be spray coated on ITO electrodes and n-doping behaviour and electrochromic properties of the chemically produced material will be investigated. The reason for why QUIN-ProDOT monomer could not be electrochemically polymerized is not clear. Further electrochemical and structural analyses will be performed to understand this unusual phenomenon.

The preliminary results for PBENZ-Pro-DOT showed promising optical contrast and switching time values. The film thickness optimization will be performed to determine the highest optical contrast that can be achieved with this material. Additionally, coloration efficiency of the material will be investigated. As mentioned before PBENZ-Pro-DOT is decorated with long alkyl chains hence it expected to be a solution processable material. Hence the corresponding monomer will be polymerized under oxidative chemical polymerization conditions (ex: FeCl<sub>3</sub>, EtOAc). The resulting polymer will be reduced and purified. Then the material will be applied to ITO electrodes with spray coating and the electrochromic properties of the resulting material will be investigated in detail.

## CHAPTER 4

### CONCLUSION

Three novel conjugated polymers were designed and synthesized towards reaching two main targets: Realization of an easily dopable and stable n-type material and realization of next generation green to transmissive electrochromic polymers with enhanced properties. For the aim of stable n-type materials, PPDI-EDOT was successfully synthesized and shown to be doped in an n-type manner by both electrochemical and spectral means. Unusually low (absolute) voltages were required for this doping process which clearly indicated the ease of n-doping in this system. Accordingly, it is expected that stability of the n-type state should be superior compared to classical examples of donor-acceptor type polymers which require much higher voltages for the n-doping process. Interestingly the polymer was produced by electrochemical polymerization which is quite rare for true n-type materials with extremely low voltage requirements. Further analysis of this quite interesting system is currently underway. For the aim of realizing next generation green to transmissive electrochromic polymers two novel materials were designed and synthesized successfully. Previous work from our group established the design strategy for green to transmissive polymers. Most of these materials utilized EDOT as the donor unit. It has been shown that ProDOT homopolymer outperforms PEDOT. However, it has been shown that while benzothiadiazole-EDOT couple gives a true green color, benzothiadiazole-ProDOT couple is cyan. The absorption maxima are generally blue shifted when EDOT is exchanged with ProDOT. Here we envisioned that switching benzothiadiazole with benzooxadiazole or quinoxaline might result in a better donor-acceptor match towards the realization of a green to transmissive polymer with superior properties. Unfortunately, and surprisingly, in the case of quinoxaline substitution an electroactive polymer could not be produced. In the case of benzooxadiazole substitution an electroactive polymer was produced by means of electropolymerization. Polymer revealed two absorption bands

as expected from a donor-acceptor material which were centered at 400 nm and 720 nm. Even though absorption centered at 720 nm is quite good for having a green color the absorption band centered at 400 is not appropriate. For observing a green color the lower wavelength band should be centered between 430-450 nm range. Additionally, there was a quite big mismatch between the absorption intensities of the two peaks. This resulted in observation of a blueish-green color in the neutral state. The preliminary studies on the electrochromic properties of the material was promising where a 30% optical contrast was achieved in the visible region with less than 2 seconds switching times.

## REFERENCES

- [1] S. C. Rasmussen. Electrically Conducting Plastics: Revising the History of Conjugated Organic Polymers. In *100+ years of plastics*; Strom, T., Rasmussen. S. C., Eds.; American Chemical Society: Washington D.C., 2011.; pp 147-163.
- [2] H. Shirakawa, *Rev. Mod. Phys.* **2001**, *73*, 713-718.
- [3] N. Miyaura, K. Yamada, A. Suzuki, *Tetrahedron Lett.* **1979**, *20*(36), 3437-3340.
- [4] W. A. Gazotti, A. F. Nogueira, E. M. Giroto, L. Micaroni, M. Martini, S. das Neves, M. De Paoli, *Adv. Mater.* **1998**, *10*, 60-64.
- [5] J. L. Brédas, R. R. Chance, R. Silbey, *Phys. Rev. B.* **1982**, *26*, 5843-5854.
- [6] J. L. Brédas, J. C. Scott, K. Yakushi, G. B. Street, *Phys. Rev. B.* **1984**, *30*, 1023-1025.
- [7] J. L. Reddinger, J.R. Reynolds, *Adv. Polym. Sci.* **1999**, *145*, 57-122.
- [8] K.-Y. Jen, M. R. Maxfield, L. W. Shacklette, R. L. Elsenbaumer, *J. Chem. Soc., Chem Comm.* **1987**, *4*, 309-311.
- [9] R. J. Waltman, J. Bargon, A. F. Diaz, *J. Phys. Chem.* **1983**, *87*, 1459-1463.
- [10] J. M. Toussaint, J. L. Brédas, *Synth. Met*, **1993**, *61*, 103-106.
- [11] J. Roncali, R. Garreau, A. Yassar, P. Marque, F. Garnier, M. Lemaire, *J. Phys. Chem.* **1987**, *91*, 6706-6714.
- [12] R. D. McCullough, *Adv. Mater.* **1998**, *10*, 93-116.
- [13] H. Sirringhaus, P. J. Brown, R. H. Friend, M. M. Nielsen, K. Bechgaard, B. M. W. Langeveld-Voss, A. J. H. Spiering, R. A. J. Janssen, E. W. Meijer, P. Hervig, D. M. de Leeuw, *Nature* **1999**, *401*, 685-688.
- [14] L. Groenendaal, F. Jonas, D. Freitag, H. Pielartzik, J. R. Reynolds, *Adv. Mater.* **2000**, *12*, 481-494.
- [15] S. Kirchmeyer, K. Reuter, *J. Mater. Chem.* **2005**, *15*, 2077-2088.
- [16] J. Roncali, *Macromol. Rapid Commun.* **2007**, *28*, 1761-1775.
- [17] U. Salzner, *J. Phys. Chem. B.* **2002**, *106*, 9214-9220.
- [18] D. M. de Leeuw, M. M. J. Simenon, A. R. Brown, R. E. F. Einerhand, *Synth. Met.* **1997**, *87*, 53-59.

- [19] Y. Takeda, T. L. Andrew, J. M. Lobez, A. J. Mork, T. M. Swager, *Angew. Chem.* **2012**, *124*, 9176–9180.
- [20] Z. A. Bao, A. J. Lovinger, J. Brown, *J. Am. Chem. Soc.* **1998**, *120*, 207–208.
- [21] A. Facchetti, M.-H. Yoon, C. L. Stern, H. E. Katz, T. J. Marks, *Angew. Chem., Int. Ed. Engl.* **2003**, *42*, 3900-3903.
- [22] M. Mamada, H. Shima, Y. Yoneda, T. Shimano, N. Yamada, K. Kakita, T. Machida, Y. Tanaka, S. Aotsuka, D. Kumaki, S. Tokito, *Chem. Mater.* **2015**, *27*, 141-147.
- [23] A. R. Brown, S. M. de Leeuw, E. J. Lous, E. E. Havinga, *Synth. Met.* **1994**, *66*, 257–261.
- [24] B. A. Jones, A. Facchetti, T. J. Marks, M. R. Wasielewski, *Chem. Mater.* **2007**, *19*, 2703–2705.
- [25] G. Horowitz, F. Kouki, P. Spearman, D. Fichou, C. Nogues, X. Pan, F. Garnier, *Adv. Mater.* **1996**, *8*, 242–245.
- [26] H. E. Katz, A. J. Lovinger, J. Johnson, C. Kloc, T. Siegrist, W. Li, Y. Y. Lin, A. Dodabalapur, *Nature* **2000**, *404*, 478–481.
- [27] H. Li, F. S. Kim, G. Ren, E. C. Hollenbeck, S. Subramaniyan, S. A. Jenekhe, *Angew. Chem., Int. Ed. Engl.* **2013**, *52*, 5513-5517.
- [28] A. Babel, S. A. Jenekhe, *J. Am. Chem. Soc.* **2003**, *125*, 13656–13567.
- [29] Z. Chen, Y. Zheng, H. Yan, A. Facchetti, *J. Am. Chem. Soc.* **2009**, *131*, 8–9.
- [30] H. Yan, Z. Chen, Y. Zheng, C. Newman, J. R. Quinn, F. Dotz, M. Kastler, A. Facchetti, *Nature* **2009**, *457*, 679–686.
- [31] X. Guo, F. S. Kim, M. J. Seger, S. A. Jenekhe, M. D. Watson, *Chem. Mater.* **2012**, *24*, 1434–1442.
- [32] H. Li, F. S. Kim, G. Ren, S. A. Jenekhe, *J. Am. Chem. Soc.* **2013**, *135*, 14920–14923.
- [33] J. Choi, H. Song, N. Kim, F. S. Kim, *Semicond. Sci. Technol.* **2015**, *30*, 064002.
- [34] R. J. Mortimer, *Chem Soc. Rev.* **1997**, *26*, 147-156.
- [35] S. K. Deb, *Appl. Opt. Suppl.* **1969**, *3*, 192-195.
- [36] P. D. Beer, O. Kocian, R. J. Mortimer, C. Ridgway, *J. Chem. Soc., Faraday Trans.* **1993**, *89*, 333-338.

- [37] H. Byker, in *Electrochromic Materials 11*, Ho, K.-C., MacArthur, D. A., Eds., *Electrochem. Soc. Proc. Ser.* Pennington: New Jersey, 1994.
- [38] M. Green, *Chem. Ind.* **1996**, *17*, 641-644.
- [39] A. Kraft, *Bull. Hist. Chem.* **2008**, *33*, 61-67.
- [40] P. M. S. Monk, R. J. Mortimer, D. R. Rosseinsky, *Electrochromism: Fundamentals and Applications*, VCH: New York, 1995.
- [41] J. J. Berzelius, *Afb. Fys. Kemi Miner.* **1815**, *4*, 293.
- [42] F. Wöhler, *Ann. Phys.* **1824**, *2*, 350-358.
- [43] P. M. S. Monk, R. J. Mortimer, D. R. Rosseinsky, *Electrochromism and Electrochromic Devices*, Cambridge Univ. Press: Cambridge, 2007.
- [44] C. G. Granqvist, *Handbook of Inorganic Electrochromic Materials*, Elsevier: Amsterdam, 1995.
- [45] T. A. Skotheim, J. R. Reynolds, *Handbook of Conducting Polymers*, CRC: Boca Raton, 2007.
- [46] J. Roncali, *Chem. Rev.*, **1992**, *92*, *4*, 711-738.
- [47] A. L. Dyer, E. J. Thompson, J. R. Reynolds, *ACS Appl. Mater. Interfaces* **2011**, *3*, 1787-1795.
- [48] C. M. Amb, J. A. Kerszulis, E. J. Thompson, A. L. Dyer, J. R. Reynolds, *Polym. Chem.* **2011**, *2*, 812-814.
- [49] R. C. Gonzalez, R. E. Woods, *Digital Image Processing*, Addison-Wesley, 1993.
- [50] W. K. Pratt, *Digital Image Processing*, John Wiley & Sons: New York, 1991.
- [51] C. Ponyton, *Digital Video and HD: Algorithms and Interfaces*, San Francisco: Elsevier, 2003.
- [52] N. Boughen, *Lightwave 3D 7.5 Lighting*, Wordware Publishing: Texas, 2003
- [53] T. Deutschmann, S. Roth, E. Oesterschulze, *J. Micromech. Microeng.* **2013**, *23*, 065032.
- [54] A. Balan, G. Gunbas, A. Durmus, L. Toppare, *Chem. Mater.* **2008**, *20*, 7510-7513.
- [55] B. Karabay, L. C. Pekel, Atilla Cihaner, *Macromolecules* **2015**, *48*, 1352-1357.
- [56] M. I. Ozkut, S. Atak, A. M. Onal, A. Cihaner, *J. Mater. Chem.* **2011**, *21*, 5268-5272.
- [57] C. M. Amb, P. M. Beaujuge, J. R. Reynolds, *Adv. Mater.* **2010**, *22*, 724-728.

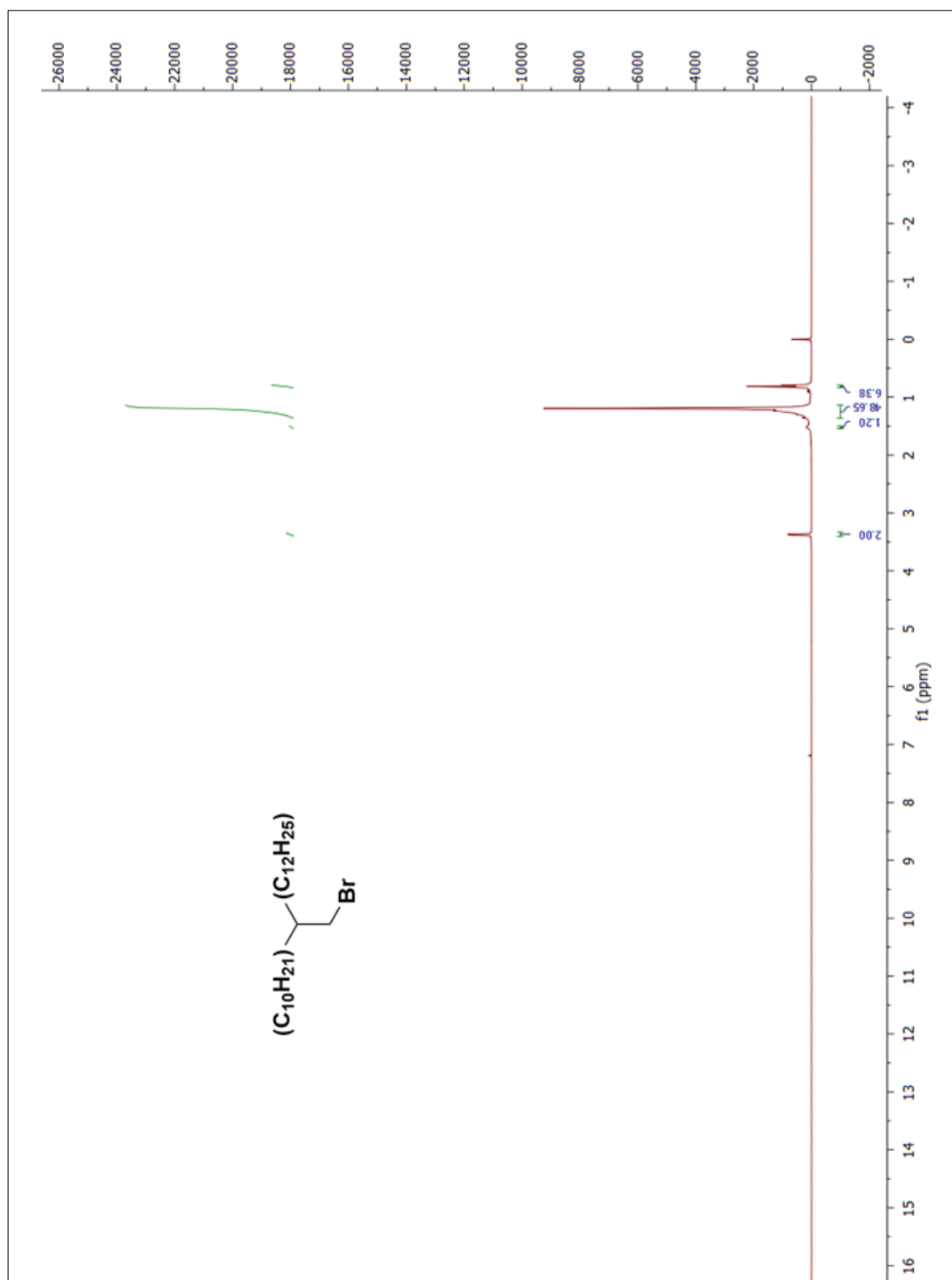
- [58] R. Yuksel, E. Ataoglu, J. Turan, E. Alpugan, S. O. Hacioglu, L. Toppare, A. Cirpan, H. E. Unalan, G. Gunbas, *J. Polym. Sci., Polym. Chem.* **2017**, *55*, 1680–1686.
- [59] G. Sonmez, C. K. F. Shen, F. Rubin, F. Wudl, *Angew. Chem., Int. Ed.* **2004**, *43*, 1498-1502.
- [60] A. Durmus, E. G. Gunbas, P. Camurlu, L. Toppare, *Chem. Commun.* **2007**, 3246-3248.
- [61] G. Gunbas, A. Durmus, L. Toppare, *Adv. Mater.* **2008**, *20*, 691-695.
- [62] G. Gunbas, A. Durmus, L. Toppare, *Adv. Funct. Mater.* **2008**, *18*, 2026-2030.
- [63] P. M. Beaujuge, S. Ellinger, J. R. Reynolds, *Adv. Mater.* **2008**, *20*, 2772-2776.
- [64] A. L. Dyer, M. R. Craig, J. E. Babiarz, K. Kiyak, J. R. Reynolds, *Macromolecules*, **2010**, *43*, 4460-4467.
- [65] X. Chen, Z. Xu, S. Mi, J. Zhenga, C. Xu, *New J. Chem.* **2015**, *39*, 5389-5394.
- [66] Z. Xu, X. Chen, S. Mi, J. Zheng, C. Xu, *Org. Electron.* **2015**, *26*, 129-136.
- [67] G. Atakana, G. Gunbas, *RSC Adv.* **2016**, *6*, 25620–25623.
- [68] J. Roncali, *Chem. Rev.* **1997**, *97*, 173-206.
- [69] F. Babudri, G. M. Farinola, F. Nasa, R. Ragni, *Chem. Commun.* **2007**, 1003-1022.
- [70] M. Losurdo, M. M. Giangregorio, P. Capezzuto, A. Cardone, C. Martinelli, G. M. Farinola, F. Babudri, F. Naso, M. Büchel, G. Bruno, *Adv. Mater.* **2009**, *21*, 1115-1120.
- [71] R. J. Mortimer, *Electrochim. Acta.* **1999**, *44*, 2971-2981.
- [72] J. C. Lacroix, K. K. Kanazawa, A. J. Diaz, *Electrochem. Soc.* **1989**, *136*, 1308-1313.
- [73] J.-C. Ching, A. G. MacDiarmid, *Synth. Met.* **1986**, *13*, 193-205.
- [74] D. M. Welsh, A. Kumar, E. W. Meijer, J. R. Reynolds, *Adv. Mater.* **1999**, *11*, 1379-1382.
- [75] C. L. Gaupp, K. Zong, P. Schottland, B. C. Thompson, J. R. Reynolds, *Macromolecules*, **2000**, *33*, 1132-1133.
- [76] P. Schottland, K. Zong, C. L. Gaupp, B. C. Thompson, C. A. Thomas, I. Giurgiu, R. Hickman, K. A. Abboud, J. R. Reynolds, *Macromolecules* **2000**, *33*, 7051-7061.
- [77] G. Sonmez, I. Schwendeman, P. Schottland, K. Zong, J. R. Reynolds, *Macromolecules* **2003**, *36*, 639-647.

- [78] G. A. Sotzing, J. L. Reddinger, A. R. Katritzky, J. Soloducho, R. Musgrave, J. R. Reynolds, *Chem. Mater.* **1997**, *9*, 1578-1587.
- [79] D. J. Irvin, C. J. DuBois, J. R. Reynolds, *Chem. Commun.* **1999**, 2121-2122.
- [80] C. J. DuBois, J. R. Reynolds, *Adv. Mater.* **2002**, *14*, 1844-1846.
- [81] A. A. Argun, P.-H. Aubert, B. C. Thompson, I. Schwendeman, C. L. Gaupp, J. Hwang, N. J. Pinto, D. B. Tanner, A. G. MacDiarmid, J. R. Reynolds, *Chem. Mater.* **2004**, *16*, 4401-4412.
- [82] D. Kumar, R. C. Sharma, *Eur. Polym. J.* **1998**, *34*, 1053-1060.
- [83] S. Sadki, P. Schottland, N. Brodie, G. Sabouraud, *Chem. Soc. Rev.* **2000**, *29*, 283-293.
- [84] G. Zotti, *Handbook of Organic Conductive Molecules and Polymers*, Nalwa, H. S. Eds., Wiley: Chichester, 1997.
- [85] M. E. G. Lyons, *Advances in Chemical Physics, Polymeric Systems*, Prigogine, I., Rice, S. A., John Wiley & Sons: New York, 1997.
- [86] G. Zotti, G. Schiavon, A. Berlin, G. Pagani, *Chem. Mater.* **1993**, *5*, 430-436.
- [87] P. Audebert, P. Hapiot, *Synthetic Metal* **1999**, *75*, 95.
- [88] K. Yoshino, S. Hayashi, R. Sugimoto, *Japanese Journal of Applied Physics* **1984**, *23*, L899.
- [89] N. Miyaura, A. Suzuki, *Synth. Commun.* **1981**, *11*, 513-519.
- [90] T. Yokozawa, H. Kohno, Y. Ohta, A. Yokoyama, *Macromolecules* **2010**, *43*, 7095-7100.
- [91] D. Milstein, J. K. Stille, *J. Am. Chem. Soc.* **1978**, *100*, 3636-3638.
- [92] Z. Bao, W. Chan, L. Yu, *Chem. Mater.* **1993**, *5*, 2-3.
- [93] T. Yamamoto, *Chem. Lett.* **2012**, *41*, 1422-1424.
- [94] E. Knoevenagel, *Chem. Ber.* **1894**, *27*, 2345-2346.
- [95] D. C. Forbes, *Tetrahedron Letters* **2006**, *47*, 1699-1703.
- [96] J. Liao, Q. Wang, *Macromolecules* **2004**, *37*, 7061-7063.
- [97] K. Tamao, M. Kumada, *J. Am. Chem. Soc.* **1972**, *94*, 4374-4392.
- [98] J. P. Corriu, J. P. Masse, *Chem. Commun.* **1972**, 144a.
- [99] S. Murahashi, *J. Organomet. Chem.* **1975**, *91*, C39.
- [100] K. Tamao, *J. Organomet. Chem.* **2002**, *653*, 23-26.

- [101] S. Xu, E. H. Kim, A. Wei, E. Negishi, *Sci. Technol. Adv. Mater.* **2014**, *15*, 044201.
- [102] K. Sonogashira, Y. Tohda, N. Hagihara, *Tetrahedron Letters* **1975**, *50*, 4467-4470.
- [103] L. B. Sessions, B. R. Cohen, R. B. Grubbs, *Macromolecules* **2007**, *40*, 1926-1933.
- [104] X. Guo, M. D. Watson, *Org. Lett.* **2008**, *10*, 5333-5336.
- [105] E. Hussain, H. Zhou, N. Yang, S. A. Shahzad, C. Yu, *Dyes and Pigment*, **2017**, *147*, 211-224.
- [106] S. Vajiravelu, L. Ramunas, G. J. Vidas, G. Valentas, J. Vygintasc, S. Valiyaveetti, *J. Mater. Chem.* **2009**, 4268–4275.
- [107] C.-W. Ge, C.-Y. Mei, J. Ling, J.-T. Wang, F.-G. Zhao, L. Liang, H.-J. Li, Y.-S. Xie, W.-S. Li, *J. Polym. Sci., Polym. Chem.* **2014**, *52*, 1200–1215.
- [108] B. Joussetme, P. Blanchard, E. Levillain, R. de Bettignies, J. Roncali, *Macromolecules* **2003**, *36*, 3020-3025.
- [109] Y.-S. Shon, T. R. Lee, *Langmuir* **1999**, *15*, 1136-1140.
- [110] X. Chen, B. Liu, Y. Zou, W. Tang, Y. Li, D. Xiao, *RSC Adv.* **2012**, *2*, 7439-7448.
- [111] M. Imit, P. Imin, A. Adronov, *Polym. Chem.* **2016**, *7*, 5241–5248.
- [112] P. M. Beaujuge, S. V. Vasilyeva, D. Y. Liu, S. Ellinger, T. D. McCarley, J. R. Reynolds, *Chem. Mater.* **2012**, *24*, 255-268.
- [113] P. Camurlu, *RSC Adv.*, **2014**, *4*, 55832–55845.
- [114] P. I. Lee, S. L. C. Hsu, P. Lin, *Macromolecules* **2010**, *43*, 8051-8057.
- [115] A. V. Patil, W. H. Lee, E. Lee, K. Kim, I. N. Kang, S. H. Lee, *Macromolecules* **2011**, *44*, 1238-1241.
- [116] G. Gunbas, L. Toppare, *Chem. Commun.* **2012**, *48*, 1083–1101.

## APPENDICES

### A. NMR Spectra of Synthesized Monomers



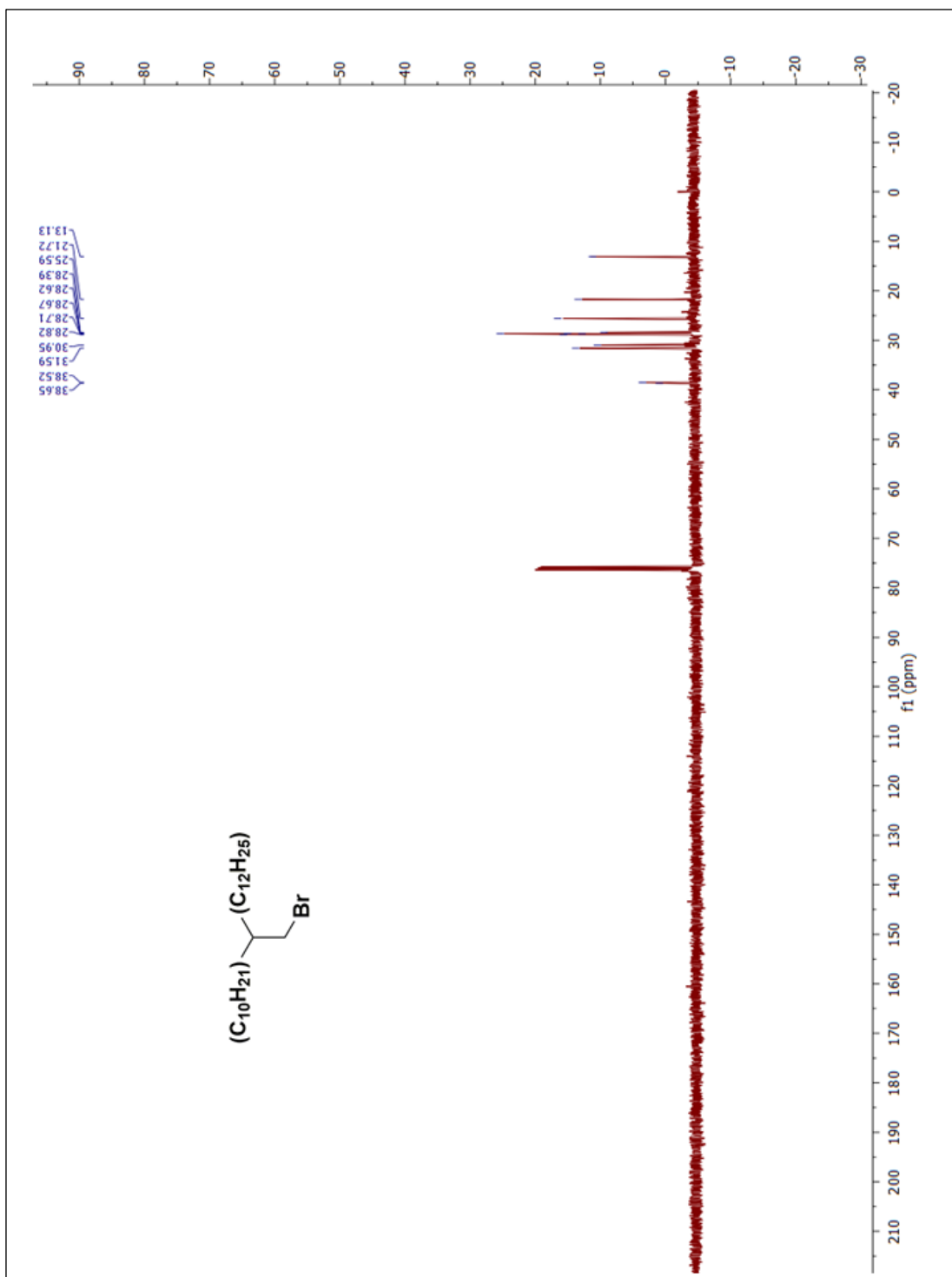


**Figure A.1.2:**  $^{13}C$ -NMR spectrum of 2-decyl-1-tetradecylbromide

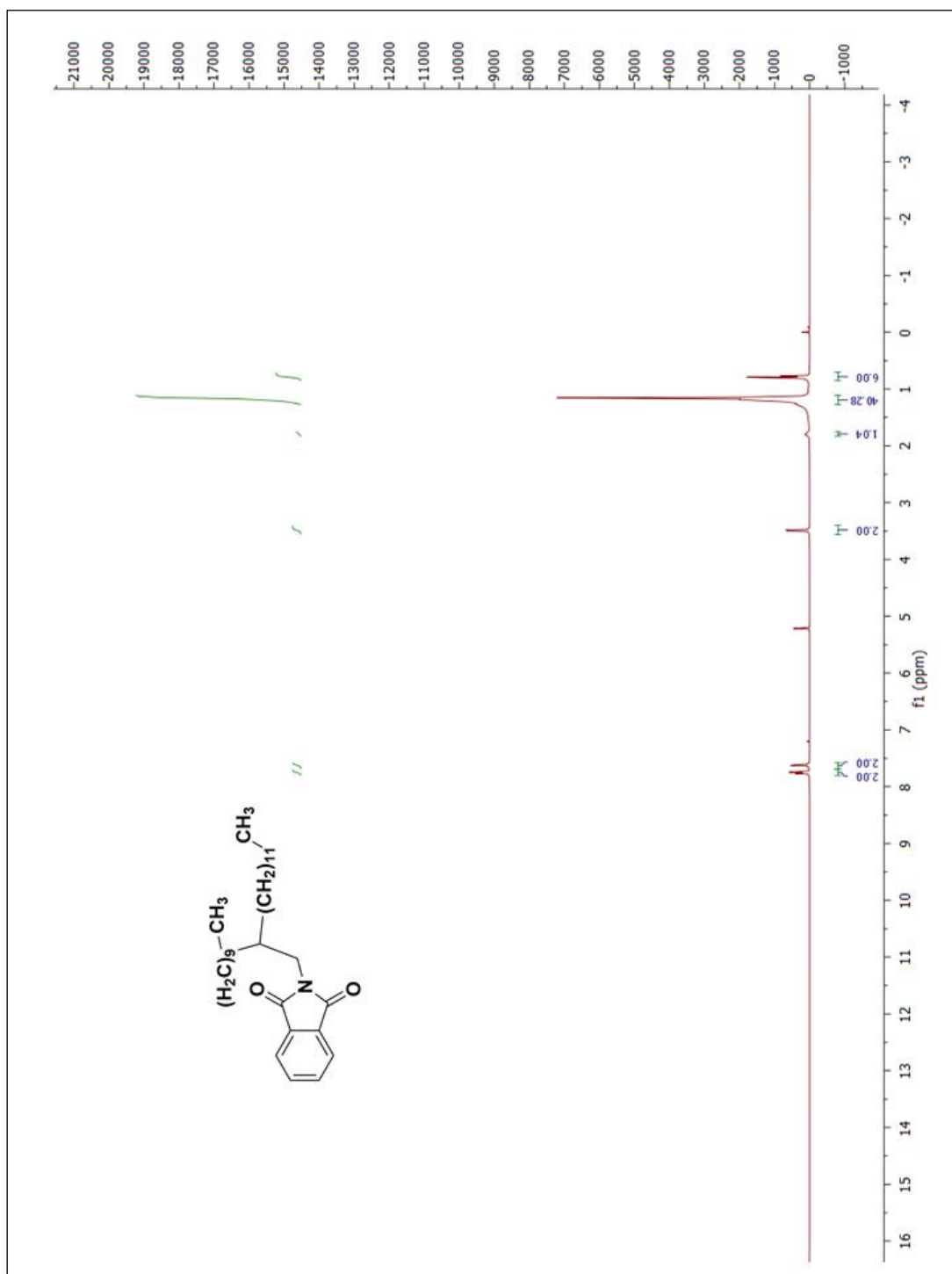


**Figure A.2.1:** <sup>1</sup>H-NMR spectrum N-(2-decyltetradecyl)phthalimide

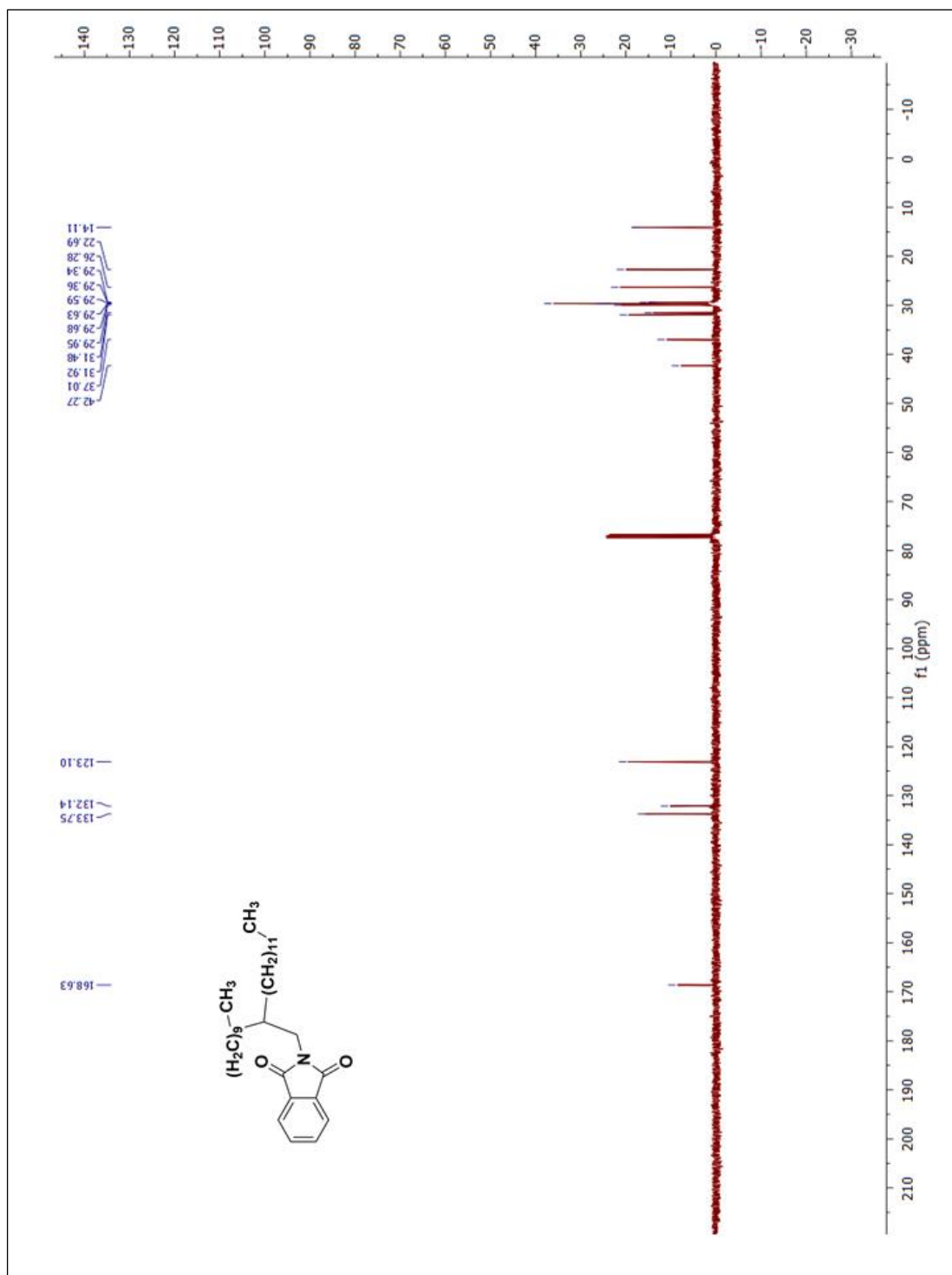


**Figure A.2.2:**  $^{13}\text{C}$ -NMR spectrum of N-(2-decyltetradecyl)phthalimide

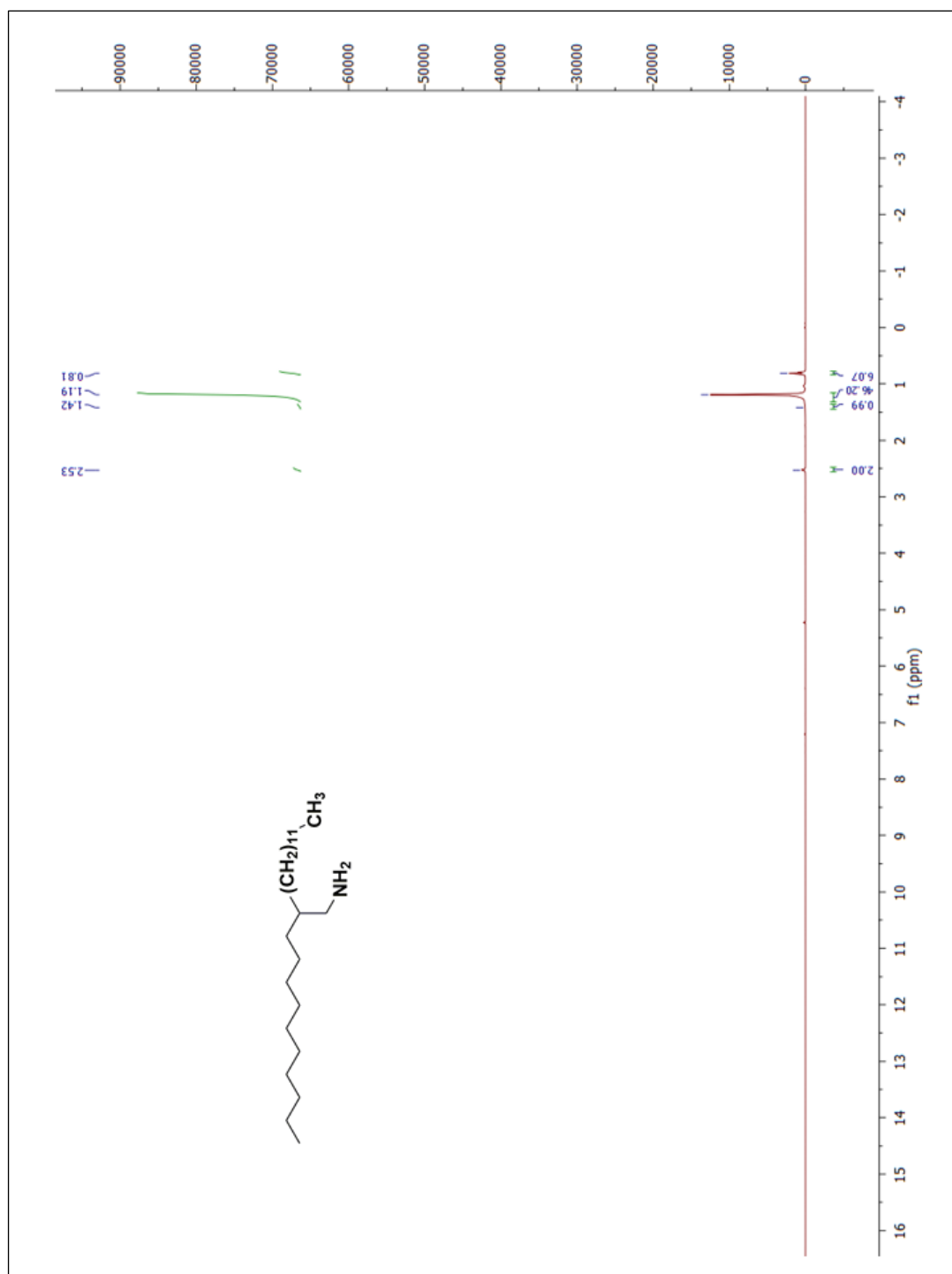


**Figure A.3.1:**  $^1\text{H-NMR}$  spectrum 2-decyl-1-tetradecylamine

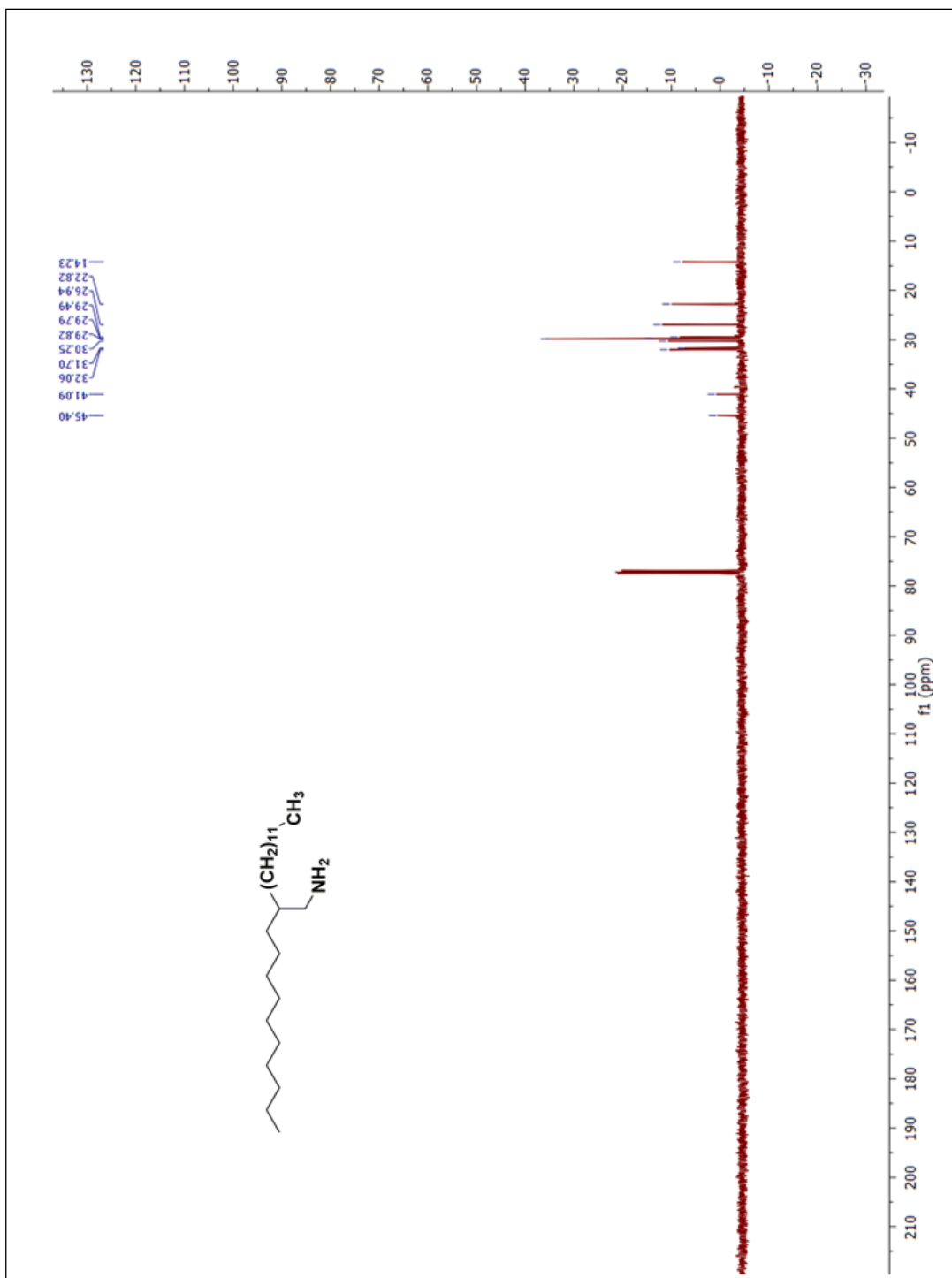


**Figure A.3.2:**  $^{13}\text{C-NMR}$  spectrum of 2-decyl-1-tetradecylamine

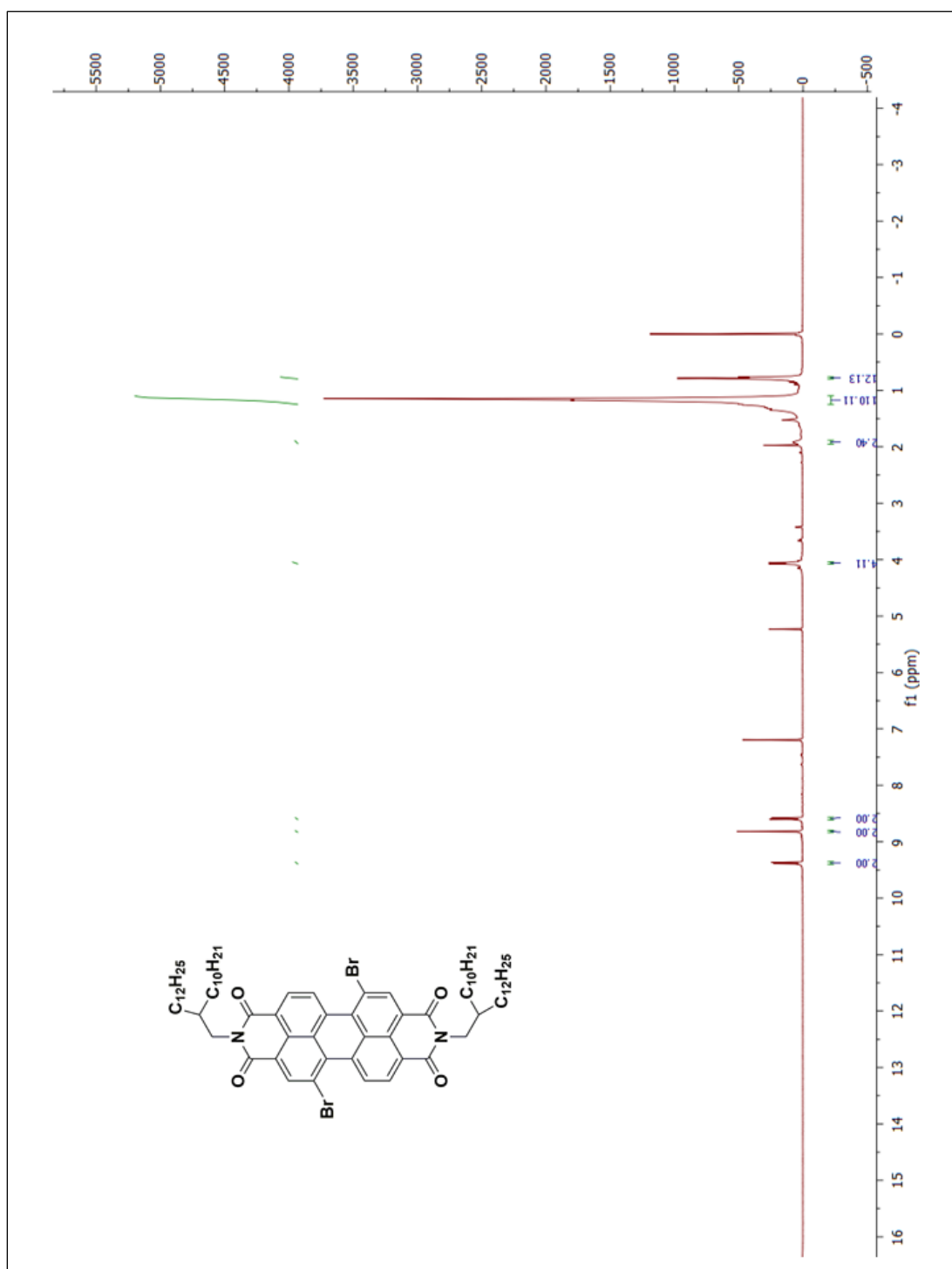


**Figure A.4.1:**  $^1\text{H-NMR}$  spectrum  $N,N'$ -bis(2-decyltetradecyl)-1,6-dibromo-3,4,9,10-perylene diimide

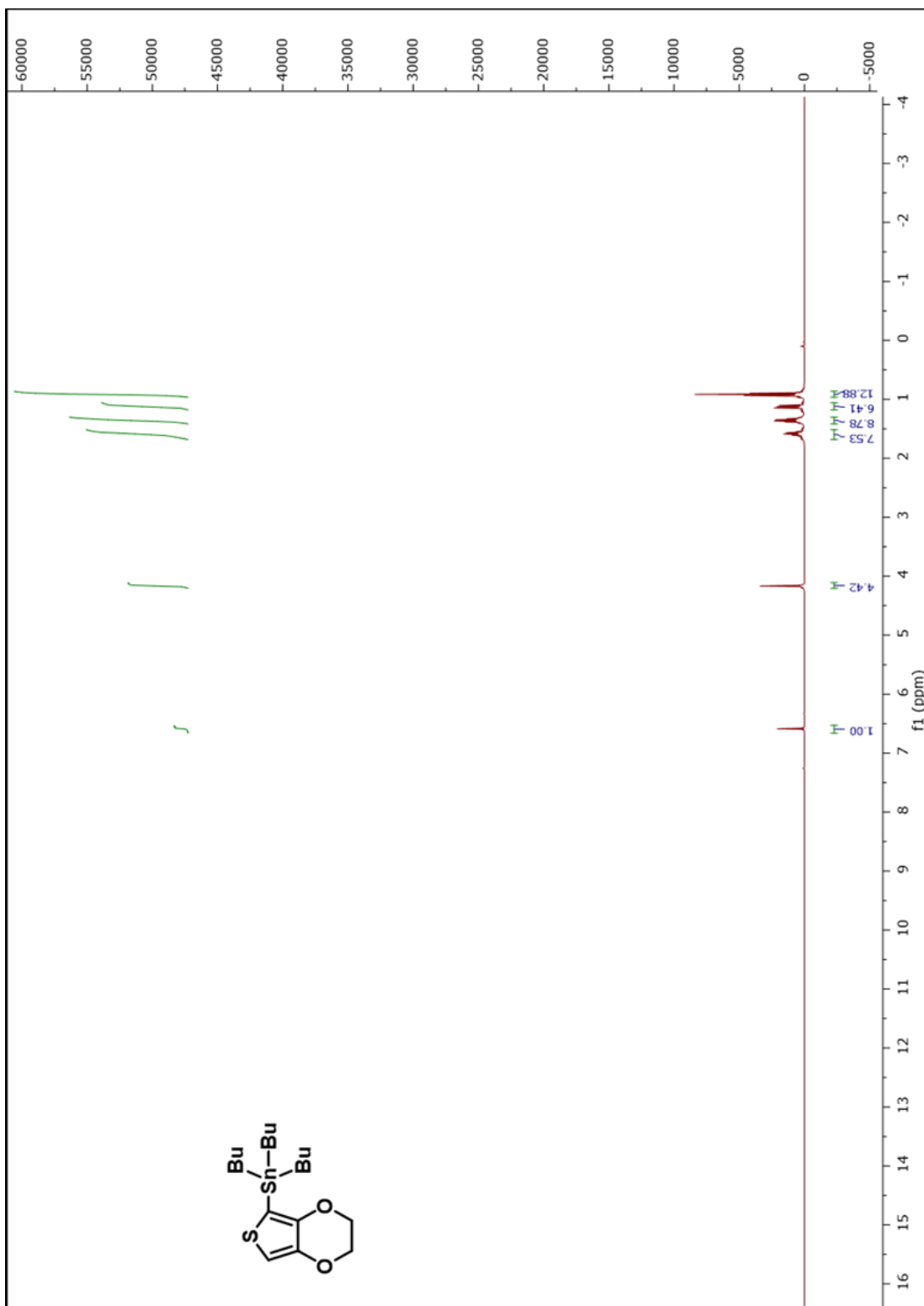


**Figure A.5.1:** <sup>1</sup>H-NMR spectrum of tributyl(2,3-dihydrothieno[3,4-b][1,4]dioxin-5-yl)stannane

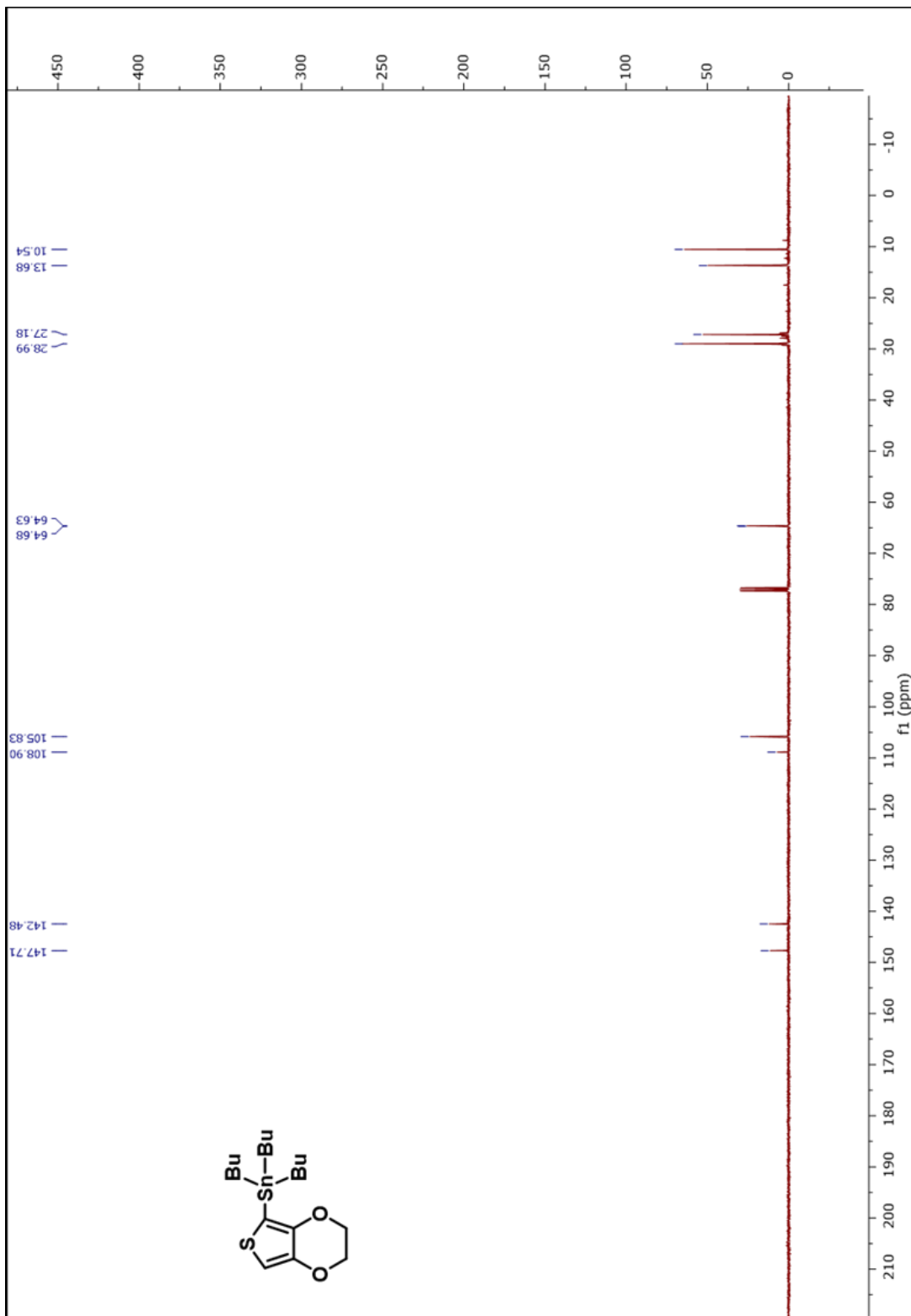


**Figure A.5.2:**  $^{13}\text{C}$ -NMR spectrum of tributyl(2,3-dihydrothieno[3,4-b][1,4]dioxin-5-yl)stannane

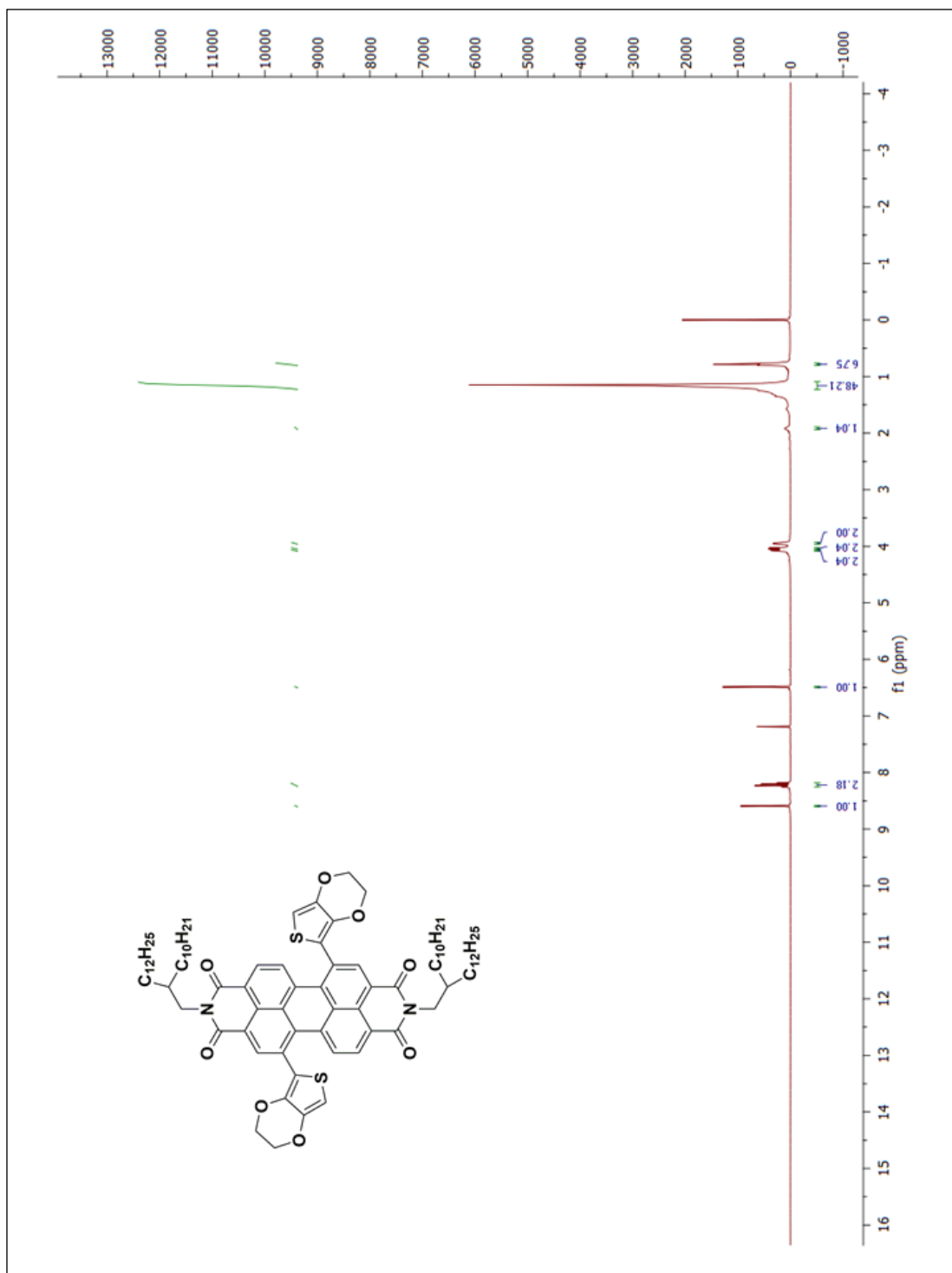


**Figure A.6.1:**  $^1\text{H-NMR}$  spectrum of PDI-e-Dot

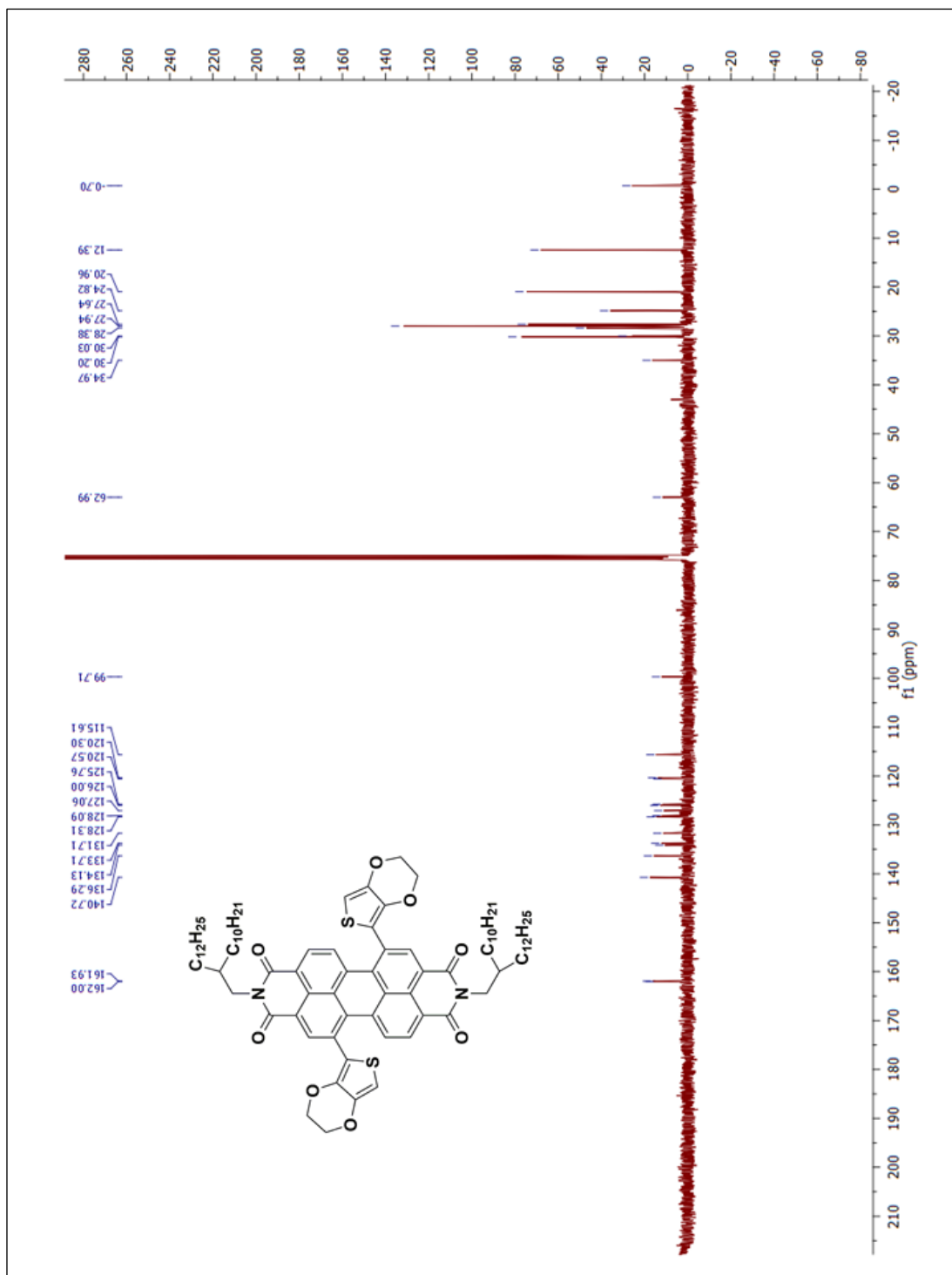


**Figure A.6.2:**  $^{13}\text{C}$ -NMR spectrum of PDI-e-Dot

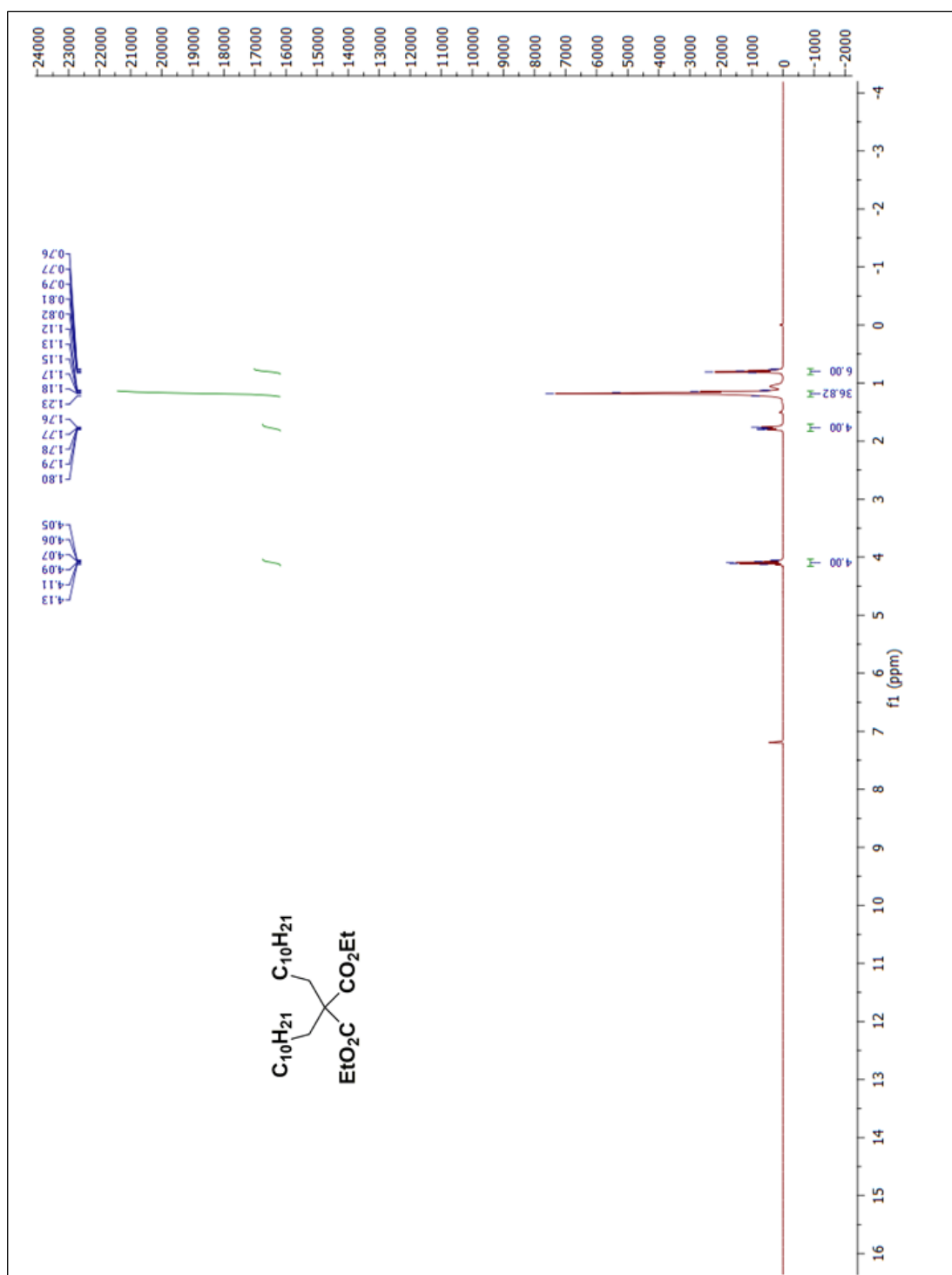


**Figure A.7.1:**  $^1\text{H-NMR}$  spectrum diethyl 2,2-dipentadecylmalonate

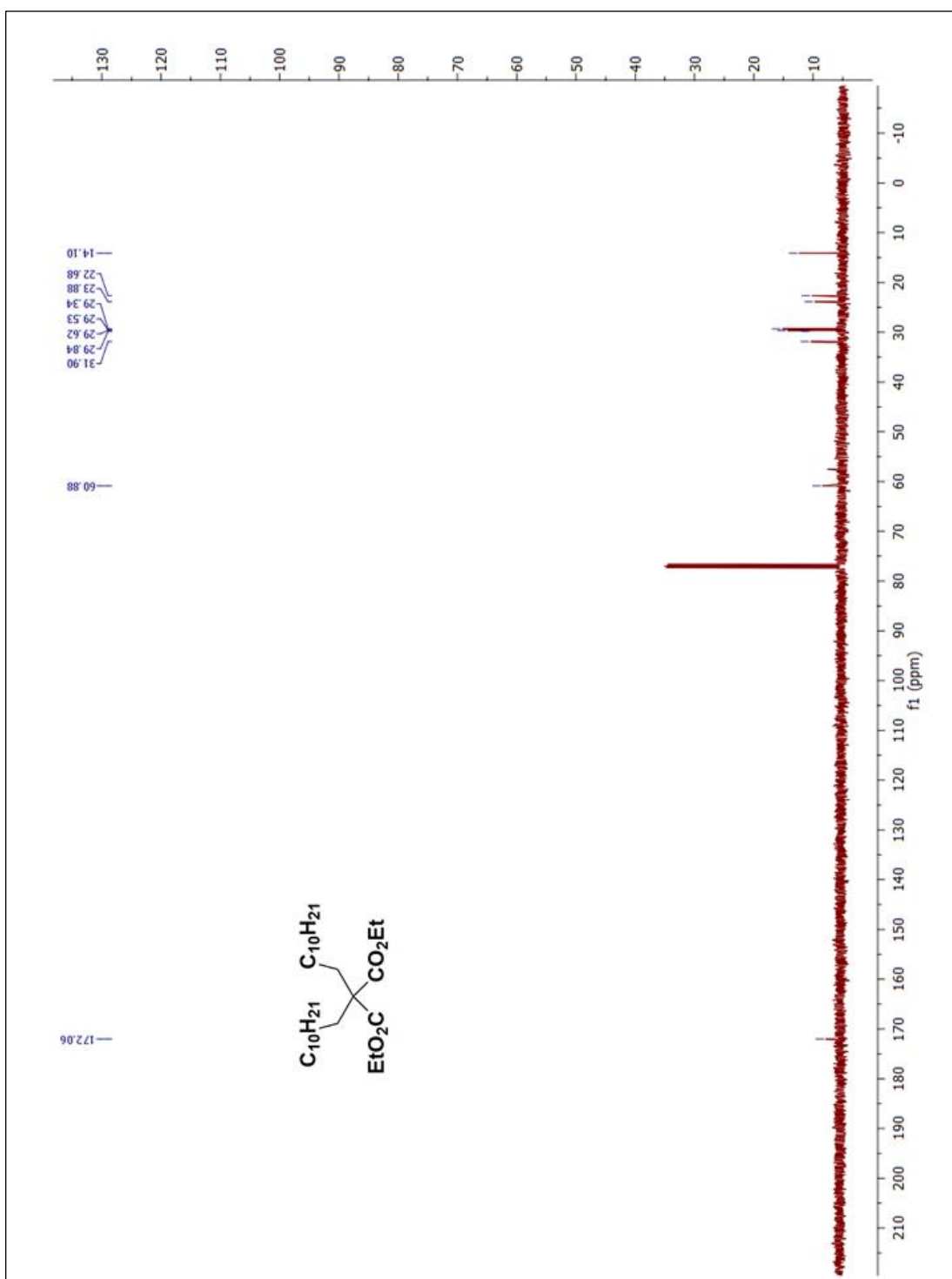


**Figure A.7.2:**  $^{13}\text{C}$ -NMR spectrum diethyl of 2,2-dipentadecylmalonate

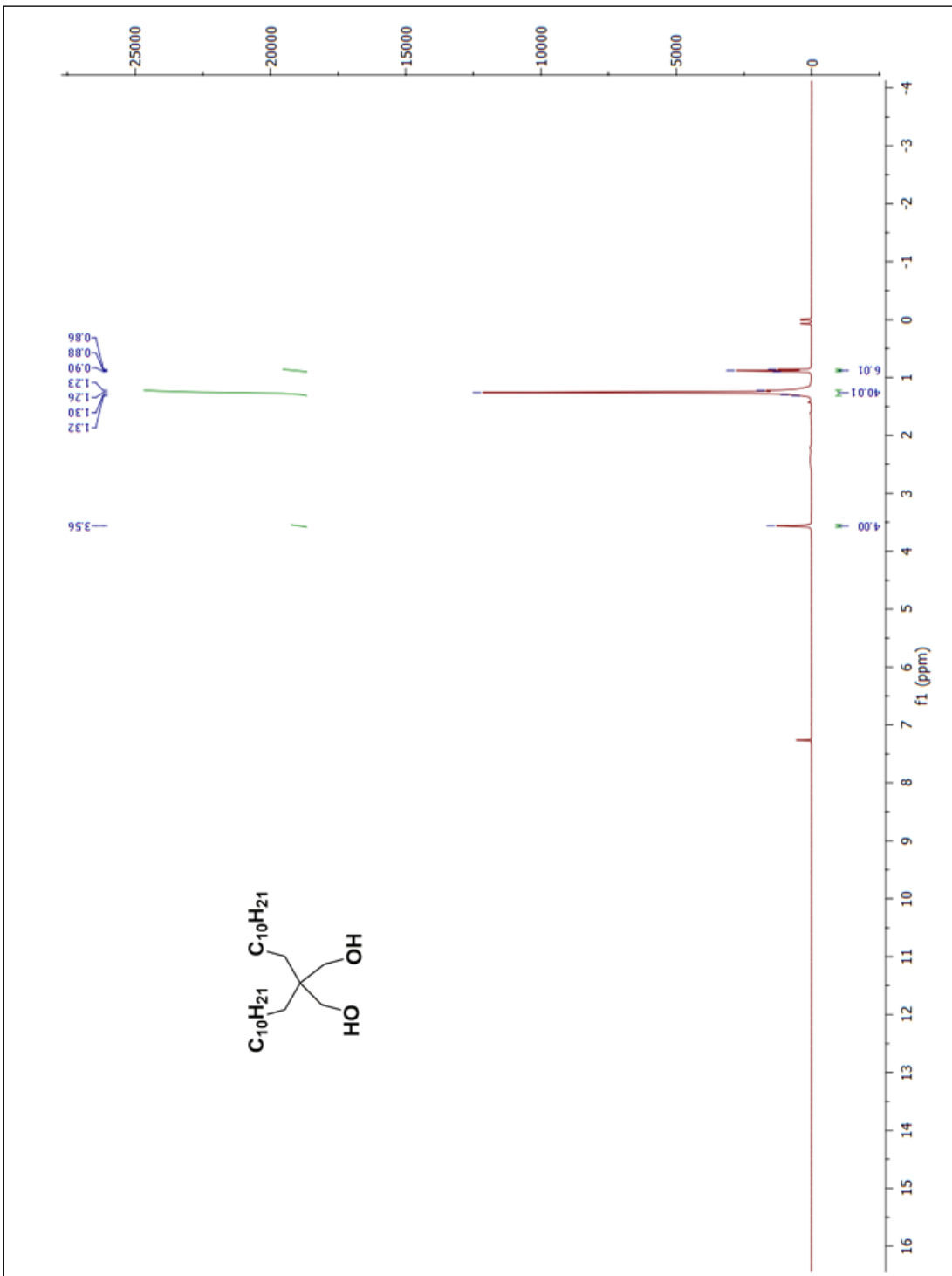


**Figure A.8.1:**  $^1\text{H-NMR}$  spectrum of 2,2-dipentadecyl-1,3-propanediol

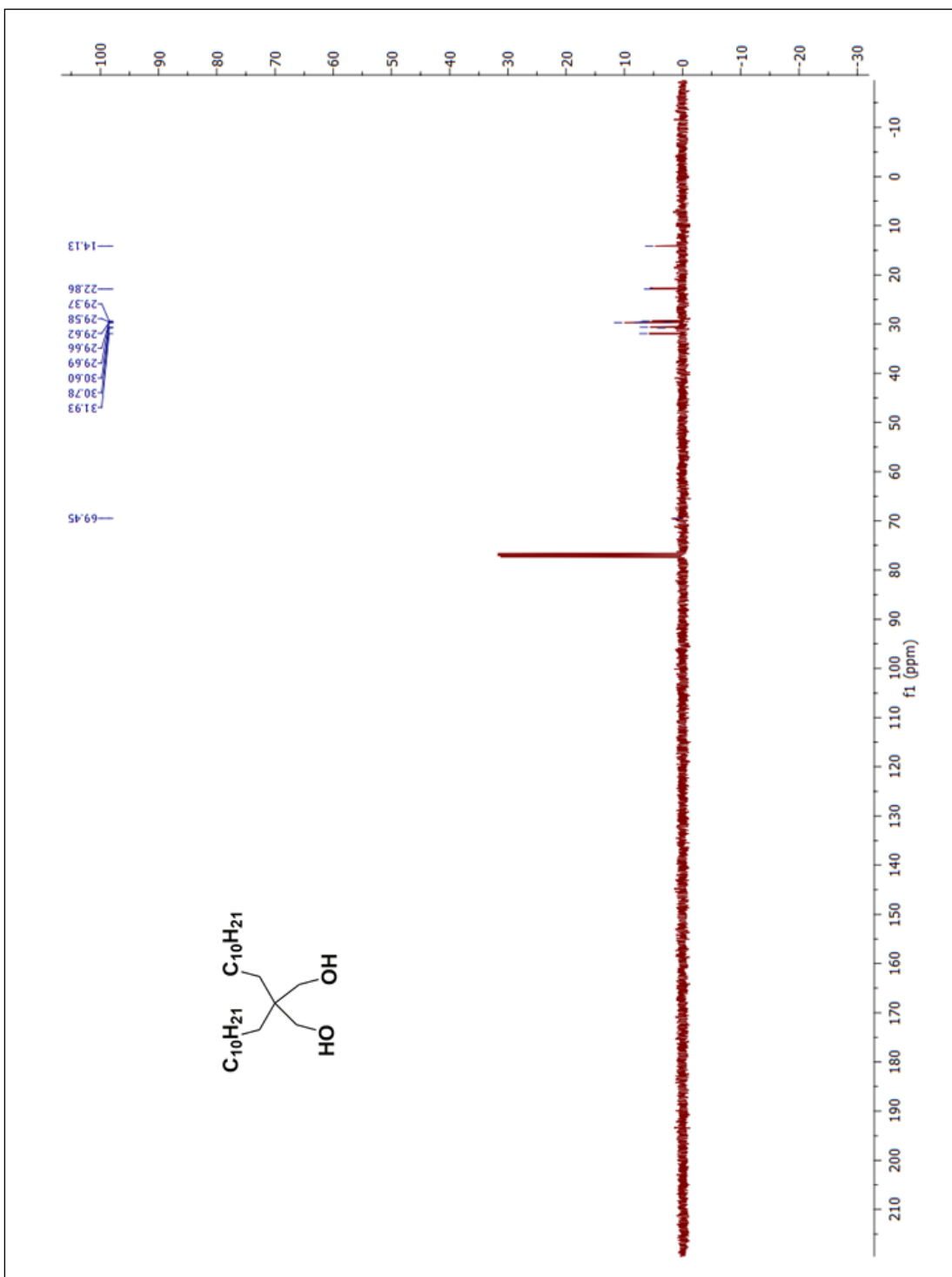


**Figure A.8.2:**  $^{13}\text{C}$ -NMR spectrum of 2,2-dipentadecyl-1,3-propanediol

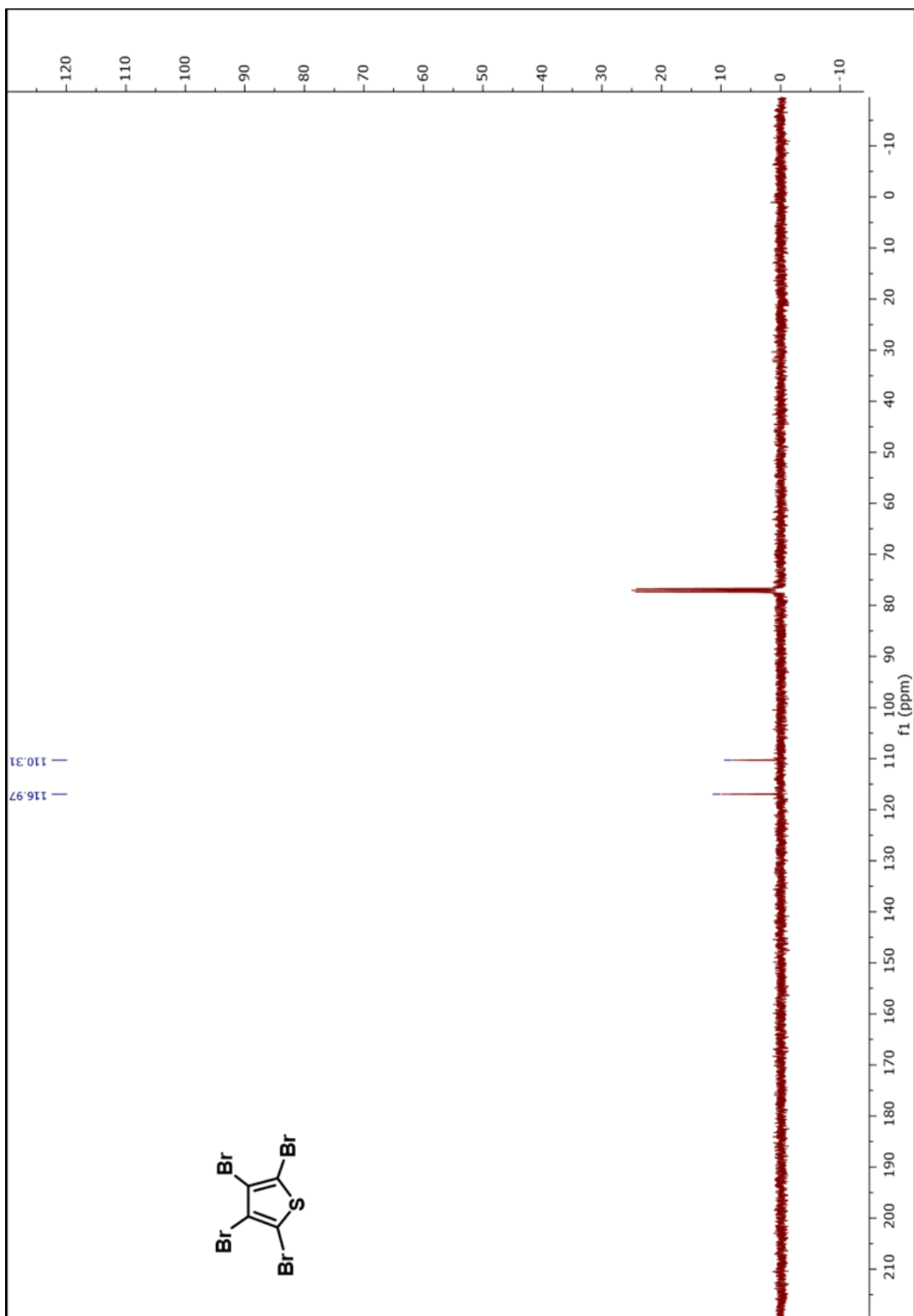
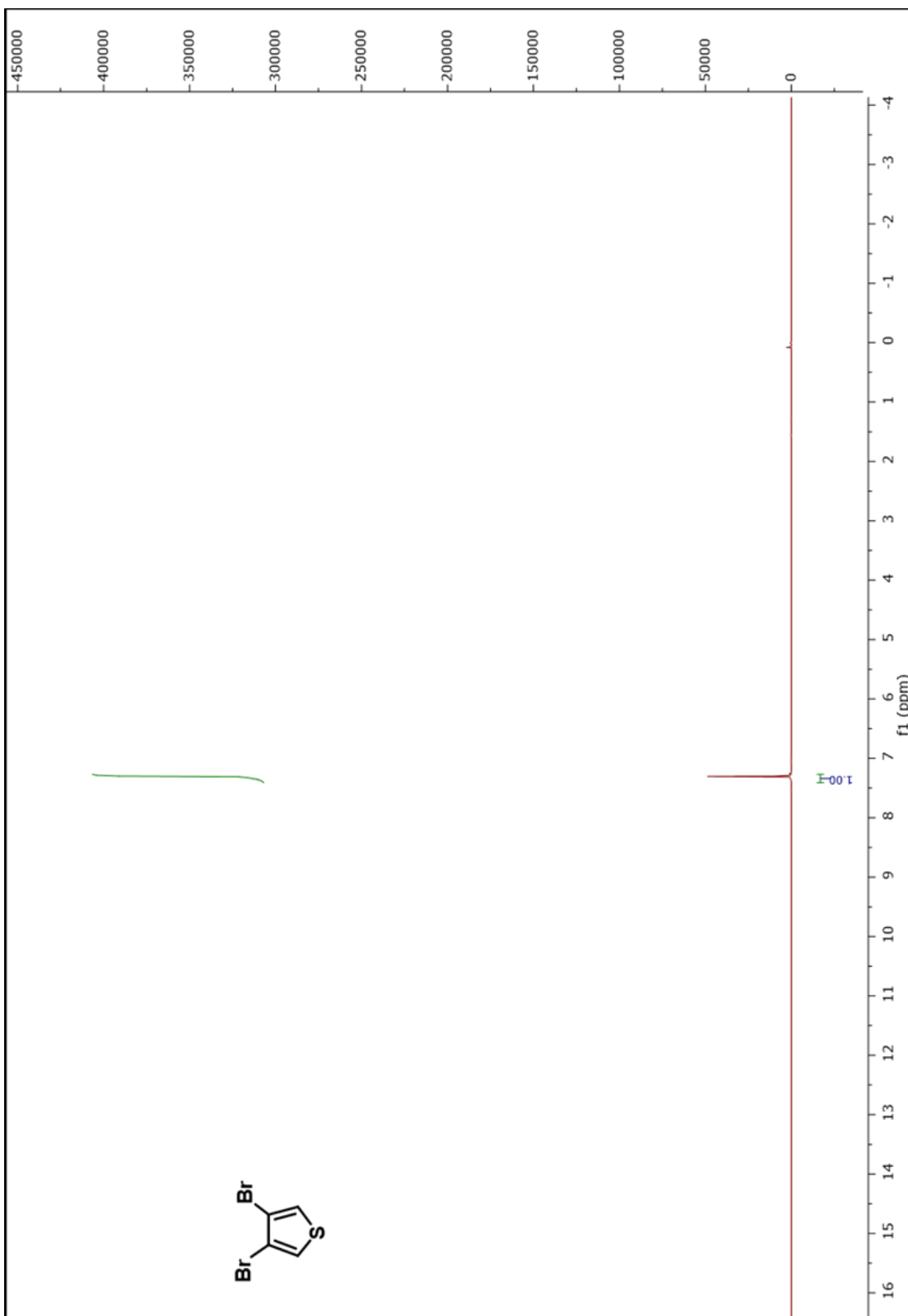
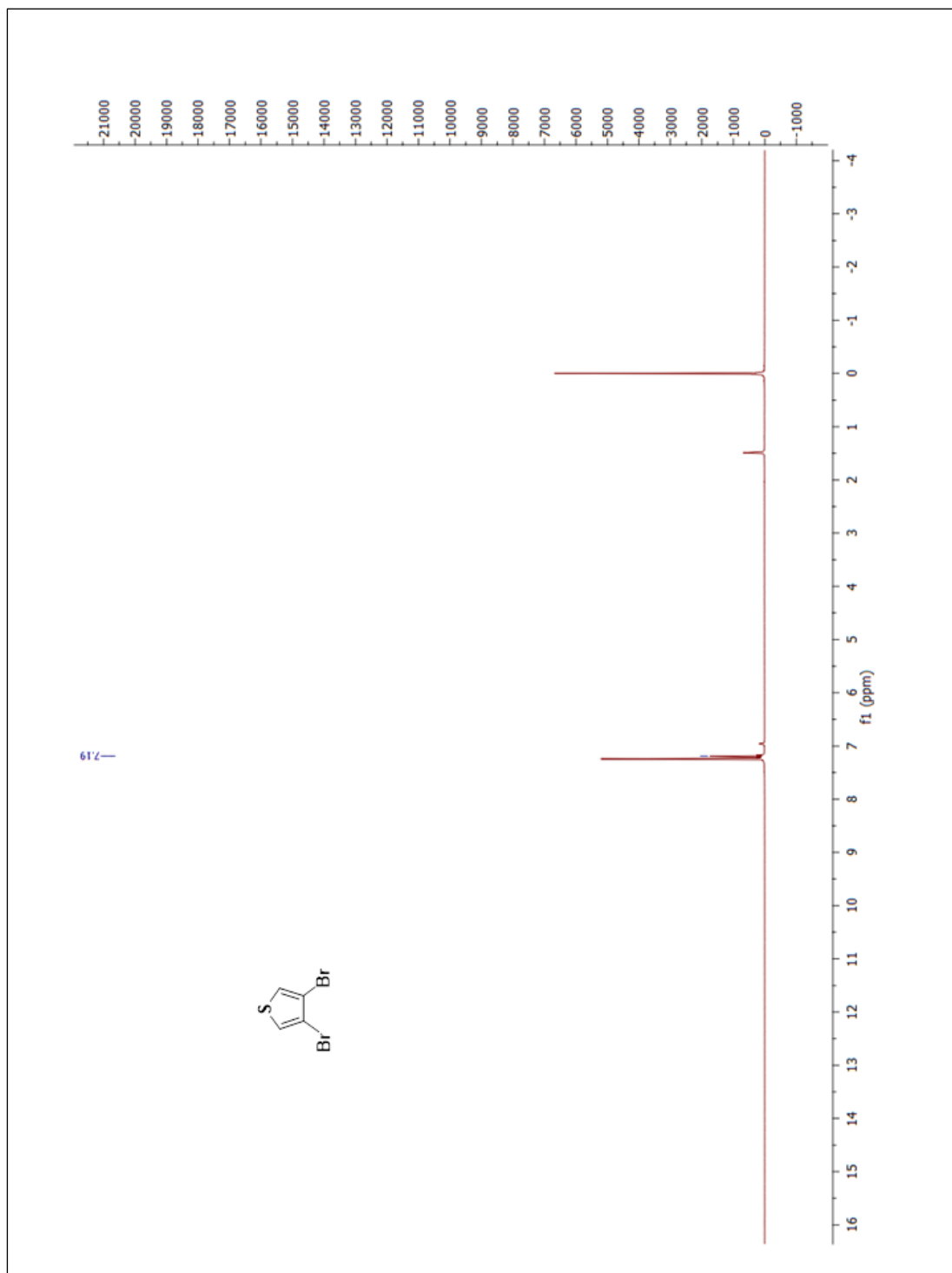


Figure A.9.2:  $^{13}\text{C}$ -NMR spectrum of 2,3,4,5-tetrabromothiophene



**Figure A.10.1:**  $^1\text{H-NMR}$  spectrum of 3,4-dibromothiophene



**Figure A.10.2:**  $^{13}\text{C}$ -NMR spectrum of 3,4-dibromothiophene

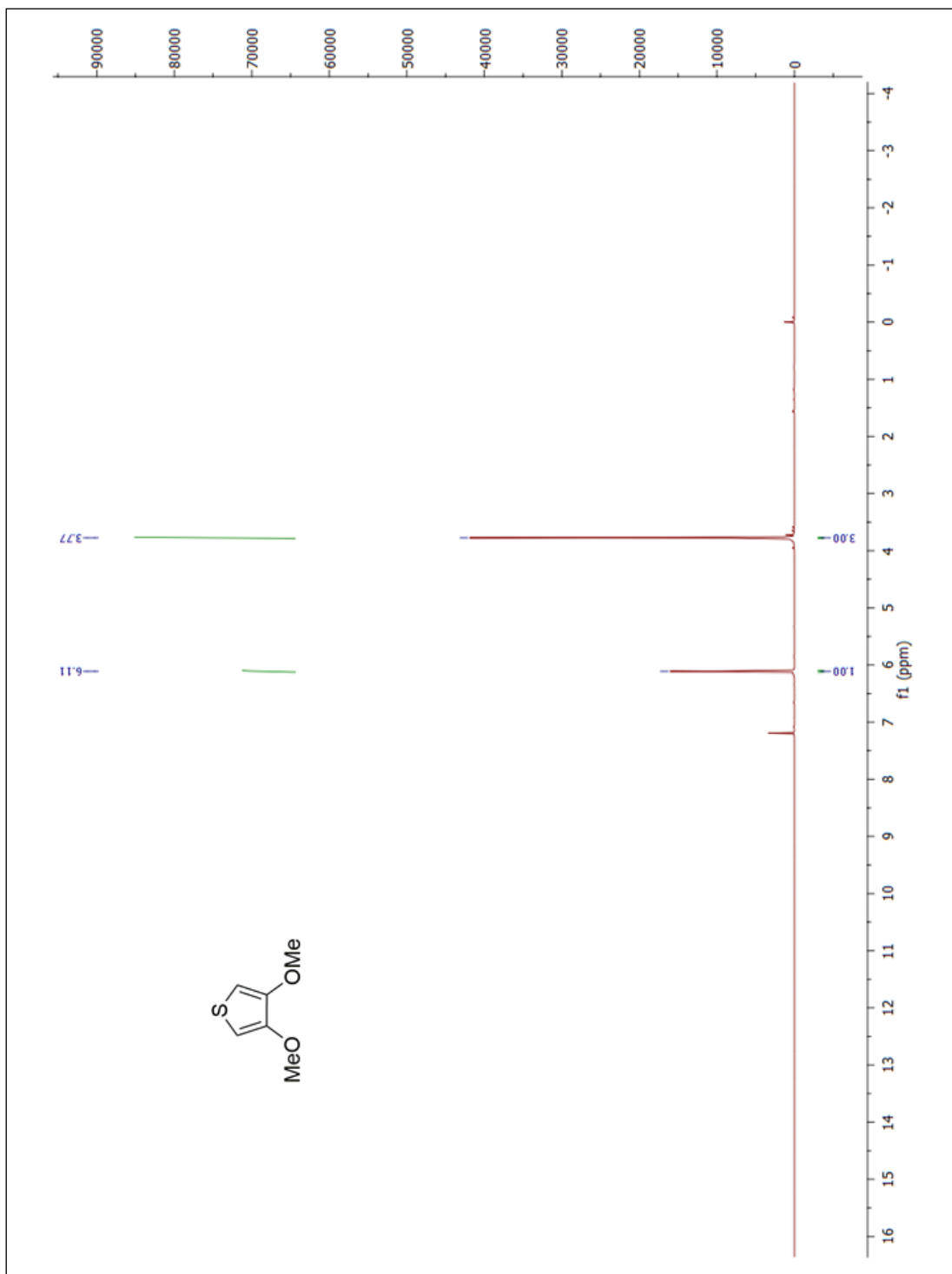


**Figure A.11.1:** <sup>1</sup>H-NMR spectrum of 3,4-dimethoxythiophene

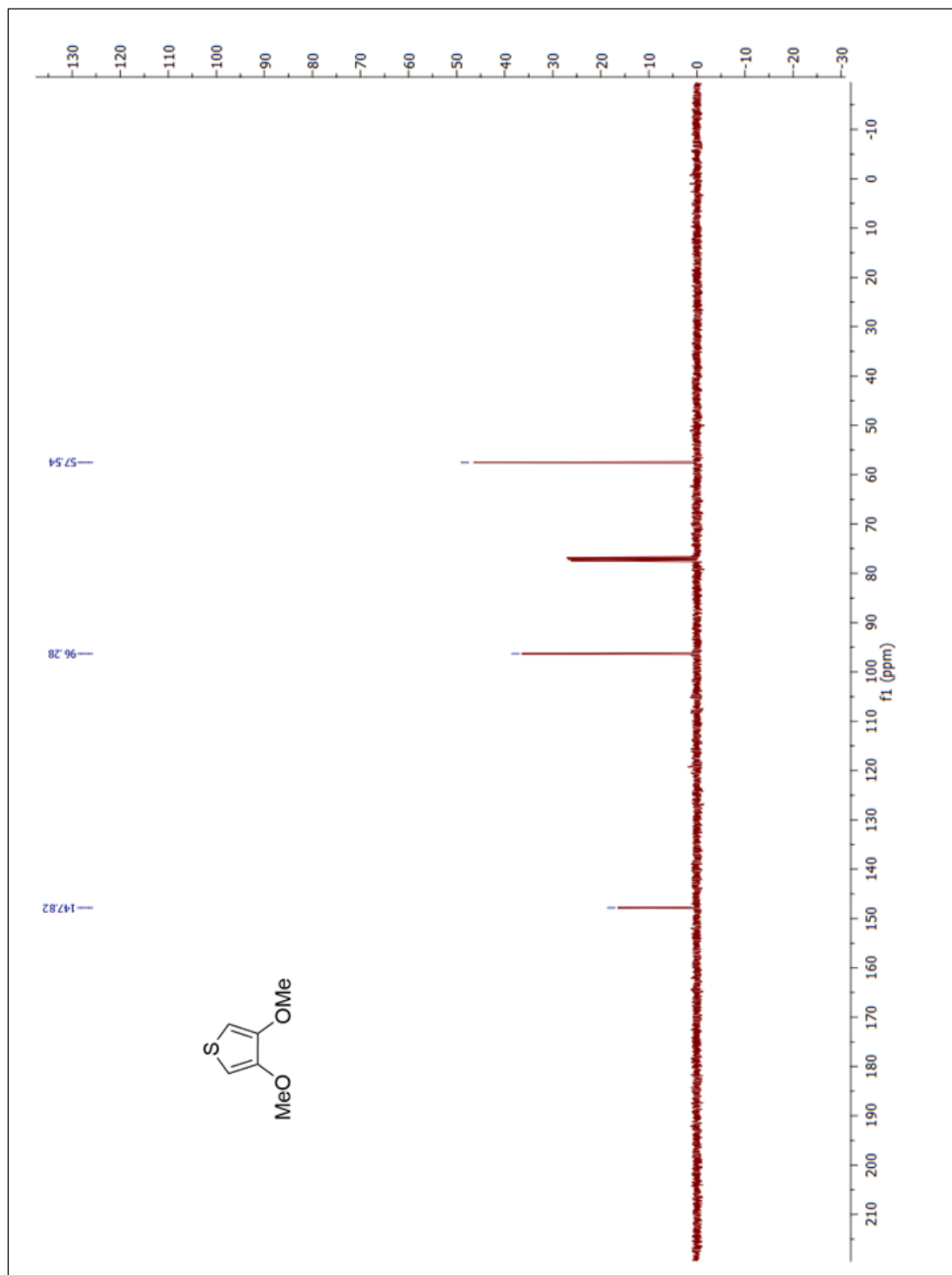


**Figure A.11.2:**  $^{13}\text{C}$ -NMR spectrum of 3,4-dimethoxythiophene

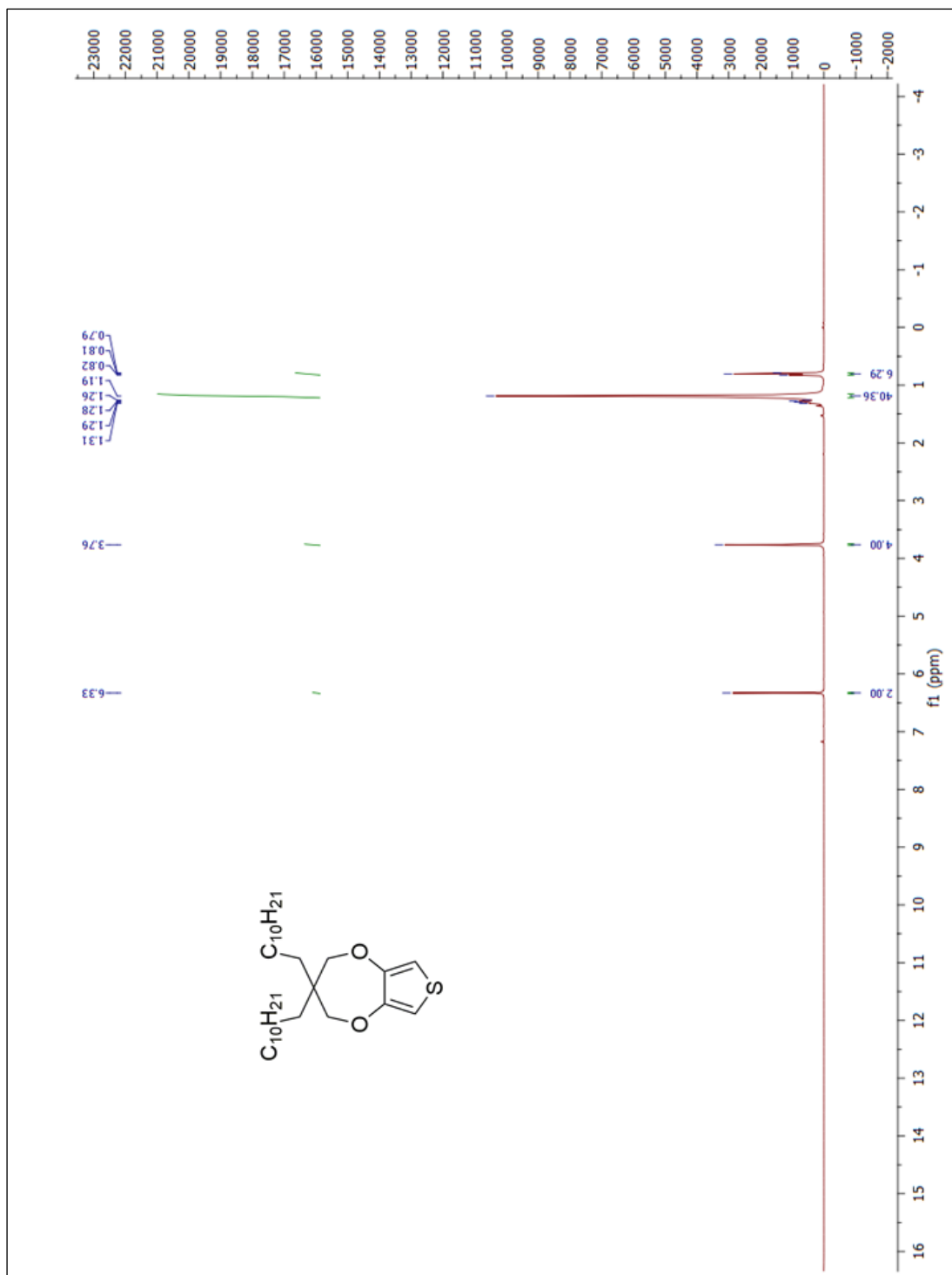


**Figure A.12.1:** <sup>1</sup>H-NMR spectrum of 3,3'-didodecyl-3,4-dihydro-2H-thieno[3,4-b][1,4]dioxepine(ProDOT)

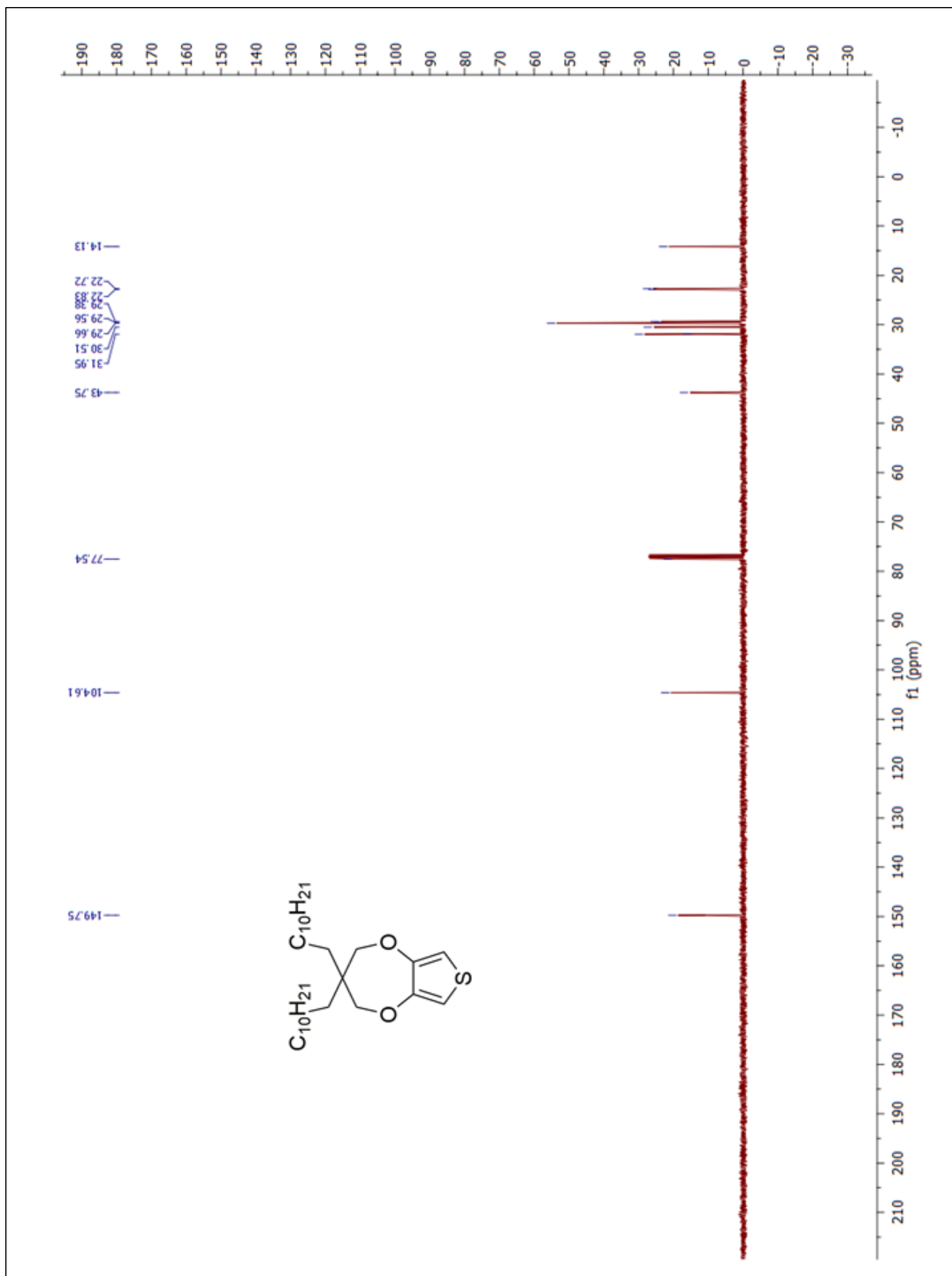


**Figure A.12.2:**  $^{13}\text{C}$ -NMR spectrum of 3,3'-didodecyl-3,4-dihydro-2H-thieno[3,4-b][1,4]dioxepine(ProDOT)







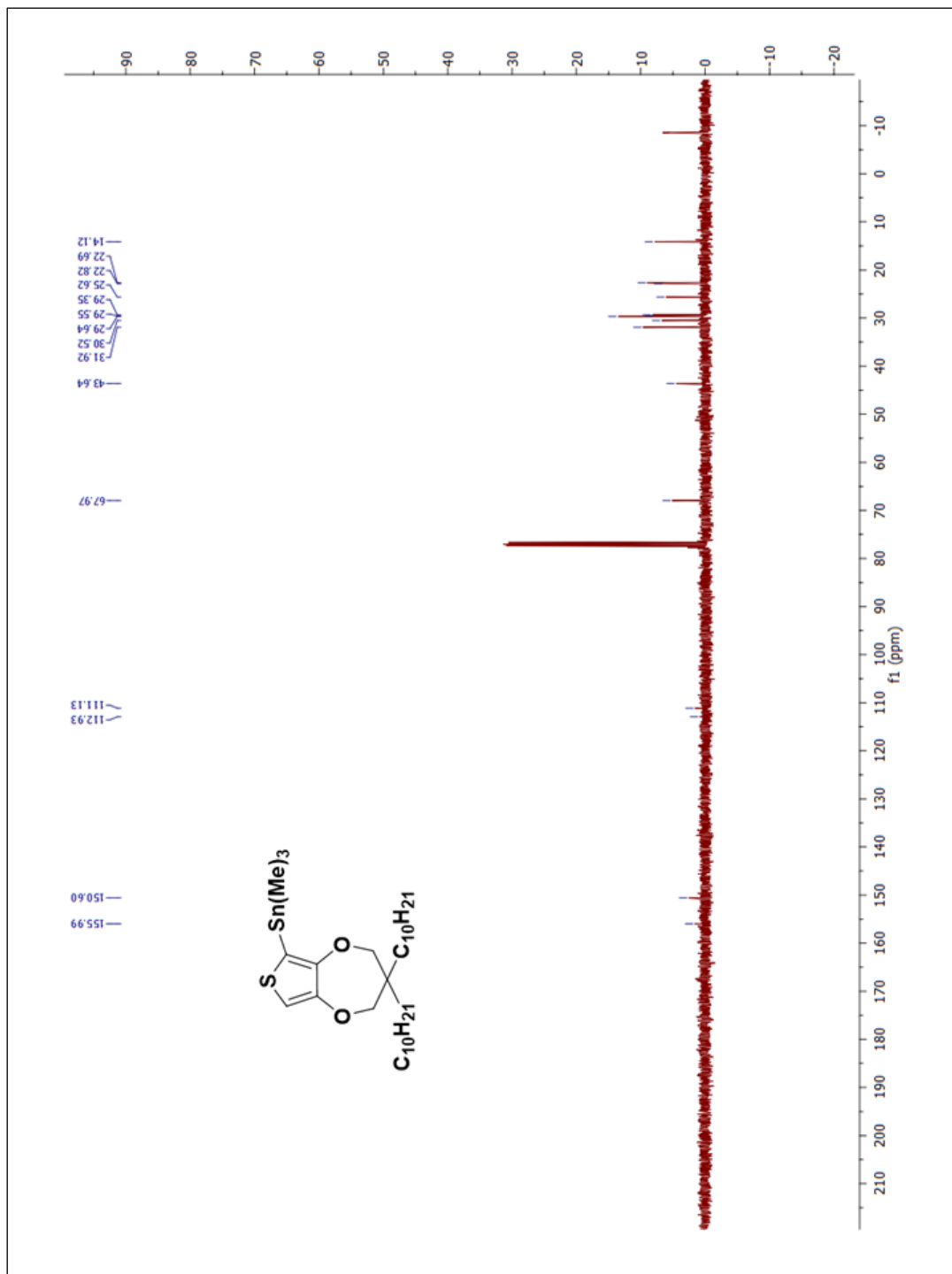


**Figure A.14.2:**  $^{13}\text{C}$ -NMR (3,3-didecyl-3,4-dihydro-2H-thieno[3,4-b][1,4]dioxepin-6-yl)trimethylstannane

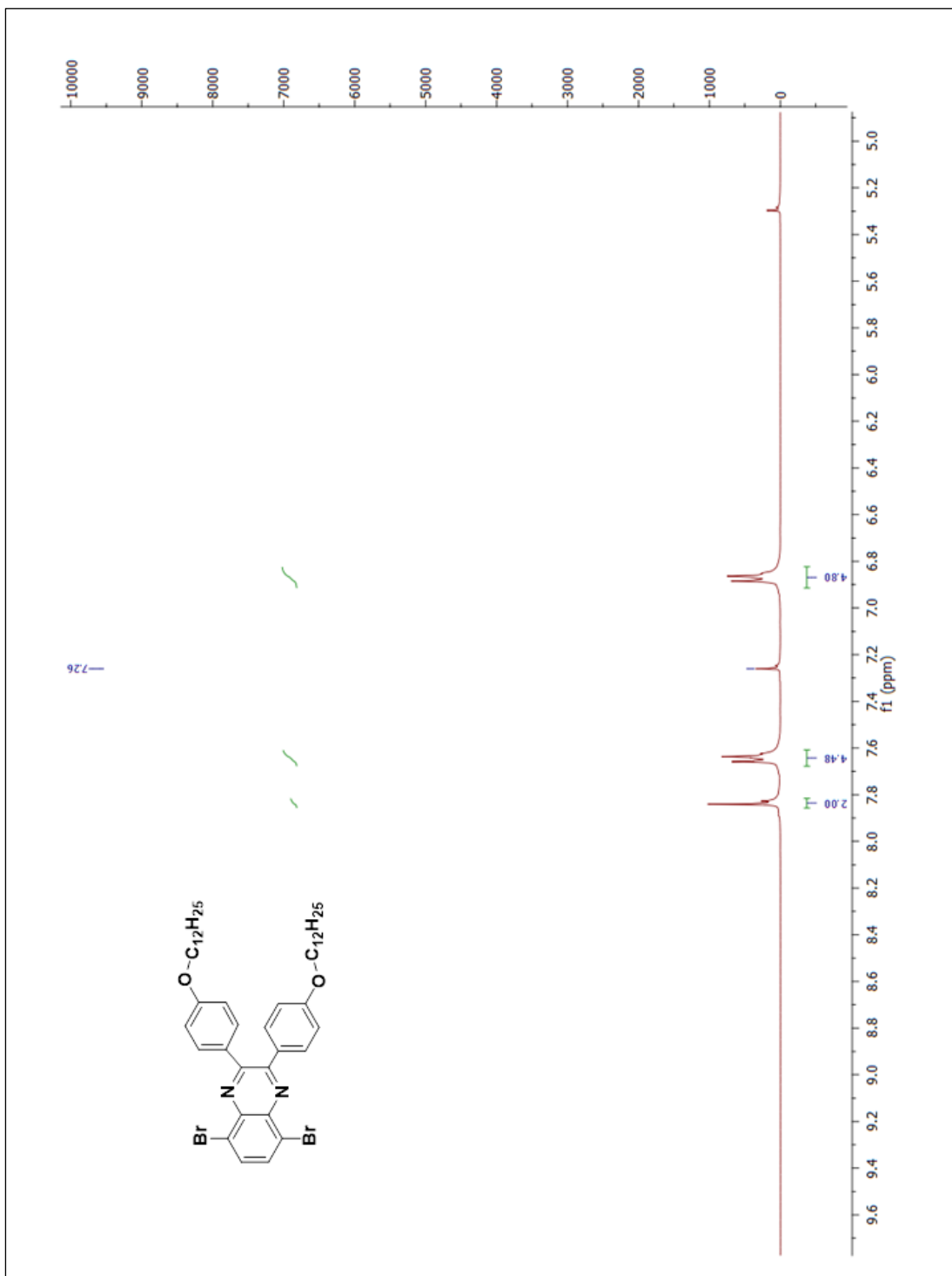


**Figure A.15.1:** <sup>1</sup>H-NMR spectrum of 5,8-dibromo-2,3-bis(4-((2-octyl)dodecyl)oxy)phenyl)quinoxaline

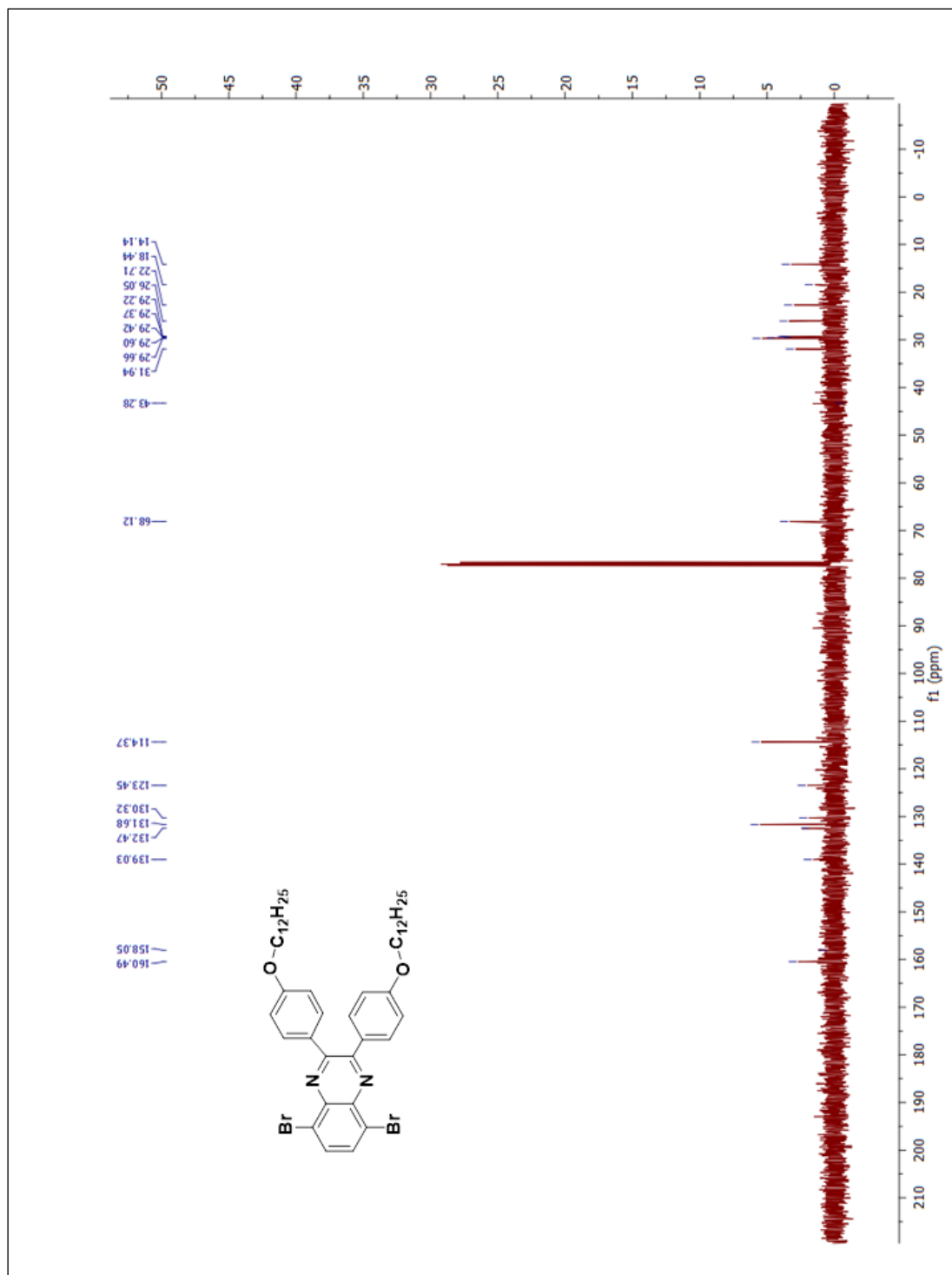


**Figure A.15.2:** <sup>13</sup>C-NMR spectrum of 5,8-dibromo-2,3-bis(4-((2-octyldecyl)oxy)phenyl)quinoxaline

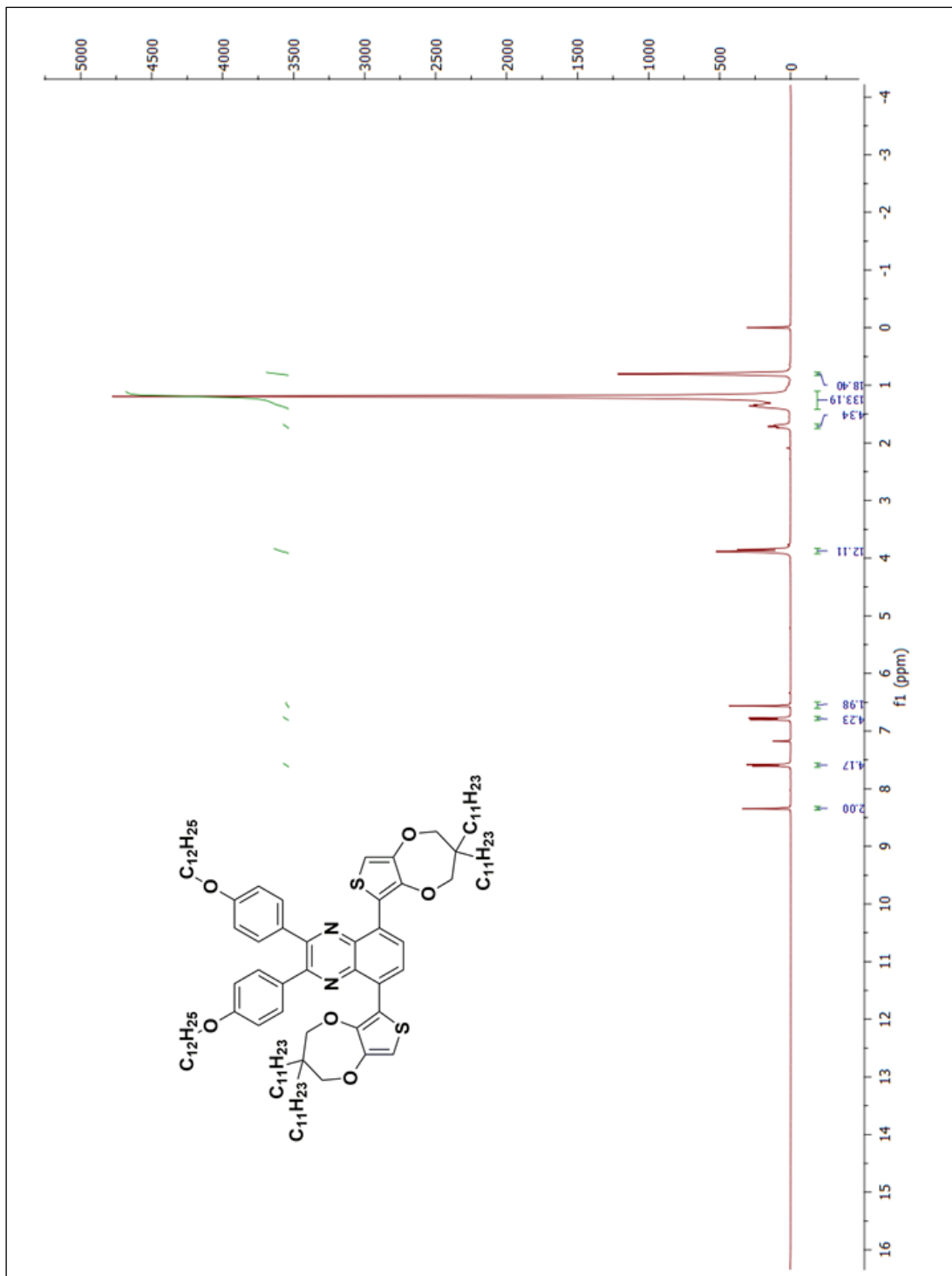


**Figure A.16.1:** <sup>1</sup>H-NMR spectrum of 5,8-bis(3,3-diundecyl-3,4-dihydro-2H-thieno[3,4-b][1,4]dioxepin-6-yl)-2,3-bis(4-(dodecyloxy)phenyl)quinoxaline

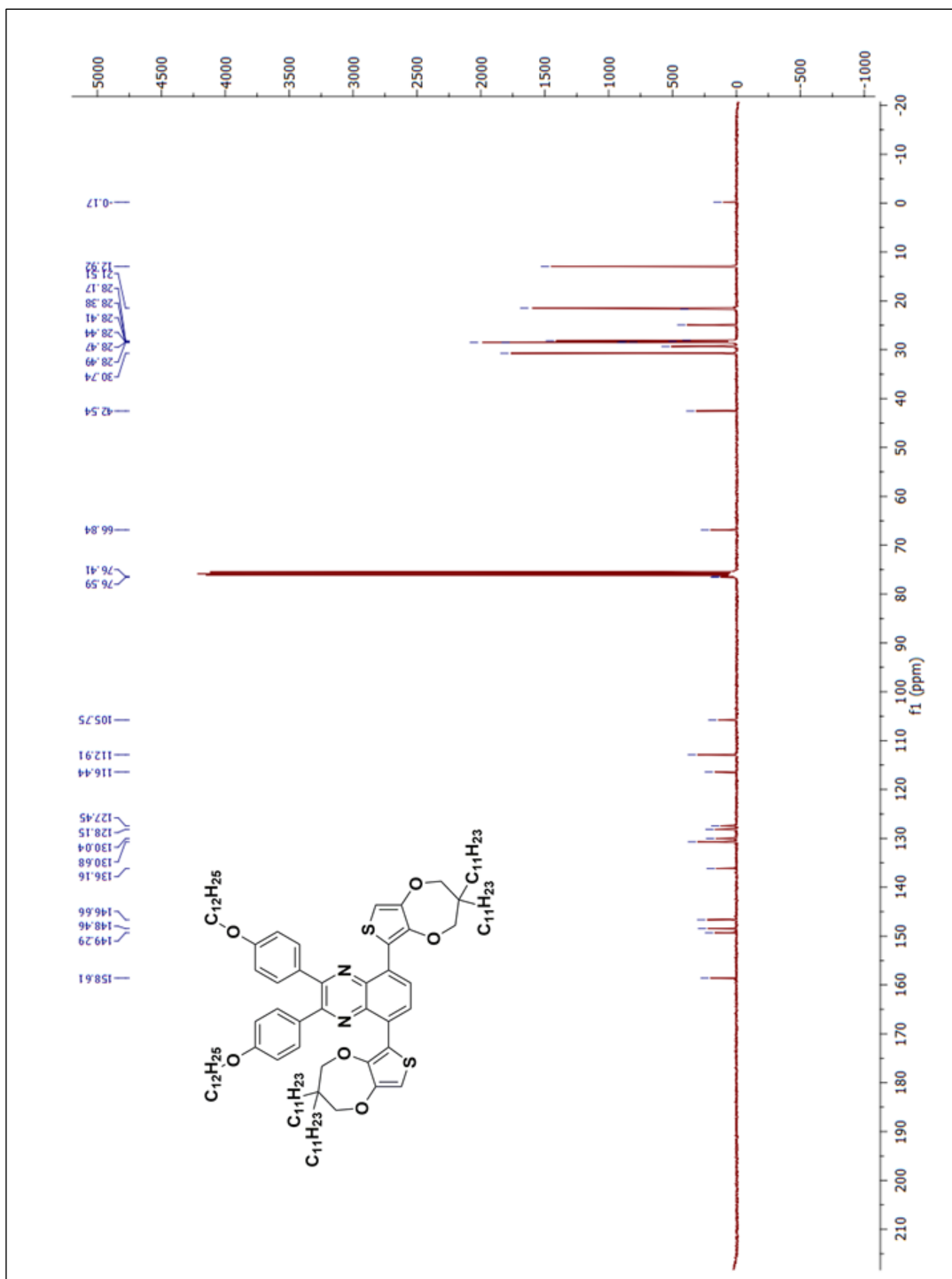


**Figure A.16.2:**  $^{13}\text{C}$ -NMR spectrum of 5,8-bis(3,3-diundecyl-3,4-dihydro-2H-thieno[3,4-b][1,4]dioxepin-6-yl)-2,3-bis(4-(dodecyloxy)phenyl)quinoxaline

y)benzo[c][1,2,5]oxadiazole FF

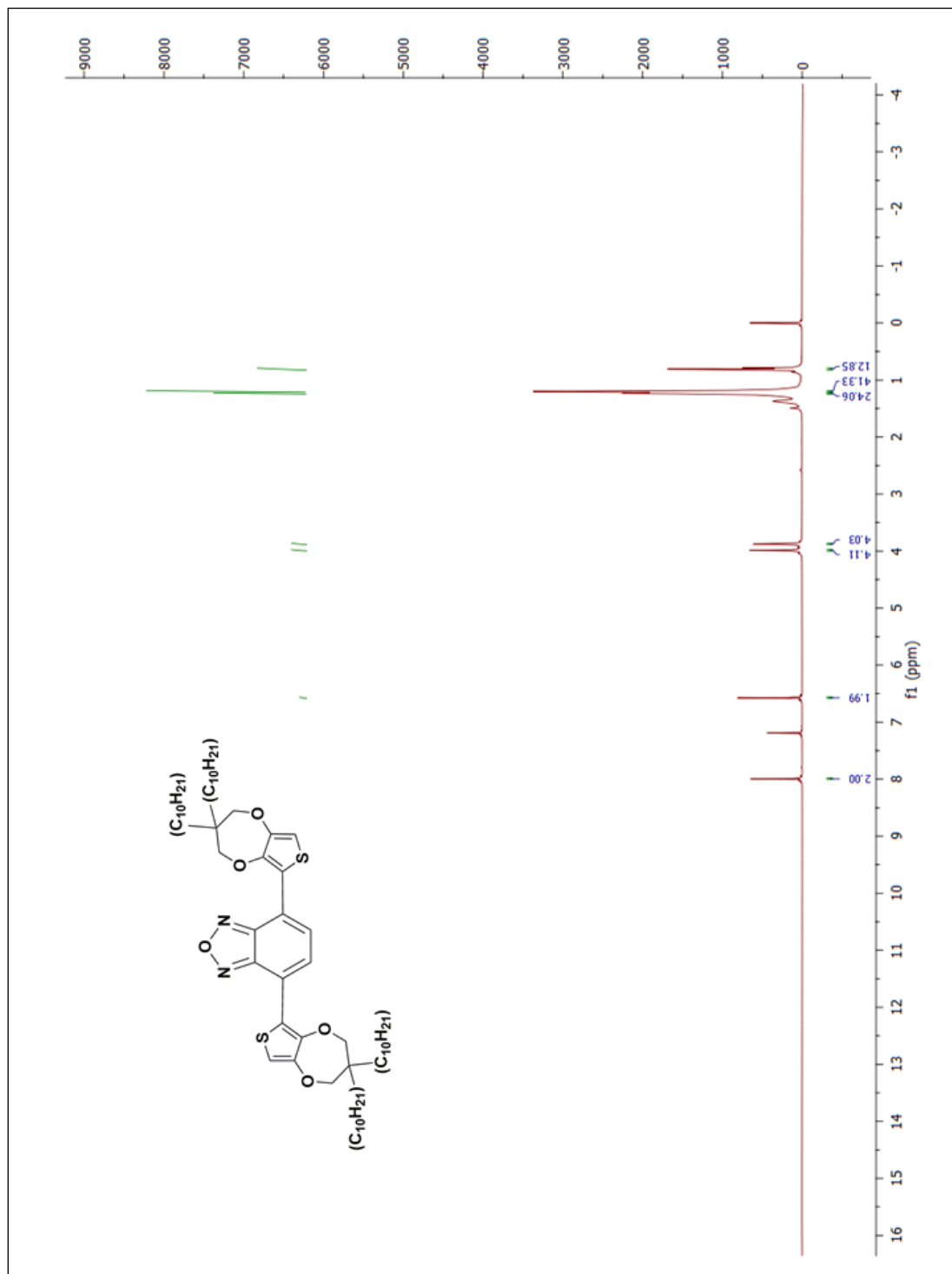


Figure A.17.1: <sup>1</sup>H-NMR spectrum of 4,7-bis(3,3-didecyl-3,4-dihydro-2H-thieno[3,4-b][1,4]dioxepin-6-